Chromosomal Aberrations in Hepatocellular Carcinoma : A Study by Comparative Genomic Hybridization and Interphase Cytogenetics

LEE Siu-wah

A Thesis Submitted in Partial Fulfilment
of the Requirements for the Degree of
Master of Philosophy
In
Medical Sciences

December 1999

UL

Chromosomal Aberrations in Hepatocellular Carcinoma : A Study by Comparative Genomic Hybridization and Interphase Cytogenetics

Submitted by LEE Siu-wah

for the degree of Master of Philosophy in Medical Sciences

at The Chinese University of Hong Kong in December 1999

Abstract

Hepatocellular Carcinoma (HCC) is a highly malignant tumour that is prevalent in Southeast Asia, including Hong Kong. Epidemiological studies have shown that there is a strong association between HCC and viral hepatitis infection of type B and C, cirrhosis, aflatoxin exposure and alcohol consumption. Although molecular and cytogenetic studies have indicated frequent loss of 1p, 4q, 6q and 8p in HCC, the mechanism for the underlying pathogenesis is still poorly understood. Comparative genomic hybridization (CGH) is a molecular cytogenetic technique that allows the rapid screening of DNA sequence gains, losses and amplifications in the entire genome. As an attempt to delineate the genetic alterations involved in the progression of HCC, we have applied CGH to the study of overall genomic imbalances in 67 HCC (55 with underlying liver cirrhosis and 12 without liver cirrhosis) and 12 surrounding cirrhotic liver tissues.

Our CGH analysis on HCC revealed a high incidence of 1q copy number gain (48/67 cases, 72%). Frequent gains were also found on 8q (32/67 cases, 48%), 20q (25/67 cases, 37%) and 17q (19/67 cases, 28%). Common losses were detected on 4q (29/67 cases, 43%), 13q (26/67 cases, 39%), 8p (25/67 cases, 37%) and 16q (19/67 cases, 28%). When genetic aberrations were correlated with clinical parameters such as tumour

staging and tumour size, we found that there is no significant difference in the pattern of genomic imbalances between stages T2 and T3. However, tumours greater than 3cm in diameter have a higher average aberrations per tumour than tumours smaller than 3cm (P = 0.036). A significant copy number loss of 4q11-q23 was identified in tumours larger than 3cm (P = 0.009). This might suggest that tumour suppressor gene(s) involved in HCC progression harboured on 4q11-q23. Of particular interest was a consistent 8q gain in non-cirrhotic HCC (100%) in comparison to HCC arising from cirrhotic livers (36%). This might suggest that genes on 8q played an essential role in the transformation of normal hepatocytes to malignant HCC. Although no genetic aberrations were identified in the 12 surrounding cirrhotic liver tissues, a smaller number of chromosomal aberrations detected in the cirrhotic HCC than the non-cirrhotic HCC supported the role of underlying cirrhosis in enhancing HCC development.

A remarkably high incidence of chromosome 1q gain (72%) found and the finding of a novel amplicon on 1q21-q25 by CGH implicated that genes important in liver carcinogenesis of HCC might reside on 1q. We therefore performed interphase FISH analysis with YAC probes on 1q21-q25 to fine map this amplicon. Our results confirmed the presence of 1q21-q25 copy number gain and confined the regional amplicon to 1q21.1. The YAC 955_e_11 defining the region of highest copy number increase should provide basis for further positional cloning of a gene that may be relevant to the development of HCC.

摘要

肝細胞癌 (HCC) 是一種在東南亞包括香港在內的常發性惡性疾病。病因學研究証明：肝細胞癌跟 B 及 C 型肝炎病毒所引起的肝炎、肝硬化、食用受黃曲霉毒素污染的食物與及酗酒有強烈的關係。儘管分子生物學和細胞遺傳學上的研究顯示，肝細胞癌患者染色體於 1p、4q、6q 和 8p 位點上時常發生缺失，但是總的病理發展尚未了解。比較基因組雜交(CGH)是一種嶄新的分子細胞遺傳技術，它能對整個腫瘤基因 DNA 序列缺失、增加及擴增區域進行快速的篩選。爲了勾劃肝細胞癌在演進過程中的遺傳變異，本研究應用 CGH 分析 67 例 HCC (其中 55 病例肝臟出現肝硬化，12 病例肝臟並沒有出現肝硬化) 和 12 病例於腫瘤週邊的肝硬化組織。

研究結果顯示染色體 1q 出現非常高比率的 DNA 序列增加 (48/67 病例，72%)，DNA 序列增加亦常見於 8q (32/67 病例，48%)，20q (25/67 病例，37%)，和 17q (19/67 病例，28%)，而 DNA 序列缺失則常見於 4q (29/67 病例，43%)，13q (26/67 病例，39%)， 8p (25/67 病例，37%) 和 16q (19/67 病例，28%)。我們亦分析了染色體變異跟腫瘤分期和腫瘤大小等的臨床指標的相關關係，發現 T2 和 T3 分期跟染色體變異模式並沒有顯著的關係，然而相對於直徑少於 3 厘米的腫瘤，直徑大於 3 厘米的腫瘤卻有較多染色體變異 ($P = 0.02$)，而 4q11-q23 的 DNA 序列缺失亦較顯著地出現於直徑大於 3 厘米的一組腫瘤上 ($P = 0.009$)，此點反映在 4q11-q23 上可能會有跟 HCC 演進相關的抑制腫瘤基因。另外，所有沒有肝硬化的 HCC 均出現 8q 增加，這點反映於 8q 上的基因在由正常肝細胞演進成惡性 HCC 中扮演重要的角色。儘管於 12 例肝硬化組織中並沒有發現染色體變異，但是相對沒有肝硬化的 HCC，有肝硬化的一組 HCC 卻出現較少的染色體變異，這顯示肝硬化在 HCC 的演進過程亦扮演重要的角色。

基於高比率的 1q 增加 (72%)以及於 1q21-q25 發現一擴增子，顯示 1q 會有對 HCC 發展有重要影響的基因。我們運用了間期 FISH 技術和酵母人工染色體

去仔細定位 1q21-q25 這擴增子，結果確定了 1q21-q25 出現 DNA 序列的增加和局限擴增子於 1q21.1 這區域。出現最高拷貝數目增加的酵母人工染色體 955_e_11，將會對和 HCC 發展有關的基因的定位克隆提供一條途徑。

Acknowledgements

First of all, I would like to thank my supervisors, Prof. Philip J Johnson and Dr. Nathalie Wong for their support and supervision amid the MPhil programme. I especially want to express my gratitude for their understanding, patience and arrangements during the preparation of this thesis. Special thanks are given to Dr Nathalie Wong for her technical advice on the use of molecular cytogenetic techniques and critical comments during the write-up of this thesis.

Sincere thanks are also given to my colleagues, Liz, Su, Yoke, Fanny, Andrew and Joyce who have made my past two years of study enjoyable and memorable. Also, I appreciate the help and encouragement of the staff working in the Cancer Centre, PWH during difficulties in my experiment.

Finally, I would like to thank my family who has backed me up during my study.

Contents

List of Figures

List of Tables

Abbreviations

ADH3	Alcohol Dehydrogenase 3 Gene
Anti-HBc	Antibody to Hepatitis B Virus Core Antigen
AP	Alkaline Phosphatase
BAC	Bacterial Artificial Chromosome
CCD	Charge-coupled Device
CDK4	Cyclin-dependent Kinase 4
CE	Cell Envelope
CGH	Comparative Genomic Hybridization
DAPI	4,6-diamino-2-phenylindole
EDC	Epidermal Differentiation Complex
FISH	Fluorescence *in situ* Hybridization
FITC	Fluorescein Isothiocynante
hJTB	Jumping Translocation Breakpoint
HBV	Hepatitis B Virus
HBsAb	Antibody to Hepatitis B Virus Surface Antigen
HBcAg	Hepatitis B Virus Core Antigen
HBsAg	Hepatitis B Virus Surface Antigen
HCC	Hepatocellular Carcinoma
HCV	Hepatitis C Virus
IGFIIr	Insulin Growth Factor II Receptor
LOH	Loss of Heterozygosity
M6P	Mannose-6-Phosphate
MUC1	Mucin 1 Gene
PAC	P1-derived Artificial Chromosome
Rb	Retinoblastoma Gene
SUP4-o	Ochre Suppressing Gene
TRITC	Tri-rhodamine Isothiocynante
YAC	Yeast Artificial Chromosome

Chapter 1.

Introduction

1.1 Hepatocellular Carcinoma (HCC)

Hepatocellular carcinoma (HCC) is a highly malignant tumour of the liver parenchyma, and represents over 95% of primary malignancy originated from the liver. HCC is the fifth most common cancer world-wide and constitutes 5.4% of total cancer cases (Parkin *et al.*, 1999). Coinciding with geographical distribution of chronic carriers of hepatitis B virus (HBV), HCC is endemic in Southeast Asia, China and Sub-Saharan Africa but rare in western countries. Age-standardised rates in men range from 2.7 per 100,000 in Northern Europe to 35.8 per 100,000 in China. However, due to the spread of hepatitis C (HCV) infection in the western populations that resulted in an increasing incidence of HCC, this malignancy is gaining more concern in the West (Ince and Wands, 1999). Besides persistent viral hepatitis B and C infections, other etiological factors associated with HCC include cirrhosis, aflatoxin exposure, alcohol consumption and chemical carcinogens.

Hong Kong lies in an area of high HCC incidence. The HCC incidence in Hong Kong is considerably higher than the West but falls in the mid-range among Asian cities (Table 1.1). Our local age-standardised incidence is 36.2 per 100,000 in male and 9.5 per 100,000 in female. The sex ratio was 3.4 male cases for every female. In 1994, 1700 new HCC cases were diagnosed, of which 87% were aged above 45 (HA Statistical Report, 1999). In 1997, HCC was the second and fourth most frequent cause of death in males and females respectively in Hong Kong (Department of Health Annual Report, 1999).

The prognosis of HCC is poor. To date, there is no effective systemic treatment for this malignancy. Surgical resection remains the only hope for long-term survival. Nevertheless, most patients present at a late stage with hepatomegaly and the liver function has deteriorated or the tumour has metastased to a secondary

site. Surgical resection is therefore applicable to only about 15% of the HCC cases. The median survival of the remaining 85% of HCC patients is about 3 months.

Table 1.1 World Age-standardised Incidence Rate (per 100,000) of HCC in Selected Countries, 1988-1992

Country/City	Males	Females
China, Qidong	72.1	19.1
China, Shanghai	28.2	9.8
China, Tianjin	22.7	8.9
Hong Kong	36.2	9.5
Japan, Osaka	46.7	11.5
Singapore :		
Chinese	22.1	5.8
Indian	6.3	2.8
Malay	11.6	3.9
Australia, NSW	2.5	0.6
Canada	3.1	1.2
UK, England & Wales	2.0	1.0
US, Los Angeles :		
Black	5.1	2.2
Chinese	16.1	4.4
Non-Hispanic White	2.9	1.1

Source : Cancer Incidence in five continents Vol. VII, IARC

1.2 Etiology of Hepatocellular Carcinoma

Whilst the mechanism for HCC development is still not clear, several factors have been found to be closely associated with HCC. Epidemiological studies have shown that there is a strong association between HCC and viral hepatitis of type B and C, cirrhosis, aflatoxin exposure in diet and alcohol consumption.

1.2.1 Viral Infection

Hepatitis B and C viruses together account for 82% of liver cancer cases worldwide (World Health Report, 1996). The association of HBV and HCV with HCC stems from the observation that HBsAg or anti-HCV is detected at a higher percentage in HCC patients than in normal population. However, the pattern of association varies in different geographic regions. In Chinese and African populations, HBsAg is detected in 62 to 80% of patients, while anti-HCV is present in 7 to 29% of cases (Okuda *et al.*, 1997). On the other hand, in Japan, Italy and Spain, anti-HCV is detected in more than 65% of patients, whereas HBsAg is detected in about 25% (Kiyosawa *et al.*, 1991, Simonetti *et al.*, 1989, Bruix *et al.*, 1989). In the remaining countries, the two viruses are deemed to play a minor but equal role. Also, it is known that the two viruses do not occur exclusively and patients can be coinfected with both HBV and HCV. It is generally thought that coinfection is more severe than infection with only one, both histologically and in the degree of clinical decompensation (Fong *et al.*, 1991).

1.2.1.1 Hepatitis B Virus

HBV is the etiological factor that has received the most extensive research. Much information has accumulated from viral biology, epidemiology and molecular studies. First discovered in 1965, hepatitis B virus is a member of hepadnaviruses

(*hepatic DNA viruses*). The 3.2kb viral genome is packaged in an envelope containing the hepatitis B surface antigen (HBsAg). In the first step of infection, HBsAg interacts with a specific HBV receptor on the plasma membrane of susceptible hepatocytes. The inner core of the virus is a nucleocapsid which contains the core antigen (HBcAg). The detection of HBsAg in serum for more than 6 months is an indicator for chronic infection, while the presence of antibody to the surface antigen (HBsAb) indicates past infection and immunity. When antibody to the core antigen (anti-HBc) is present alone, it indicates ongoing replication.

A direct cause-and-effect relationship between HCC and HBV has been demonstrated recently (Chang *et al.*, 1997). Following the implementation of hepatitis B vaccination program in 1984 in Taiwan, the incidence of hepatocellular carcinoma in children aged 6 to 14 declined from 0.7 per 100,000 between 1981 to 1986 to 0.36 per 100,000 between 1990 to 1994 ($P < 0.01$). The incidence of brain tumour in the same age group, which was used as a control, remained similar during the same period of time. It therefore provides a strong evidence that active immunisation can reduce the incidence of HCC. The incidence of adult HCC in relation to immunisation however remains to be verified.

Another study in Taiwan provided further epidemiological evidence for the association of HBV with HCC (Beasley, 1988). Between 1975 and 1986, 22707 men in Taiwan were studied prospectively. Serological tests showed that 15.2% were HBsAg-positive, 9.9% were anti-HBc-positive, 68.6% were anti-HBs-positive and 5.6% were negative for all three HBV markers. At the end of the study, 161 subjects developed HCC of which 152 were HBsAg carriers. Besides, in nine cases that were positive for anti-HBc, seven were also positive for anti-HBs. HCC was not found in men who were negative for all three markers for HBV infection. Based on these

findings, the authors suggested that chronic HBV infection preceded the onset of HCC and HBsAg-positive individuals are at a higher risk than uninfected individuals in developing HCC.

The ability of HBV to cause malignant transformation has been demonstrated by transfecting the entire HBV genome into mouse hepatocytes which were subsequently transformed to cell lines (Hohne *et al.*, 1990, Chen *et al.*, 1992). However, the mechanism underlying the HBV-related hepatocarcinogenesis is still unclear. One proposed mechanism is insertional mutagenesis by HBV DNA. The 3.2kb HBV genome frequently integrates into the host genome (Brechot *et al.*, 1980) and about 80% of HCC contained multiple HBV DNA integration sites in their chromosome (Chen *et al.*, 1982). Although the integration of HBV appears to be random, two reports have suggested the viral insertion of HBV in cellular genes like the growth-regulating genes (cyclin A) (Wang *et al.*, 1990) and the retinoic acid receptor genes (Dejean *et al.*, 1986). Another possibility is the transactivation of critical cellular genes by the *HBX* gene, which encodes the HBx protein. The HBx protein is a protein of 154 amino acids that is highly conserved among the different subtypes of HBV. It is multifunctional and is a known pleiotropic transactivator with no DNA-binding activity. Some studies have shown a direct interaction between the HBx protein and the p53 protein (Feitelson *et al.*,1993, Wang *et al.*, 1994).

1.2.1.2 Hepatitis C Virus

HCV is not a DNA virus but a positive-stranded RNA molecule of approximately 9500 nucleotides. The nucleotide sequence of HCV is variable, and can be divided into at least six subtypes (Simmonds *et al.*, 1994). The pattern of HCV genotypes may change significantly according to the histological severity of the liver disease (Nousbaum *et al.*, 1995). The presence of HCV RNA in serum

indicates active viral replication and seropositivity of anti-HCV is often used to confirm hepatitis C infection.

In most geographic areas, anti-HCV is detected in less than 2% of the general population (Alter, 1995, Mansel and Locarnini, 1995). However, it was detected in more than 58% of HCC patients in countries like Japan, Italy, France and Spain (Ohkoshi *et al.*, 1990, Levrero *et al.*, 1991, Nalpas *et al.*, 1991, Bruix *et al.*, 1989). Undoubtedly, persistent HCV infection initiates a series of pathological changes similar to HBV infection. These include inflammation, cellular injury, hepatic regeneration, and cirrhosis, all of which may contribute to the oncogenic process (Ince and Wands, 1999).

1.2.2 Cirrhosis and Chronic Inflammation

Hepatocytes in the normal adult liver rarely divide, but replications take place following parenchymal injury or loss. Cirrhosis is the liver response to chronic hepatocellular necrosis, inflammation and fibrosis. It is characterised by diffused, interlacing septal fibrosis and nodules of regenerating hepatocytes. Hepatic cirrhosis is found in 80 to 90% of HCC patients. Etiological factors such as viral infections and alcohol consumption can all lead to cirrhosis which in turn may progress to HCC. Cirrhosis is therefore thought to be the premalignant condition of HCC (Johnson, 1987). The risk of all genetic accidents increases in direct relation to the number of cell division. Therefore, the active regeneration of hepatocytes, which are challenged genetically by various etiological agents, may finally give rise to malignant clones. Nevertheless, cirrhosis is by no means a prerequisite for carcinoma as some HCC can arise in a non-cirrhotic liver.

1.2.3 Aflatoxin

Aflatoxin is a carcinogen produced by food spoilage fungi, *Aspergillus flavus* and *A. parasiticus*. It contaminates food supplies like corn, peanuts, and grains in humid tropical and subtropical regions, such as Qidong province of China and Africa. Chronic feeding of aflatoxin B_1 has been demonstrated to induce liver cancer in many animal species (Tulpule, 1981). Aflatoxin B_1 is bioactivated by cytochrome P450 monooxygenases to a reactive electrophile, aflatoxin-8,9-epoxide, which can bind covalently to guanine residues. An aflatoxin B_1 associated TGC to TTC point mutation occurred in codon 249 of the p53 tumour suppressor gene (Ozturk *et al.*, 1991). It is possible that such mutation has led to the inactivation of p53, that results in the upregulation of cellular proliferation.

1.3 Genetic Studies of Hepatocellular Carcinoma

1.3.1 Conventional Cytogenetics

Conventional cytogenetic studies can provide an overall view on the genetic alterations present. However, in the case of HCC, karyotypic information has been limited due to poor *in vitro* growth of the hepatocytes and the suboptimal chromosome morphology that precluded accurate analysis.

So far, there have been only five reports on the karyotypes of primary HCC (Table 1.2). The tumours displayed multiple and complex abnormalities in both chromosome number and structure. Changes of chromosome 1 were the most common chromosomal aberrations reported. Deletion of the short arm of chromosome 1 and loss of chromosomes 16, 21 and 22 was frequently detected.

Table 1.2. Cytogenetic Analysis of Hepatocellular Carcinoma From Short-term Cultures.

Source	Histology	Chromosomes: Modal no.	Aberrations	Viral exposure	Reference
65 yr. man	Epithelial	46	XY, -13, -16, +del(1)(p22), del(6)(q13), inv(9)(p12q12), +der(1)t(1;?)(p32;?), +der(5)t(5;?)(q34;?), der(22)t(22;?)(q12;?)	HBV-	Simon *et al.*, 1990
77 yr.	Well differentiated	46 (normal)	-	-	Bardi *et al.*, 1992
70 yr.	Moderately differentiated	45	-Y	-	Bardi *et al.*, 1992
79 yr. man	Well differentiated	71-79	XX, -Y, <3n>, +3, -8, -16, -17, -21, der(1)t(1;?)(p36;?), del(1)(p11), +der(1)t(1;?)(q21;?), +del(1)(q32), +der(3)t(1;?;3)(3qter→3p11::?::1p12→1p36::?), der(6)t(6;8)(q12;q13), +der(6), 9p+, +der(9)(q13), del(10)(q24), der(12)t(12;?)(p13;?), inv dup(12)(q11q24), der(13)t(10;13)(q11;p13), +1-9mar	-	Bardi *et al.*, 1992
58 yr. man		76-79	XXY, +der(1)t(1q;?), +del(1)(q25), der(1)del(1)(p34)del(1)(q42), +del(1)(p13), +7, +11, +12, +18, +mar1, +mar2	-	Werner *et al.*, 1993

17 yr. man	Fibrolamellar, metastasis	62-92	XX, -Y, <3n>, +3, +6, +6, +7, +7, +8, +10, +13, +15, +16, +20, -21, -22, +mar1X2, +mar[cp6]	HBV-, HCV-	Lowichik *et al.*, 1996
17 yr. man	Fibrolamellar, metastasis	78	XX, -Y, <3n>, der(1)t(1;1)(p36.1;q21), +4, +6, +6, +7, +7, i(8)(q10), +10, +15, +20, -21, -22, +mar1X2, +mar2[3]	HBV-, HCV-	Lowichik *et al.*, 1996
Patient 1		106-113	XXXYY, del(1)(p22), -4, -5, -8, i(8)(q10), i(9), add(9)(p24), -10, -13, -13, -15, add(16)(q24), -16, -17, -17, -18, ad(21)(q10)x2, -22, +7-13mar [cp10]	HBV-, HCV+	Chen *et al.*, 1996
Patient 2		72-76	XY, -X, del(1)(p32), +add(1)(q10), +del(6)(q15), +7, -8, -9, -10, -11, -12, +13, +15, -16, -17, +18, +20, -21, -22, +4-8mar [cp12]	HBV+	Chen *et al.*, 1996
Patient 3		45	X, -Y, del(1)(p34), del(1)(p22), -4, -5, -13, der(16)add(16)(q24), +2mar [cp8]	HBV+	Chen *et al.*, 1996
Patient 4		46	XY [cp8]	HBV+	Chen *et al.*, 1996
Patient 5		66-72	XY, -X, +del(1)(p32), +add(1)(q10), -4, -6, +7, -8, +11, der(13;15)(q10;p10), i(14)(q10), -16, -17, -21, -22, +1-3mar [cp10]	-	Chen *et al.*, 1996

1.3.2 Molecular Cytogenetics

The number of chromosome copies can also be enumerated by fluorescence *in situ* hybridization (FISH), using peri-centromeric probes on interphase nuclei. Using this approach, trisomy or polysomy of chromosomes 1, 8 and 17 in HCC was first reported (Nasarek *et al.*, 1995, Kimura *et al.*, 1996). By the use of a panel of peri-centromeric probes, Ohsawa (1996) reported numerical aberrations in chromosomes 7, 8, 9, 10, 12, 17, 18, X and Y in 71% (27/38) of HCC cases studied. Similarly, Zimmermann *et al.* (1997) reported polysomy of chromosomes 1, 6, 7, 8 and 16, and monosomy of chromosomes 4, 16 and 17 in HCC. However, these studies have the major drawback in being dependent on the probes chosen and the peri-centromeric probes used do not necessarily represent the whole intact chromosome.

In contrast, a recently developed molecular cytogenetic technique comparative genomic hybridization (CGH) allows the genome-wide survey for chromosomal imbalances in tumours without prior knowledge of the aberrations present. There are so far two reports on the application of CGH in primary HCC. Recurring chromosomal losses on 4q, 8p, 16q, 17p, 13q, 6q and 1p as well as gains on 8q, 1q, 6p and 17q were suggested (Marchio *et al.*, 1997, Kusano *et al.*, 1999).

1.3.3 Molecular Genetic Studies

1.3.3.1 Proto-oncogenes

Studies on proto-oncogenes in HCC have focused on mutations or expression of known proto-oncogenes including the *ras* family, *c-met, c-myc and bcl-2*. Although common in human pancreatic carcinomas, mutation of the *ras* family is infrequent in HCC (Tsuda *et al.*, 1989, Tada *et al.*, 1990). However, overexpression

of *N-ras*, usually in the absence of a mutation, has been detected in 50 to 100% of human HCC by Northern blot analysis (Wang *et al.*, 1991). Similarly, a 2- to 10-fold increase in *c-met* expression was detected (Boix *et al.*, 1994). By Southern blot hybridization, *c-myc* amplification has been reported in 36.4% (28/77) of HCC (Zhang *et al.*, 1993) while immunohistochemical study of *bcl-2* revealed an abnormal expression in 13.5% of cases (Zhao *et al.*, 1994). Thus far, no candidate proto-oncogene has been suggested to be strongly associated with the development of HCC.

1.3.3.2 Tumour Suppressor Genes

A number of allelotype studies have been performed on HCC. Frequent loss of heterozygosity (LOH) on chromosomes 1p, 4q, 6q, 8p, 10q, 13q, 16q, 17p and 22q had been reported (Buetow *et al.*, 1989, Tsuda *et al.*, 1990, Nishida *et al.*, 1992, Emi *et al.*, 1992, Yeh *et al.*, 1994, Boige *et al.*, 1997, Nagai *et al.*, 1997, De Souza *et al.*, 1995). Further to their previous allelotyping on HCC, Pineau *et al.* (1999) undertook a high-density polymorphic marker analysis on chromosome 8p. Their results showed that 60% of the tumours exhibited LOH at one or more loci at 8p with three distinct minimal deleted areas. Nevertheless, few studies have succeeded to associate the LOH at a chromosomal locus to the inactivation of a specific tumour suppressor gene in hepatocarcinogenesis. One exception is the LOH at the mannose 6-phosphate/insulin-like growth factor II receptor (*M6P/IGFIIr*) locus. Following the observation of reduced expression of IGFIIr in both rat and human HCC, De Souza *et al.* (1995) found LOH at *M6P/IGFIIr* loci in 64% (14/22) of liver tumours. They then demonstrated that in HCC with LOH at the *M6P/IGFIIr* locus, there were accompanying mutations in the remaining allele that result in truncated receptor

protein and major amino acid substitutions (De Souza *et al.*, 1995). These findings suggested that *M6P/IGFIIr* played an important role in human liver carcinogenesis.

1.3.3.3 Cell Cycle Genes

TP53 exhibits several functions of a checkpoint gene in mammalian cells and is involved in maintaining genomic integrity. Subsequent to a report of mutational hotspot in the p53 gene in HCC by Ozturk *et al.*(1991), a number of studies have been reported on the prevalence of p53 mutations in HCC from various geographic regions (Bressac *et al.*, 1991, Kress *et al.*, 1992, Sheu *et al.*, 1992, Nose *et al.*, 1993, Ng *et al.*, 1994). A specific G to T transversion at the third base of codon 249 was frequently identified in HCC from aflatoxin-endemic areas like Qidong province of China and South Africa, but not from other parts of the world (Ozturk *et al.*, 1991). This in turn might be suggestive of a codon 249 mutation of the p53 gene as a genetic trait in HCC from areas of high aflatoxin exposure.

The interplay between $p16^{INK4}$, cyclin-dependent kinase 4 (CDK4), cyclin D1 and retinoblastoma (Rb) genes is one of the pathways that regulate the G1/S transition. Phosphorylation of retinoblastoma protein, pRb in G1 phase is required to allow progression from G1 to S phase. The product of p16 binds to CDK4 and inhibits the kinase activity of cyclin D1-CDK4 complex, leading to dephosphorylation of pRb that inhibits the progression of the cell cycle.

Frequent loss of chromosome 13q14 including the loci of Rb in HCC and concomitant loss of Rb protein expression has been reported (Zhang *et al.*, 1994). In human HCC, the cyclin D1 gene was overexpressed in 13% of the tumours (Zhang *et al.*, 1993). However, amplification or rearrangements of the CDK4 gene were not detected (Kita *et al.*, 1996). Although homozygous deletions and mutations of p16

were relatively rare in HCC (Kita *et al.*, 1996, Hui *et al.*, 1996), Liew *et al.* (1999) found a high frequency of hypermethylation of the 5' CpG island of the p16 gene (62.5%, 32/48 of HCC tumours). Furthermore, hypermethylation in conjunction to homozygous deletion and missense mutation resulting in p16 alteration was detected in 70.8% (34/48) of HCC. This suggested an important role of p16 in the development of HCC.

1.4 Background of Study

Genomic imbalances are common in solid tumours. Previous cytogenetic and molecular studies in HCC have mainly indicated areas of recurrent genetic losses. Information on chromosomal gains, on the other hand, is mainly provided by FISH studies. The use of peri-centromeric probes in FISH studies however does not distinguish regional chromosome gains or a gain of the whole chromosome.

Comparative genomic hybridization (CGH) is a recently developed molecular cytogenetic technique. It offers the advantage of rapid and simultaneous screening of DNA sequence gains and losses in the entire tumour genome in one single experiment. The correlation of genetic changes identified with clinical parameters, such as tumour staging and tumour size would improve our understanding of the role of individual genetic aberration in the progression of HCC. As cirrhosis is considered as the premalignant state for HCC, it is also worthy to investigate if genetic aberrations are present in cirrhotic tissues surrounding the tumour.

Another advantage offered by CGH is its ability to reveal sites of DNA amplification. These sites of DNA amplification can be thought of chromosome regions harbouring potential proto-oncogenes. Therefore, characterisation of novel site(s) of DNA amplification found in CGH would provide basis for positional cloning of gene(s) that may be involved in the development of HCC.

1.5 Objectives of Study

1. To screen and analyse recurrent genetic changes in hepatocellular carcinoma by CGH and identify the possible correlation of the identified genetic changes with clinical stage, tumour size and the presence of underlying cirrhosis in tumour specimens.

2. To investigate the surrounding cirrhotic liver tissues of the tumours for the presence of genetic alterations.

3. To validate and characterise amplified site identified by CGH with interphase cytogenetics.

Chapter 2.

Materials and Methods

2.1 Materials

Preparation of Normal Human Metaphase chromosomes

1. Phytohaematoglutinine (GibcoBRL Life Technoiogies, Gaitherburg, MD)
2. RPMI 1640 (GibcoBRL)
3. Fetal calf serum (GibcoBRL)
4. Penicillin/streptomycin (GibcoBRL)
5. Colchicine (Sigma)
6. RNase (Boehringer Mannheim)
7. 2xSSC: 0.3*M* NaCl (Sigma), 0.03*M* trisodium citrate (Sigma)

Extraction of High Molecular Weight DNA

8. Phenol/chloroform/isoamyl alcohol 25:24:1 (v/v/v)
9. β-mercaptoethanol (Sigma)
10. Lyticase solution: 5U/μl lyticase (Sigma), 50m*M* Tris-HCl, 1m*M* EDTA, 50% glycerol (Sigma)
11. SCE buffer: 1*M* sorbitol (Sigma), 0.1*M* trisodium citrate (Sigma), 0.1*M* EDTA (Sigma), pH 7.0
12. QIAamp tissue kit (Qiagen, GmbH Germany)

Labeling of DNA by Nick Translation

13. Biotin-16-dUTP (1m*M*) (Boehringer Mannheim, Mannheim, Germany)
14. Digoxigenin(dig)-11-dUTP (1m*M*) (Boehringer Mannheim)
15. Nick translation buffer: 0.05*M* Tris-HCl, 5m*M* $MgCl_2$, 0.05mg/ml BSA, 0.01*M* β-mercaptoethanol (pH 8.0)
16. Deoxyribonucleotides: dATP, dCTP and dGTP (Boehringer Mannheim)
17. DNA polymerase I (Amersham Life Science)

18. DNase I (Boehringer Mannheim)

19. Agarose (Biowest)

20. 1xTAE buffer: 0.04*M tris*-base, 1.14ml acetic acid and 1*M* EDTA (pH 8.0)

21. 1kb plus DNA ladder (GibcoBRL)

Labeling Efficiency

22. Nick spin column (Pharmacia Biotech)

23. NBT/BCIP: (Gibco BRL)

24. 1xTE buffer: 10m*M Tris*-HCl, 1m*M* EDTA (pH 7.4)

25. Maleic acid buffer: 0.1*M* maleic acid, 0.15*M* NaCl (pH 7.5)

26. Blocking solution: 1% blocking reagent (Boehringer Mannheim) in maleic acid buffer (pH 7.5)

Preparation of Probe

27. Human Cot-1 DNA (1mg/ml) (GibcoBRL)

28. Hybrisol VII (Oncor): 70% formamide, 2xSSC, 10% dextran sulphate (pH 7.0)

Fluorochrome-conjugated Antibodies

29. Monoclonal mouse anti-digoxigenin (Sigma Chemical Co., St Louis, MO); 1:100 dilution

30. Rabbit anti-mouse TRITC (Sigma); 1:100 dilution

31. Goat anti-rabbit TRITC (Sigma); 1:100 dilution

32. FITC-avidin DCS (Vector Laboratories, Burlingame, CA); 5μg/ml

33. Goat biotinylated anti-avidin D (Vector Laboratories); 1:100 dilution

34. Sheep anti-digoxigenin FITC (Boehringer Mannheim); 1:10 dilution

35. Rabbit anti-sheep FITC (Sigma); 1:20 dilution

36. Avidin Texas-Red (Vector Laboratories); 1:80 dilution

Fluorescence Microscopy and Image Analysis

37. 4,6-diamino-2-phenylindole (DAPI) (Sigma)

38. Anti-fade solution (Vectashield, Vector Laboratories, Burlingame, CA)

39. Cytovision (Applied Imaging, Sunderland, UK).

Culture of Yeast Artificial Chromosomes

40. Yeast host strain: *Saccharomyces cerevisiae* AB1380 (*trp1⁻, ura3⁻, ade2-1*)

41. AHC plate: 0.17% yeast nitrogen base without amino acid and ammonium sulfate (Difco), 0.5% ammonium sulfate (Sigma), 1.4% casein hydrolysate acid (Oxoid), 0.002% adenine hemisulfate (Sigma), 2% agar (Difco), 3.5U/ml penicillin and 3.5μg/ml streptomycin (GibcoBRL)

42. YPD broth (Difco): 1% yeast extract, 2% peptone, 2% dextrose

43. Shaking Incubator: Thermolyne Rosi 1000™

Inter-Alu-PCR

44. Primer sequences ALE1: GCCTCCCAAAGTGCTGGGATTACAG

ALE3: CCACTGCACTCCAGCCTGGG

45. PCR amplification buffer: 10mM Tris HCl pH 8.3, 2mM $MgCl_2$, 0.2mM dNTP, 0.2μM of each of primers ALE1 and ALE3, 1.75U of polymerase [95% AmpliTaq Gold (5U/μl, Perkin-Elmer), 5% pfu polymerase (2.5U/μl, Stratagene)].

46. Programmable thermal cycler (PTC-200, MJ Research Inc)

47. High Pure PCR Product Purification kit (Boehringer Mannheim)

48. GeneQuant (Pharmacia Biotech, Sweden).

49. 3-aminopropyltriethoxylsilane (Sigma)

50. Sodium thiocyanate (Sigma)

51. Pepsin (Boehringer Mannheim)

2.2 Analysis of Chromosomal Imbalances by Comparative Genomic Hybridization

2.2.1 Comparative Genomic Hybridization

First introduced in 1992, comparative genomic hybridization (CGH) represents a major breakthrough in the field of molecular cytogenetics (Kallioniemi *et al.*, 1992). It allows the identification of chromosomal gains and losses in the whole tumour genome in a single experiment. Whilst conventional cytogenetic studies on solid tumours are often hampered by sub-optimal tumour growth *in vitro* and poor chromosome morphology, CGH allows the study of genetic alterations in solid tumours without the need of cell culture. Also, CGH is a useful tool to detect and map amplified DNA sequences in the tumour genome, which in the past are only revealed by conventional cytogenetics as homogeneously staining regions and double minute chromosomes (Alitalo and Schwab, 1986).

Essentially, the technique of CGH consists of two components: (a) fluorescence in situ hybridization of labeled DNA on metaphase chromosomes, and (b) digital analysis of fluorescent images (Fig. 2.1). The first component involves the four steps of FISH: denaturation, hybridization, post-hybridization wash and detection (see section 2.3.1). The probes used in CGH can be labeled either directly by fluorochrome-conjugated deoxynucleotides or indirectly by hapten-conjugated deoxynucleotides. After denaturation into single-stranded DNAs, equal amounts of labeled total tumour DNA and normal genomic reference DNA are co-hybridized onto normal human metaphase chromosomes, in the presence of excess unlabeled human Cot-1 DNA. Homologous sequences present in both test and reference DNA will compete for the same target sites on metaphase chromosomes. For indirectly labeled probes, fluorescent signals can be visualized with green and red fluorescing

antibodies against the haptens. The final hybridized signals appear as tiny fluorescent granules on the chromosome. The denser the granules, the better the hybridization quality. The ratio of fluorescent intensity between the two DNA at a particular chromosomal locus reflects the relative copy number of DNA sequences in the tumour genome. In our laboratory, tumour DNA is labeled with green fluorescent agent (FITC) and normal reference DNA as red (TRITC), although the reverse labeling is also possible. Gains of DNA sequences in the test DNA are visualized as increased green-to-red fluorescent signal ratio. Similarly, losses are indicated as an increased red fluorescent signal of reference DNA over green signals.

Although high-level amplifications can be readily observed under the fluorescence microscope, digital image analysis is required to give a better estimation of regions of low-level copy number changes. The green and red fluorescent images and the blue DAPI images are captured with a cooled charge-coupled device (CCD) camera. Reverse DAPI-banding pattern generated by the computer resembles that of crude G-band and therefore allows chromosome identification according to standard karyotyping (Fig. 2.2A). Fluorescent ratios were then calculated by integrating the value of the green and red signals across the width of a line orthogonal to the chromosome axis (Fig. 2.2B). After normalization, the image profiles of 8 to 12 metaphases were averaged to give a copy number karyogram (Fig. 2.2C & D). The spatial resolution of CGH mapping is approximately 10 mega base pair (Mbp) for low-copy-number gains and losses and 2 Mbp for high-copy-number amplifications (Piper *et al.*, 1995, Bentz *et al.*, 1998). The introduction of CGH has accelerated the identification of chromosomal aberrations in a number of human neoplasms (Zitzelsberger *et al.*, 1997, Knuutila *et al.*, 1998).

Figure 2.1 Schematic Outline of the CGH Technique. Test and reference DNA are differentially labeled (green and red, respectively) and co-hybridized to normal human metaphase chromosome spreads. Visualization of the chromosomes by fluorescence microscopy reveals differences in the fluorescent hybridization signals along the chromosomes, representative of the abundance of the test DNA sequence relative to the reference DNA sequence. Analysis of captured images can provide a colour ratio profile indicative of copy number changes in the test DNA relative to the reference DNA.

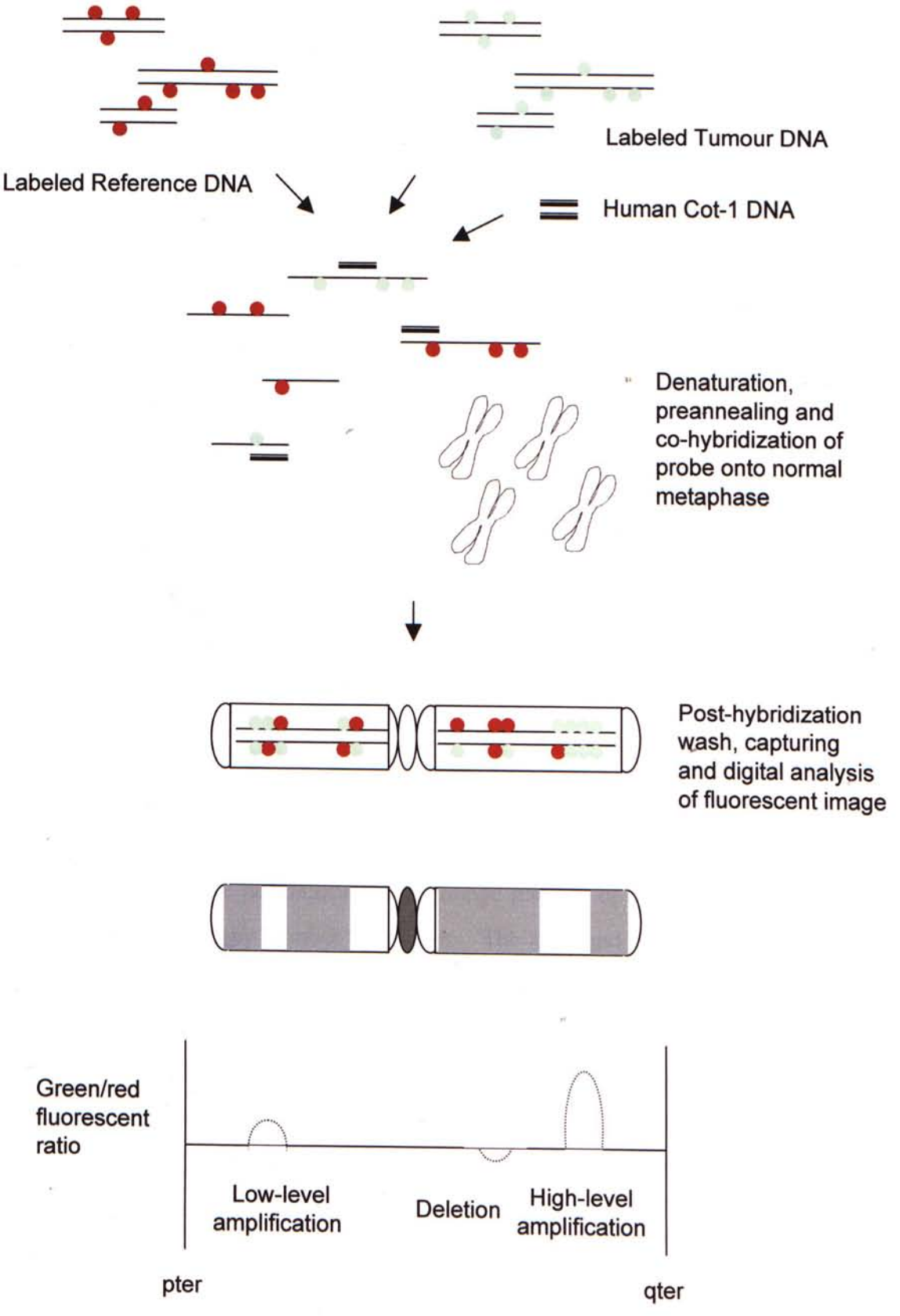
Labeled Tumour DNA
Labeled Reference DNA
Human Cot-1 DNA
Denaturation, preannealing and co-hybridization of probe onto normal metaphase
Post-hybridization wash, capturing and digital analysis of fluorescent image
Green/red fluorescent ratio
Low-level amplification
Deletion
High-level amplification
pter
qter

Figure 2.2 Digital Analysis and Detection of Chromosomal Imbalances by CGH. The green and red fluorescent images and the blue DAPI images are captured with a cooled CCD camera. (A) Hybridization pattern of the normal reference DNA labeled with digoxigenin and detected via TRITC. Using an appropriate single bandpass filter, a CCD image of only the TRITC fluorescence was captured. This gray-scale image was then digitally pseudocoloured in red. (B) Hybridization pattern of biotin-labeled total genomic DNA derived from tumour cells. The image was obtained with a single bandpass filter for FITC fluorescence, and pseudocoloured in green. (C) DAPI image of the normal metaphase. (D) Reverse DAPI image generated by digital inversion of the DAPI image. This provides banding pattern resembling that of crude G-band, therefore allows identification of the chromosomes by standard karyotyping. (E) The fluorescent intensity profile of each chromosome was calculated by a summation of the green and red fluorescence pixel value along the sequence of lines perpendicular to and spaced at unit distance along the medial axis. Thresholds for gains and losses were defined as the theoretical value of 1.25 and 0.75 respectively. (F) Karyogram of the metaphase spreads with pseudo-colours superimposed. Chromosomal gains (green) and losses (red) can be readily recognised. There is a high consistency of the ratios for both chromosome homologs. (G) After normalization, the image profiles of 8 to 12 metaphases are averaged to give a copy number karyogram. The averaged green-to-red fluorescent ratio is shown by the pink line, accompanied by the 95% confidence interval (golden lines). Red and green vertical lines represent the thresholds for chromosomal losses (0.75) and gains (1.25). The CGH profile of this specimen suggests high-level copy gains of 1q and 6p, low-level gains of 2pter-q22, 2q3-qter, 7, 8q13-qter, 10pter-q25, 15q, 17q and 20, and losses of 4q12-q28, 17p, 18p11.2-qter, 22 and Y.

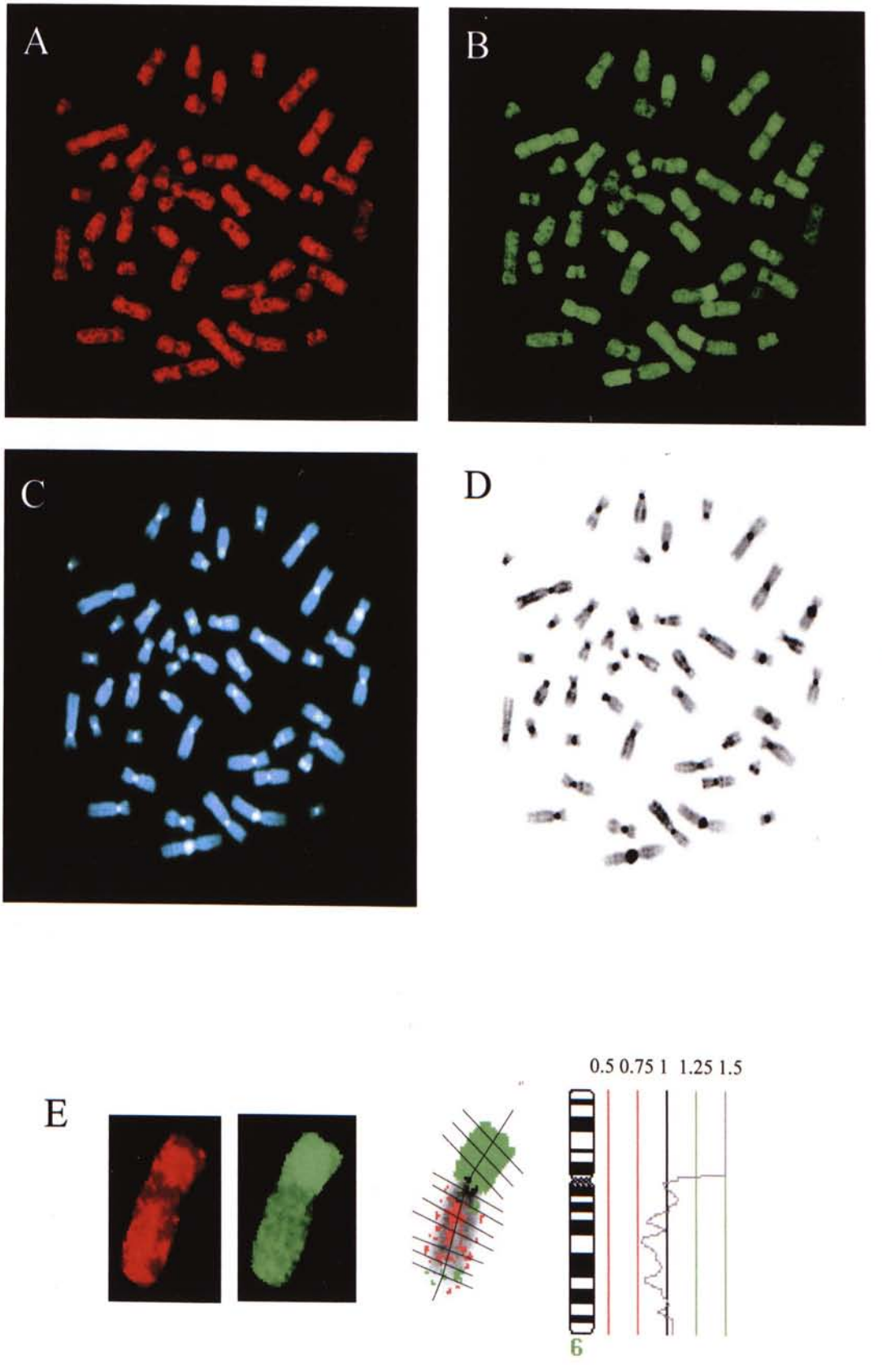
A
B
C
D
E
0.5 0.75 1 1.25 1.5
6

F

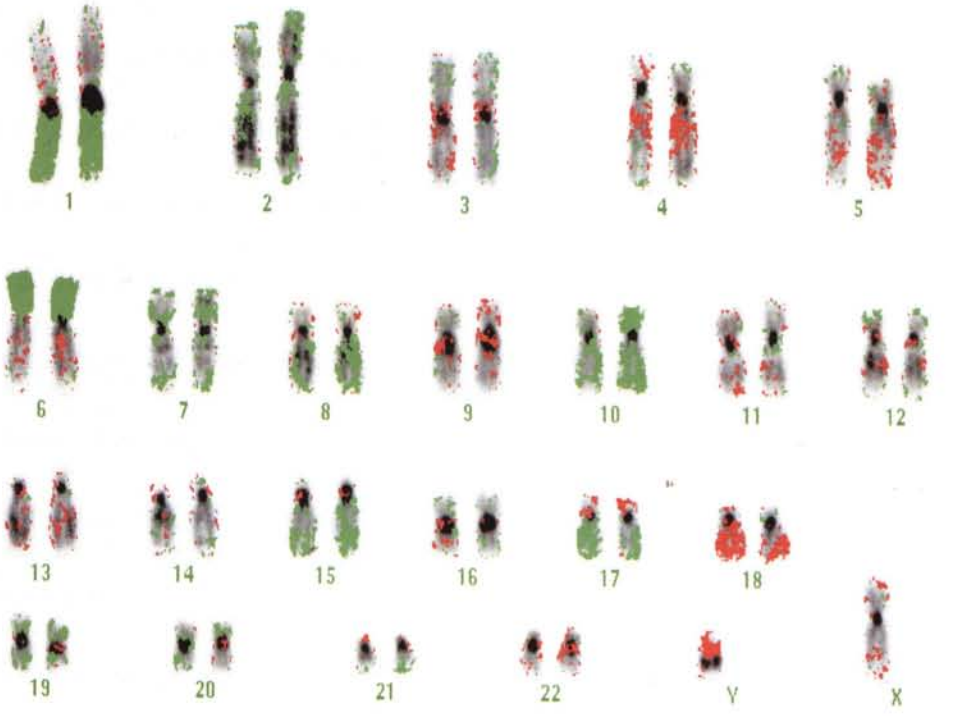
1
2
3
4
5
6
7
8
9
10
11
12
13
14
15
16
17
18
19
20
21
22
Y
X

G

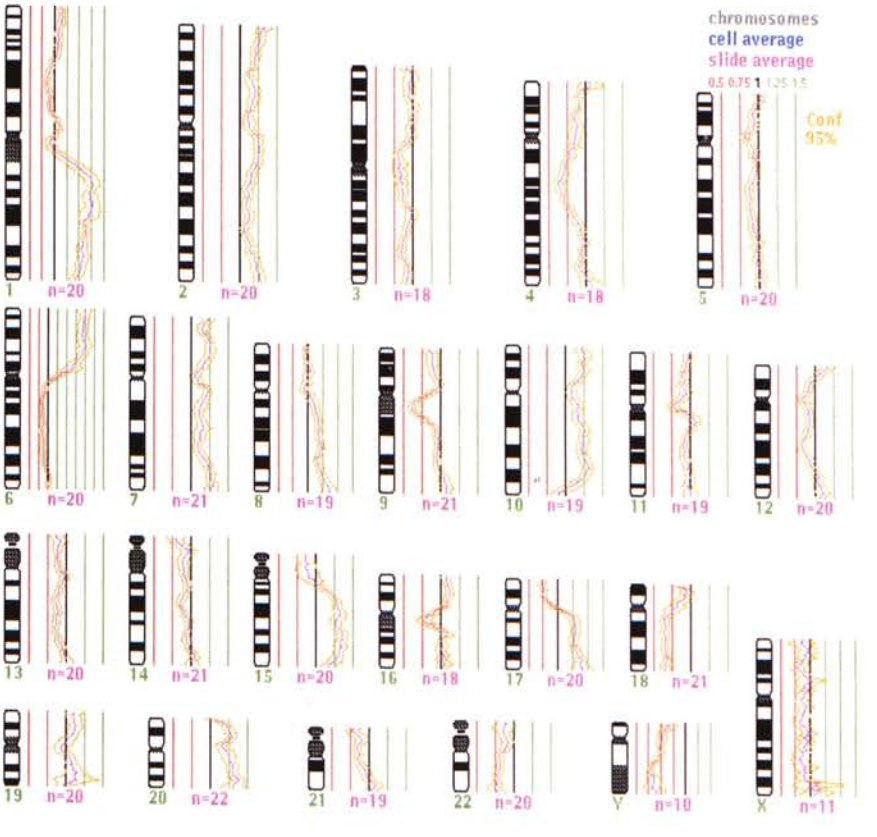
chromosomes
cell average
slide average
0.5 0.75 1 1.25 1.5
Conf 95%
1 n=20
2 n=20
3 n=18
4 n=18
5 n=20
6 n=20
7 n=21
8 n=19
9 n=21
10 n=19
11 n=19
12 n=20
13 n=20
14 n=21
15 n=20
16 n=18
17 n=20
18 n=21
19 n=20
20 n=22
21 n=19
22 n=20
Y n=10
X n=11

2.2.2 Methods

2.2.2.1 Preparation of Normal Metaphase

Normal metaphase slides were prepared from phytohaematoglutinine-stimulated peripheral blood lymphocyte cultures from a healthy male. The lymphocytes were cultivated in RPMI 1640 medium containing 20% fetal calf serum, 3.5U/ml penicillin and 3.5μg/ml streptomycin at 37°C for 72 hours. The cells were then arrested at metaphase by adding 100μl of 25μg/ml colchicine. After another hour of incubation at 37°C, cells were spun down. The collected cells were treated with hypotonic KCl (75m*M*) and fixed in methanol/acetic acid until a white pellet was obtained. Finally, the cells were spread onto clean glass slides. After aging at room temperature for one week, the slides were treated with 100μg/ml RNase at 37°C, washed three times with 2XSSC and passed sequentially through 70%, 80% and 100% ethanol series. The air-dried slides were then stored at -20°C.

2.2.2.2 Extraction of High Molecular Weight DNA

Frozen tumour blocks were sectioned in cryostat (Leica). Fixed on the cryostat plate, a 5μm section was first taken and mounted onto a glass slide. Twenty to 30 consecutive sections of 10μm were then collected in an eppendorf tube, and washed twice with autoclaved double distilled water. A final 5μm section was cut and transferred onto the same glass slide with the first 5μm section. This slide was then stained with hematoxylin and eosin (H&E) and the tumour cell content was evaluated by an experienced pathologist. For CGH analysis, only specimens with more than 75% tumour cell content were studied.

High molecular weight DNA was extracted from the sectioned tumour tissues using conventional phenol/chloroform/isoamyl alcohol method (Maniatas *et*

al., 1989). Similarly, normal reference DNA was extracted from peripheral blood lymphocytes of healthy individuals.

2.2.2.3 Labeling of DNA by Nick Translation

Tumour and normal DNA was labeled with biotin-16-dUTP and digoxigenin(dig)-11-dUTP by nick translation respectively. The nick translation was carried out in a reaction mixture containing nick translation buffer, DNA polymerase, 0.5mM each of dATP, dCTP, dGTP and hapten-conjugated dUTP and DNase I at 15°C for 1 hour 45 minutes. To evaluate the DNA fragment length obtained, the nick translated products were run on a 1% agarose gel in 1xTAE buffer. Fragment size of 200 to 1500 base pairs was desirable for CGH study (Fig. 2.3). The nick translation reaction was stopped with EDTA followed by passing through nick spin column to remove unincorporated haptens and deoxyribonucleotides.

2.2.2.4 Labeling Efficiency

Dot blot analysis was carried out to assess the labeling efficiency of the nick translated product. The purified hapten-labeled DNA was diluted to 10pg/μl with 1xTE buffer and dotted onto a piece of Hybond N+ nylon transfer membrane, on which three standards, 10pg/μl, 7.5pg/μl and 5pg/μl of labeled control DNA, were also placed. The membrane was then dried at 37°C for 1 hour to fix the DNA onto the membrane. After rehydration in maleic acid buffer, the membrane was incubated with blocking reagent. Alkaline phosphatase (AP) conjugated antibodies against the hapten (anti-biotin-AP Fab fragments or anti-dig-AP conjugate) was then applied onto the membrane for 30 minutes at room temperature. Finally, signal was developed by incubating the membrane with a colour substrate solution of

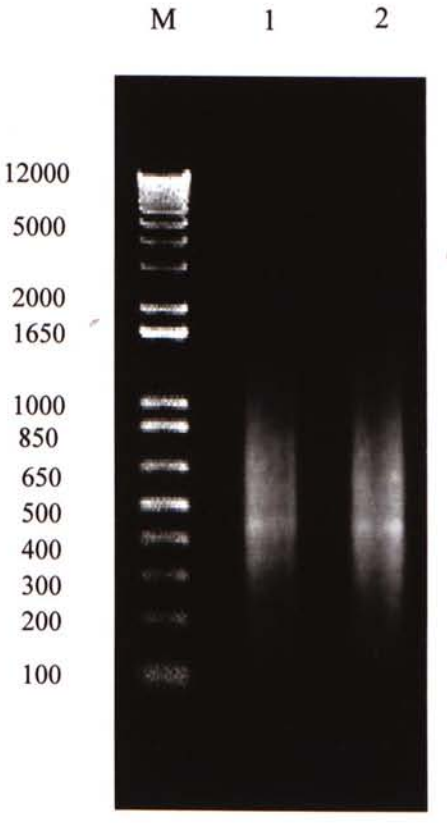

Fig 2.3 Labeling of DNA by Nick Translation. Normal and Tumour DNA were cut to fragment size of 200 to 1500bp. Lane M: 1Kb Plus DNA Ladder. Lane 1: Normal reference DNA. Lane 2: Tumour DNA.

NBT/BCIP in the dark. Dot intensities of both test and control DNA were determined by a densitometer. The labeling efficiency of test DNA can then be determined from the standard curve derived from the control DNA (Fig. 2.4)

2.2.2.5 Preparation of Probe

Five hundred nanograms each of biotinylated test DNA and digoxigenin-labeled normal reference DNA were ethanol precipitated with 70-fold human Cot-1 DNA. The human Cot-1 DNA consists of purified repetitive sequences that will block the highly polymorphic repeat sequences like the centromeric and heterochromatic regions. Ethanol precipitated DNA was dried in vacuum until a transparent pellet was obtained. The probe mixture was finally redissolved in 12μl of hybrisol VII, which contains 50% formamide, 2xSSC and 10% dextran sulphate (pH 7.0).

2.2.2.6 Hybridization

Normal metaphases prepared from section 2.2.1 were treated with 300μg/ml pepsin in 0.01M HCl (pH 2.0) for 4 minutes at 37°C. The metaphase chromosomes were then denatured in 70% formamide/2xSSC (pH 7.0) at 72°C for 2 minutes. The metaphase slide was then dehydrated through a cold ethanol series of 70%, 80% and 100% ethanol. The probe was denatured at 75°C for 5 minutes, left on ice for 5 minutes and allowed to pre-anneal at 37°C for at least 30 minutes. The probe mixture was then spun hard and added to the denatured metaphase chromosomes. The slide was covered by a glass coverslip, sealed in rubber cement and allowed for hybridization at 37°C for 2 to 3 days in a moist chamber.

A

B

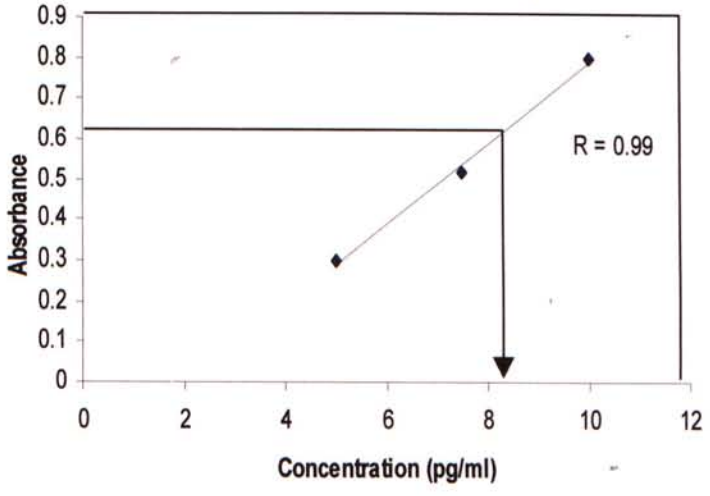

Figure 2.4. Estimation of the labeling efficiency by dot blot analysis. (A) One microliter of control DNA at a concentration of 10pg/μl, 7.5pg/μland 5pg/μl, and the test sample at 10pg/μl were spotted on, fixed to and detected with colourimetric substrate.

(B) The labeling efficiency of test sample DNA was determined from the standard curve derived from the absorbance of the control DNA. Labeling efficiency = Actual Value/Expected Value x 100%. In this case, the value read off the standard curve is 8.5. Therefore, the labeling efficiency is 8.5/10 x 100% = 85%.

2.2.2.7 Washing and Detection of Signals

Post-hybridization washes were carried out in two changes of 50% formamide/2xSSC (pH 7.0) and 2xSSC (pH 7.0) at 40°C for 5 minutes each. This is followed by blocking with 3% Marvel/4xSSC/0.1% Tween-20 for 30 minutes at 37°C. Fluorescent signals were developed immunocytochemically by the following sequence of antibodies (i) Monoclonal mouse anti-digoxigenin and FITC-avidin DCS (ii) Rabbit anti-mouse TRITC (iii) Mouse biotinylated anti-avidin D (iv) Goat anti-rabbit TRITC and FITC-avidin DCS. All antibodies were diluted 1:100 in 1% Marvel/4xSSC/0.1% Tween. Each antibody layer was allowed to incubate for 30 minutes at 37°C. Finally, the slide was counterstained with 0.4μg/ml 4,6-diamino-2-phenylindole (DAPI) in an antifade solution.

2.2.2.8 Image Acquisition and Analysis

A CCD camera mounted on a Leitz DM RB (Leica, Wetzlar, Germany) fluorescence microscope was used for image acquisition. Three consecutive fluorescent images of each metaphase were captured with a three-band-pass filter (DAPI, FITC and TRITC) in an automated filter wheel. Images acquired were analysed by the CGH version 3.1 on an imaging analyser software Cytovision (Applied Imaging, Sunderland, UK). Karyotype analysis was based on the reverse DAPI images generated. Since the absolute fluorescence intensity of fluorochromes in CGH is affected by illumination brightness, exposure time, bleaching, hybridization efficiency and metaphase quality, a normalization procedure was employed to equalize the median intensities of the test and reference images in all metaphases. The fluorescent intensity profile of each chromosome was calculated by a summation of the green and red fluorescence pixel values along the sequence of

lines perpendicular to and spaced at unit distance along the medial axis. An average ratio profile for each chromosome was calculated based on the analysis of 8 to 12 metaphases. Thresholds for gains and losses were defined as the theoretical value of 1.25 and 0.75 respectively. These values were established on the basis of an expected figure of trisomy (1.25) in a diploid tumour cell population or monosomy (0.75) of a certain chromosome in 50% of the test cells. High-level gain of a chromosomal arm or amplification of a chromosomal region was present when the ratio exceeded 1.5. Regions of amplified DNA with a green-to-red fluorescent ratio over 1.5 are known as amplicons. Chromosomal regions rich in heterochromatin (centromeres of chromosomes 1, 9 and 16, p-arm of acrocentromeric chromosomes and Yq12) were excluded in CGH analysis as excess Cot-1 DNA present suppressed hybridization to these regions (Kallioniemi *et al.*, 1994).

2.2.2.9 Control Experiments

DNA from normal individuals was used as the negative control where two differentially labeled normal DNA was hybridized against each other. DNA from the hepatoblastoma cell line HepG2 was used as the positive control. In negative control experiments, no aberrations were detected besides the occasional 1p32-pter, 16p, 19 and 22 deviation from baseline and hence these regions were analysed with caution in tumour samples (Fig. 2.5A). In positive control experiments, CGH was able to show gains in chromosome 2, 6pter-q14, 6q22-qter, 7, 16q21-qter, 17q and 20 in DNA from the hepatoblastoma cell line HepG2 (Fig. 2.5B). These aberrations agreed with the reported karyotype of HepG2 (Simon *et al.*, 1982) and were consistent in all CGH experiments.

Figure 2.5. Control Experiments. (A) In negative controls, biotin and digoxigenin-labeled DNA from normal individuals were hybridized against each other. No aberrations were detected. (B) CGH profile of the hepatoblastoma cell line HepG2. Gains in chromosome 2, 6pter-q14, 6q22-qter, 16q21-qter, 17q and 20 were consistently found in all CGH experiments.

A

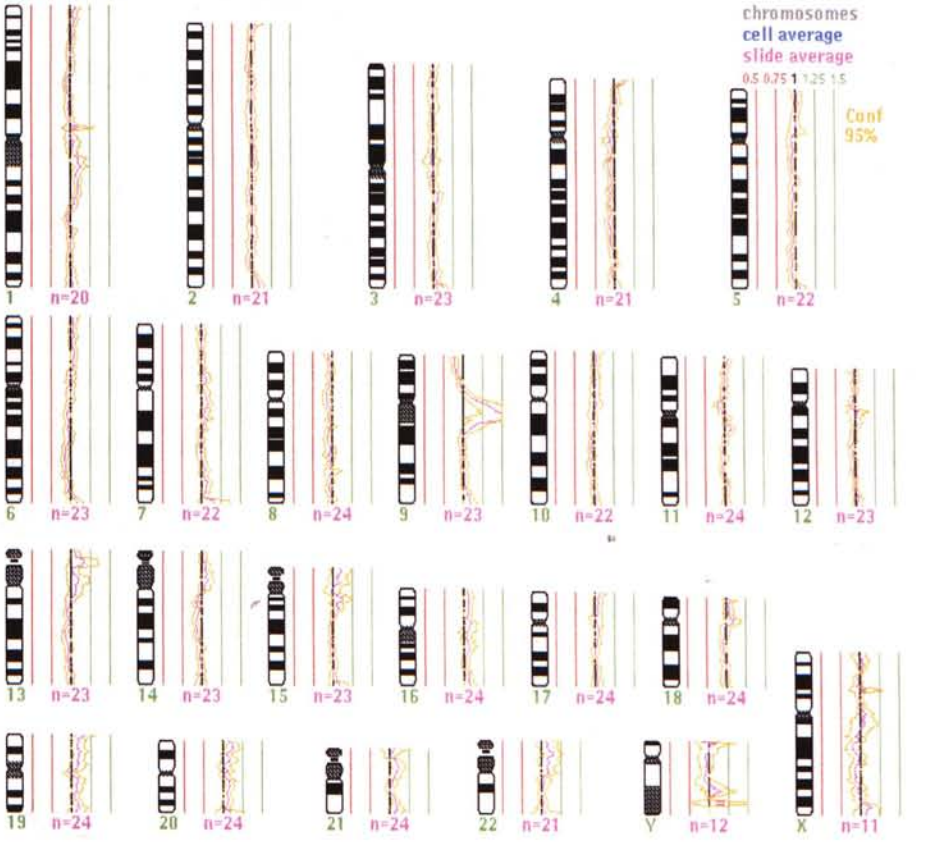
chromosomes
cell average
slide average
0.5 0.75 1 1.25 1.5
Conf 95%
1 n=20
2 n=21
3 n=23
4 n=21
5 n=22
6 n=23
7 n=22
8 n=24
9 n=23
10 n=22
11 n=24
12 n=23
13 n=23
14 n=23
15 n=23
16 n=24
17 n=24
18 n=24
19 n=24
20 n=24
21 n=24
22 n=21
Y n=12
X n=11

B

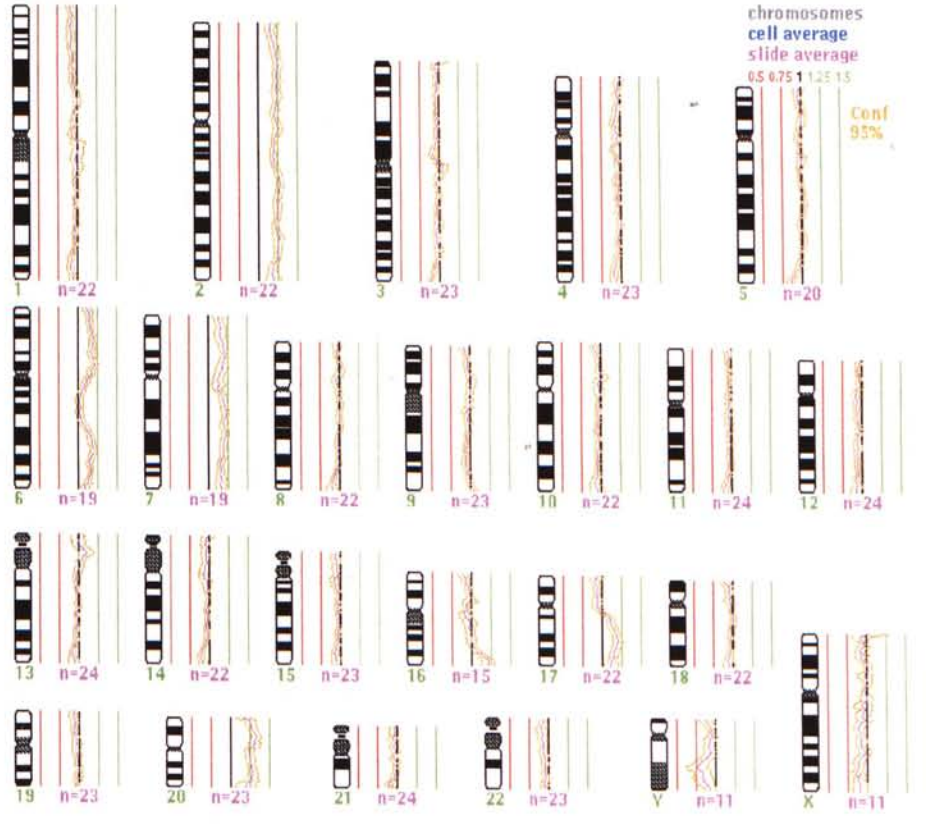
chromosomes
cell average
slide average
0.5 0.75 1 1.25 1.5
Conf 95%
1 n=22
2 n=22
3 n=23
4 n=23
5 n=20
6 n=19
7 n=19
8 n=22
9 n=23
10 n=22
11 n=24
12 n=24
13 n=24
14 n=22
15 n=23
16 n=15
17 n=22
18 n=22
19 n=23
20 n=23
21 n=24
22 n=23
Y n=11
X n=11

2.3 Positional Mapping of Novel Amplicon by Interphase Cytogenetics

2.3.1 Fluorescence *in situ* Hybridization

The ability of single-stranded complementary nucleic acids to hybridize, or renature forms the basic principle of molecular genetic techniques. DNA strands that are not highly complementary will not hybridize or interfere with the hybridization of complementary sequences.

The concept of DNA-DNA hybridization is not limited to extracted DNA, but is also applicable to DNA localised in cytological structures. In 1969, Gall and Pardue first demonstrated the hybridization of isotopically labeled RNA probes in morphologically preserved chromosomes and cells, which were visualized as silver grains under a normal microscope (Gall and Pardue, 1969). The application of this technique in cytogenetics and the replacement of radioactive isotopes with fluorochromes led to the development of *fluorescence in situ hybridization* (FISH) (Pinkel *et al.*, 1986). When FISH is applied on non-dividing cells, it is termed *interphase cytogenetics*. Unlike conventional cytogenetics, interphase cytogenetics does not require tissue culturing and allows direct correlation of genetic aberration with cell morphology.

FISH can be divided into four steps: denaturation, hybridization, post-hybridization wash and detection (Cowan, 1994) (Fig. 2.6). The hapten-labeled probe and target is first denatured to give single-stranded DNA. This is often accomplished through the use of heat and formamide (*denaturation*). After adding the probe to the chromosome preparation (*in situ*), the probe and target chromosome is incubated together to allow annealing of complementary sequences (*hybridization*). Thereafter, excess and non-specifically bound probe is removed from the slide through washing (*post-hybridization washing*). Fluorescent signals are

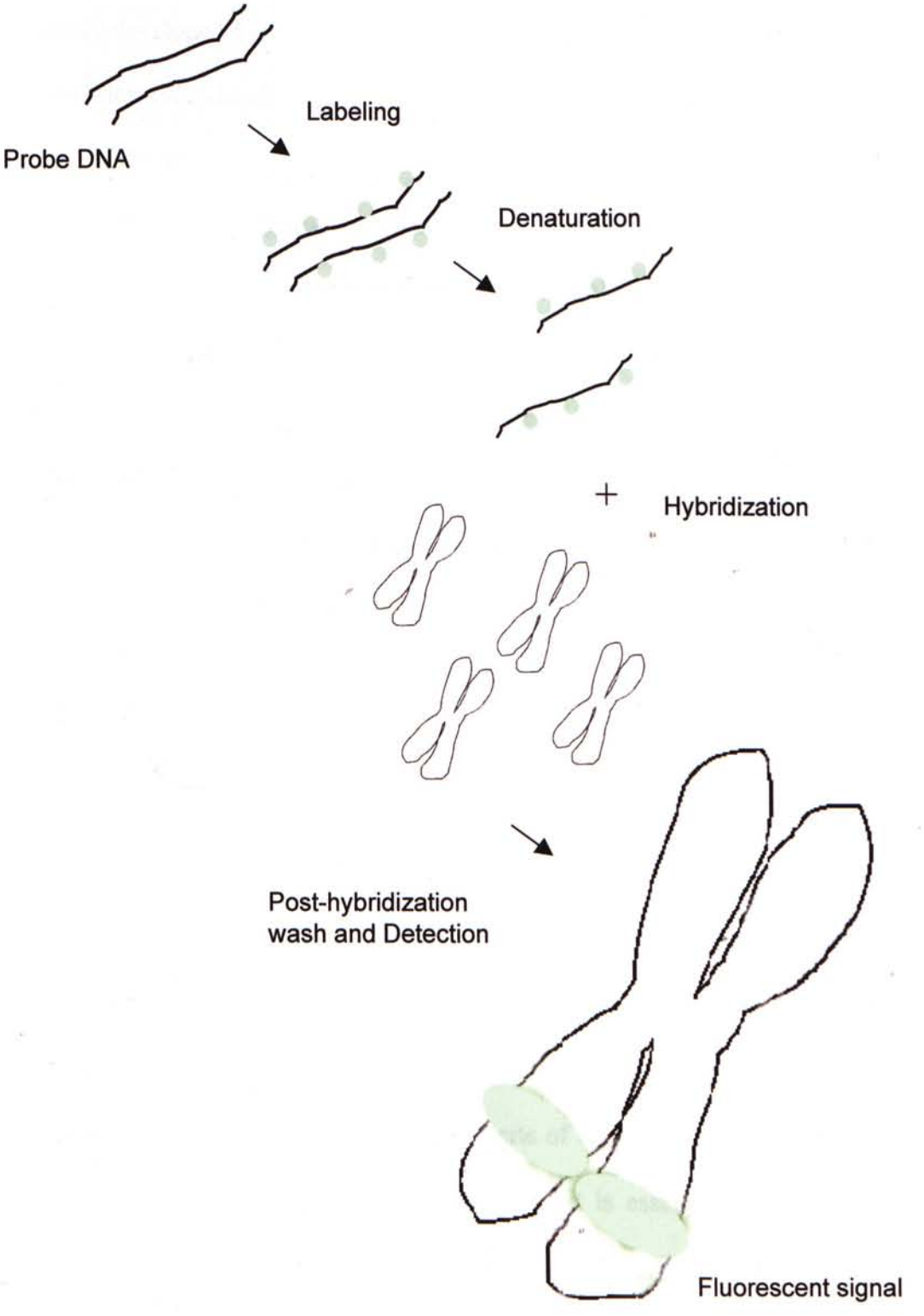

Figure 2.6 Principle of Fluorescence *in situ* Hybridization.
The probe DNA is first labeled with direct fluorochromes or haptens such as biotin and digoxigenin. After denaturation into single-stranded DNA, the probe and target chromosome are incubated together to allow annealing of complementary sequences. Finally, fluorescent signals can be seen under the fluorescence microscope.

finally developed by incubating the hybridized probe with fluorochrome-conjugated antibodies (*detection*).

The successful use of FISH is dependent on the availability of probes. There are in general three types of probes: (a) whole chromosome painting probes. They are useful to study chromosome translocations (b) repetitive DNA probes. They contain peri-centromeric, telomeric, sub-telomeric, classical satellite, beta satellite or *Alu* DNA sequences. The peri-centromeric probes are especially useful in enumerating chromosome copy number in interphase nuclei. (c) single-copy probes. They are used to study the deletion or amplification of a particular locus in the genome. Rapid progress in the human genome project has provided a wealth of FISH probes that are cloned in cosmids, P1, BACs or yeast artificial chromosomes (YAC) vectors (Luke *et al.*, 1997).

2.3.2 Using Yeast Artificial Chromosomes (YAC) as Probe

Characterisation of amplified sequences identified by CGH requires consecutive fragments of unique human DNA sequences. These are best sought from the various DNA cloning systems (Table 2.1) and their respective "genomic libraries", which contain human DNA inserts of size from a few kilobases to more than a megabase. In interphase cytogenetics, it is essential to obtain hybridized signals that are large enough to be scored by the naked eye. Yeast artificial chromosome (Burke *et al.* 1987) therefore represents the most appropriate source of cloned DNA fragments, since it can give a wide coverage of the region in question.

Table 2.1. DNA insert size of different cloning vectors

Vector	Host	Insert size
λ phage	*E. coli*	5-25 kb
λ cosmids	*E. coli*	35-45 kb
P1 phage	*E. coli*	70-100 kb
PACs	*E. coli*	100-300 kb
BACs	*E. coli*	≤ 300 kb
YACs	*S. cerevisiae*	200-2000 kb

In contrast to bacterial cloning systems, where clones are selected by dominant antibiotic resistance, YAC selection is based mainly on nutritional complementation of biosynthetic mutations. These mutations result in a growth requirement in the yeast strain that can be satisfied by the addition of a nutritional supplement to the media. The host strain used in this experiment, *S cerevisiae* AB1380 carries biosynthetic *ura3* and *trp1* mutant alleles so that it is auxotrophic for uracil and tryptophan. YAC selection is therefore maintained by the functional *URA3* and *TRP1* genes on pYAC4, and a lack of uracil and tryptophan in the growth medium (Fig. 2.7).

In addition to the auxotrophic mutations, *S cerevisiae* AB1380 carries an *ade2-1* ochre mutation and an interruptible marker, *SUP4-o* gene. An *ade2-1* ochre mutation blocks the purine biosynthetic pathway and leads to an accumulation of red-hued intermediates in adenine-deficient media. Yeast cells without a human insert remain white because the *SUP4-o* gene suppresses the formation of the red pigment. However, insertion of genomic DNA in the YAC interrupts the *SUP4-o* gene in the YAC vector. Therefore, colonies will have a red pigmentation. This colour marker allows visual identification of yeast colonies retaining the human insert (Fig. 2.8).

Figure 2.7. A Yeast Artificial Chromosome (YAC) Cloning System. A plasmid containing inverted repeats of telomeric (TEL) sequences, a centromere sequence (CEN), and selectable markers (*TRP1* and *URA3*), provides the two vector arms after cleavage with restriction enzymes at the *Eco*R1 site in the SUP4 gene and at the *Bam*H1 sites. The vector arms are dephosphorylated and ligated to large DNA fragments from a target DNA (e.g., human). The recombinant molecules are introduced into yeast, where they are maintained as extra chromosomes.
The *TRP1* and *URA3* genes are wild-type alleles of the genes mutated in the host *S. cerevisiae* AB1380. They are on opposite sides of the *Eco*R1 cloning site. The growth medium, AHC medium is deficient in uracil and trytophan, and therefore selects for both arms of the YAC vector. This favours high stability of the YAC through successive passages. (Adapted from Burke *et al.*, 1987)

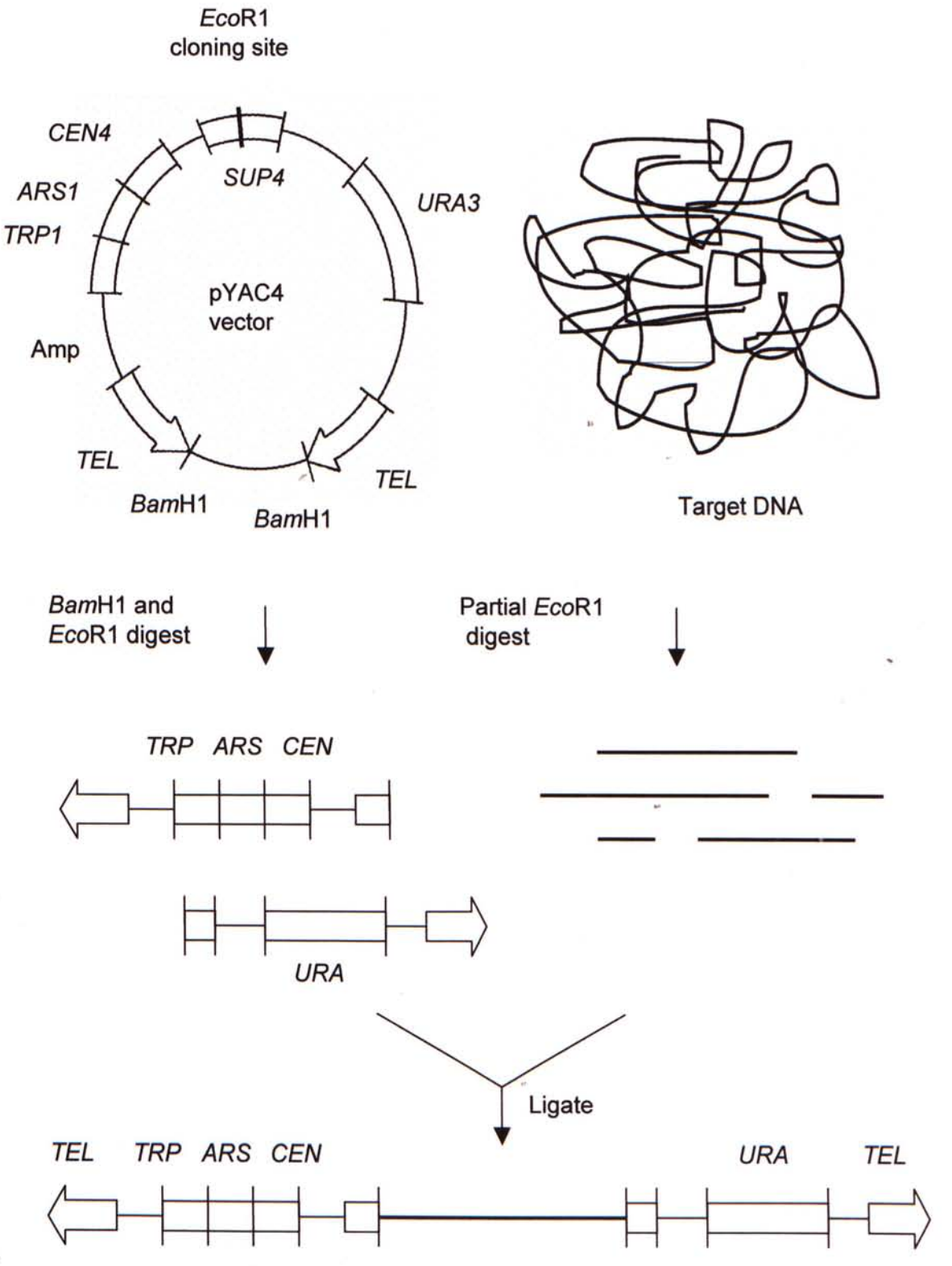
EcoR1
cloning site
CEN4
ARS1
TRP1
SUP4
URA3
pYAC4
vector
Amp
TEL
TEL
BamH1
BamH1
Target DNA
BamH1 and
EcoR1 digest
Partial EcoR1
digest
TRP ARS CEN
URA
Ligate
TEL TRP ARS CEN
URA
TEL

Figure 2.8. Red Colonies of YAC. *S. cerevisiae* AB1380 carries an *ade2-1* ochre mutation and an interruptible marker, *SUP4-o* gene. A red pigmentation will be produced when the yeasts are grown in adenine-deficient media. This allows the selection of yeast colonies retaining the human insert.

Although YAC has the highest capacity for DNA inserts, there are three major problems associated with its use.

I. Most existing total genomic YAC libraries contain 5 to 50% of chimeric clones that contains DNA sequences from two or more separate genomic regions. Chimaeras may arise by co-ligation of DNA inserts *in vitro* prior to yeast transformation, or by recombination between two DNA molecules that were introduced into the same yeast cell (Larionov *et al.*, 1994).

II. Many YAC clones are unstable and tend to delete internal regions from their inserts. These deletions varied from 20 to 260kb and can be generated both during the transformation process and during mitotic growth of transformants (Kouprina *et al.*, 1994).

III. Unlike plasmid vectors in bacteria, the structure of YAC is very similar to natural yeast chromosomes. Therefore, the 15Mb yeast host chromosome background cannot be separated from the YACs by simple methods (Chu *et al.*, 1986).

In this thesis, these limitations have been resolved by

I. Performing metaphase FISH for each YAC being used in the experiment. Those YAC that show secondary site of hybridization are indicative of chimerism and are not selected as FISH probes.

II. Performing FISH analysis on interphase nuclei. A small deletion in YAC will not interfere with visual scoring of signals under the microscope.

III. Using inter-*Alu*-PCR to selectively amplify human sequences among a yeast DNA background.

2.3.3 Methods

2.3.3.1 Culture of Yeast Artificial Chromosomes

Glycerol stock of YAC-containing yeast was revived by streaking on AHC plate. The plate was incubated at 30°C for 4 days or until single red colonies were seen. A red colony was picked with an autoclaved toothpick and inoculated into 2ml YPD broth. Shaken at 220rpm, culture was left overnight at 30°C in a shaking incubator. The next day, 800µl of the overnight culture was inoculated into another 5ml of fresh YPD. Growth was maintained at 30°C with shaking at 220rpm, until an OD_{600} of a 10-fold dilution reads 0.31 to 0.37. This absorbance corresponds to a cell density of $1x10^8$ cells/ml.

2.3.3.2 Extraction of Total YAC DNA

Yeast cells were spun down by centrifugation at 500g for 3 minutes. The supernatant was aspirated, and the pellet was washed with autoclaved double distilled water and SCE buffer. The pellet was then resuspended in 3mL of SCE buffer and 7µl of β-mercaptoethanol was added. To disrupt the yeast cell wall, yeast suspension was incubated with 50U/ml lyticase at 37°C for an hour in a shaking water bath. Total yeast DNA was subsequently extracted according to instructions of QIAamp tissue kit. In brief, the spheroplasts (yeast cells with cell wall removed) were first lysed in 180µl of tissue lysis buffer provided by the kit. After treating with proteinase K at 55°C for an hour and RNase at room temperature for 2 minutes, the yeast lysate solution was incubated with 200µl buffer AL at 70°C for 10 minutes. The solution was then mixed thoroughly with 210µl of absolute ethanol and passed through a spin column. After washing with washing buffer, total yeast DNA was finally eluted with the elution buffer.

2.3.3.3 Verification of YAC Clones for Chimerism by FISH

Each YAC clone studied in the present thesis was verified for chimerism and chromosomal location before use. One microgram of total yeast DNA containing YAC DNA was labeled with digoxigenin according to methods described in section 2.2.3. The labeled total yeast DNA was ethanol precipitated with 70-fold excess of human Cot-1 DNA and resuspended in 5µl hybrisol VII. FISH was performed on normal metaphase chromosomes. The chromosomal location of YAC was confirmed by visual inspection. The presence of second site of hybridization was considered as chimerism.

2.3.3.4 Inter-*Alu*-PCR

When total yeast DNA was used as probe and applied onto paraffin sections, a high background-to-signal ratio was found (Fig. 2.9). This may be attributed to the interference from host yeast DNA. It is known that yeast ribosomal sequences can anneal to the short arms of the human acrocentric chromosomes (Leversha, 1997). To minimize cross hybridization from host yeast DNA, we employed inter-*Alu*-PCR to selectively amplify the human sequences in the YAC from total yeast DNA.

Mammalian genomes contain short interspersed repeated sequences (SINES) (Singer, 1982). In human, the major SINES is the *Alu* DNA sequence family. These repeats are found ubiquitously in primates, though similar repeats are also found in rodents (Schmid and Jelinek, 1982). *Alu* repeats are widely distributed in the human genome, giving an average spacing between individual copies of 4 kilobases (Nelson *et al.*, 1989). Although individual *Alu* sequence contains "variable" regions, a 25-bp region between nucleotide position 23 and 47, and a 16-bp region between nucleotide position 245 and 260 are well conserved among different members in the family

(Kariya *et al.*, 1987). PCR with primers annealing to these conserved regions therefore selectively amplify the DNA regions between *Alu* segments and enrich human DNA sequences against a yeast background (Fig. 2.10).

In this thesis, 5ng of total yeast genomic DNA with human DNA insert was amplified in 50μl of PCR amplification buffer. Primer sequences ALE1 (GCCTCCCAAAGTGCTGGGATTACAG) and ALE3 (CCACTGCACTCCAGCC-TGGG), modified from Cole *et al.* (1991), were used at a final concentration of 0.2μM. The PCR reaction was conducted in a programmable thermal cycler (MJ Research Inc). After an initial denaturation at 94°C for 5 minutes, samples were subjected to 30 cycles of denaturation at 96°C for 1 minute, annealing at 55°C for 1 minute, elongation at 72°C for 5 minutes and a final incubation at 72°C for 10 minutes. Primers and free nucleotides were removed by passing through a PCR product purification column (High Pure PCR Product Purification kit). The purified PCR products were then quantitated using GeneQuant (Pharmacia). Two hundred nanograms of PCR products were run on a 1% agarose gel to check the result of the PCR reaction (Fig. 2.11). The inter-Alu PCR products were then labeled with biotin or digoxigenin by nick translation as described in section 2.2.3 to an optimum fragment size of 200 to 500 base pairs (Fig. 2.12). The labeled inter-Alu PCR products were then ethanol precipitated with excess of human Cot-1 DNA and resuspended in Hybrisol VII to a final concentration of 60ng/μl.

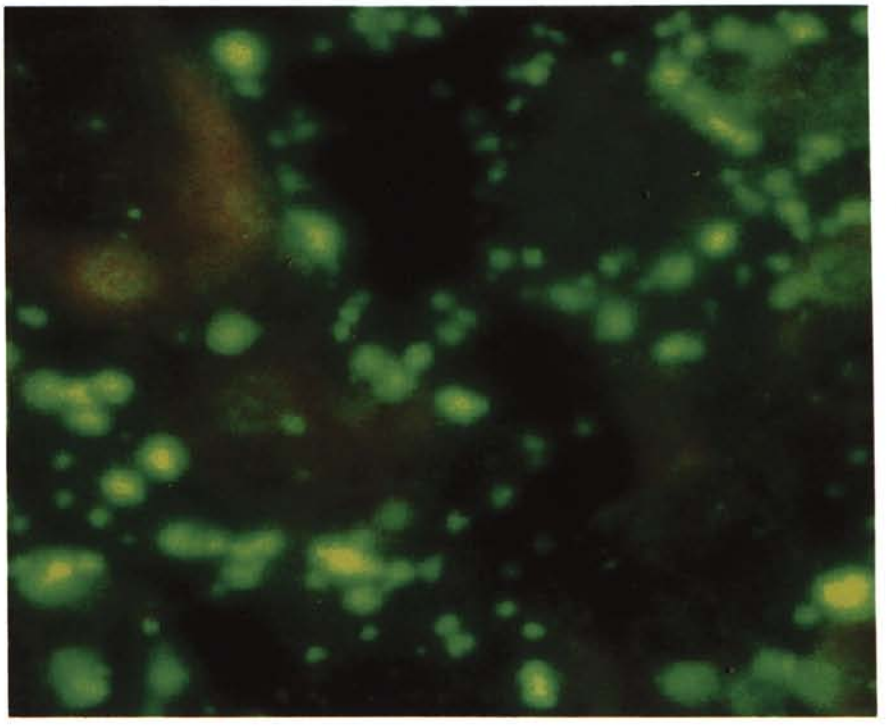

Figure 2.9. High background-to-signal Ratio in FISH Experiment. High background-to-signal ratio was found when total yeast DNA was used as probe and applied onto formalin-fixed paraffin-embedded tissue sections.

Figure 2.10 Schematic of *Alu*-PCR Experiment. *Alu*-PCR is used to isolate human-specific DNA sequences among a yeast DNA background. (A) Consensus *Alu* sequence and locations of primers for amplification. Conserved regions are shown in bold. PCR primers are shown as lines with arrowheads to indicate 5' to 3' orientation relative to the *Alu* sequence. (B) Figure shows a stretch of DNA, that contains 5 *Alu* sequences, separating four sections of DNA (1-4). The orientation of these *Alu* sequences is shown by the arrowheads. The combined use of Ale-1 and Ale-3 will selectively amplify DNA sequences between the *Alu* sequences. PCR amplification for primer Ale-3 and section 2 of the DNA is shown in detail.

A

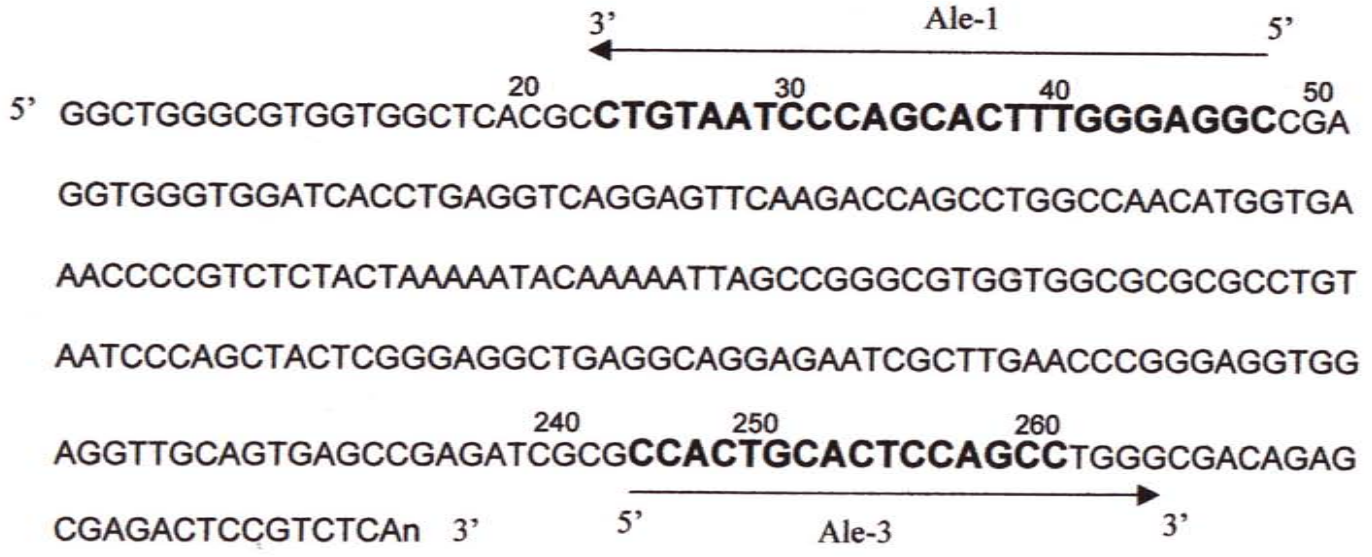

Ale-1: 5'GCCTCCCAAAGTGCTGGGATTACAG3'

Ale-3: 5'CCACTGCACTCCAGCCTGGG3'

B

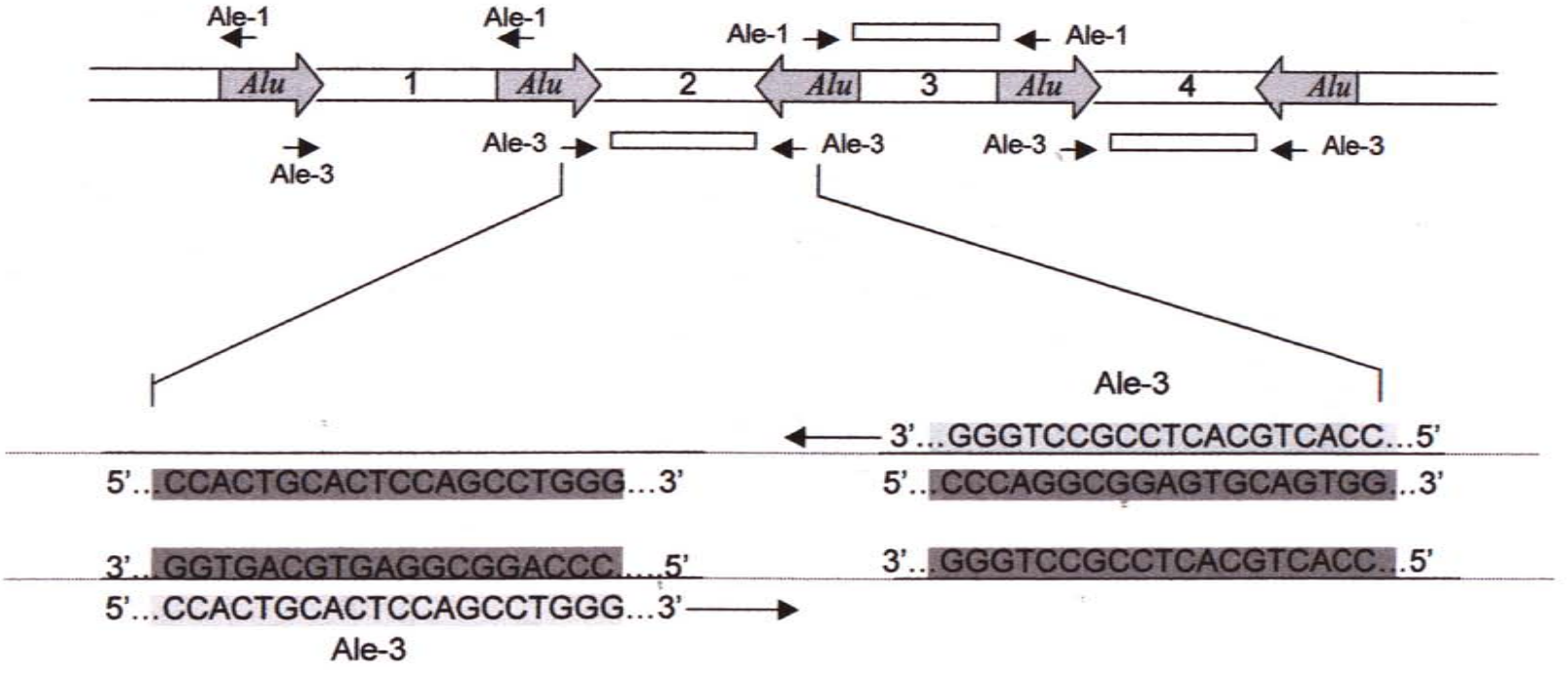
Ale-1
Ale-1
Ale-1
Ale-1
Alu
1
Alu
2
Alu
3
Alu
4
Alu
Ale-3
Ale-3
Ale-3
Ale-3
Ale-3
Ale-3
3'...GGGTCCGCCTCACGTCACC...5'
5'..CCACTGCACTCCAGCCTGGG...3'
5'..CCCAGGCGGAGTGCAGTGG..3'
3'..GGTGACGTGAGGCGGACCC....5'
3'..GGGTCCGCCTCACGTCACC..5'
5'...CCACTGCACTCCAGCCTGGG...3'
Ale-3

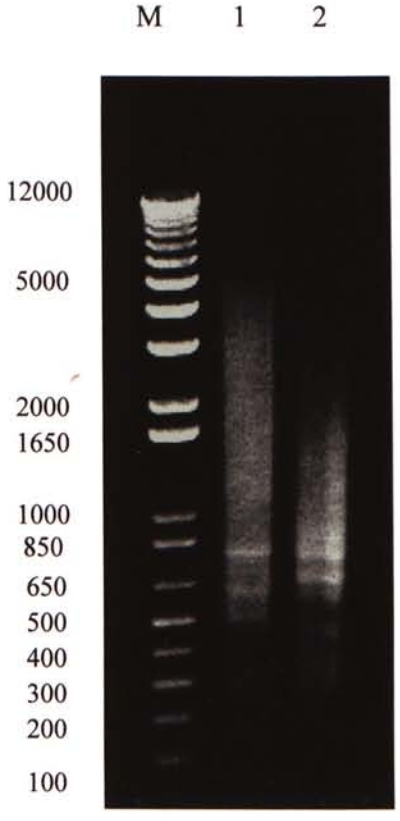

Figure 2.11. Amplification of Human DNA from Yeast Artificial Chromosomes by Using *Alu* primers, Ale-1 and Ale-3. Lane M: 1 Kb Plus DNA Ladder. Lane 1: amplification result from total yeast DNA of 955e11. Lane 2: amplification result from total yeast DNA of 910c8.

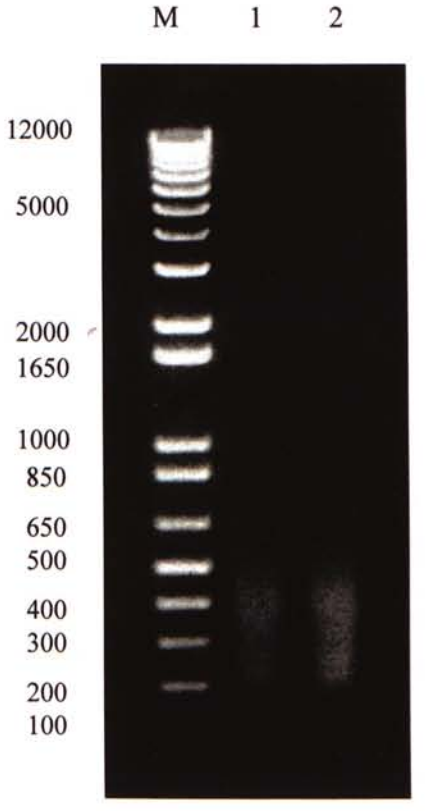

Figure 2.12. Nick Translation of Inter-*Alu* PCR Products. The inter-Alu PCR products were labeled with biotin or digoxigenin by nick translation to an optimum fragment size of 200 to 500 base pairs. Lane M: 1 Kb Plus DNA Ladder. Lane 1: nick translation result of 955e11. Lane 2: nick translation result of 910c8.

Chapter 3.

Assessment of Genetic Changes in HCC by Comparative Genomic Hybridization (CGH)

3.1 Introduction

In this chapter, CGH was used to study the entire tumour genome for regions of gains and losses in 67 HCC with an aim to identify recurrent genetic changes. A correlation of identified aberrations with clinical stages, tumour size and serum alpha-fetal protein levels was carried out. Twelve non-tumourous cirrhotic liver tissues surrounding the tumours were also analysed by CGH in order to assess whether gross genetic alterations were also involved in the putative premalignant tissue.

3.2 Materials and Methods

3.2.1 Patients and Specimens

Tumourous liver tissues were obtained from 67 ethnic Southern Chinese patients who underwent hepatic resection for curative intent at the Prince of Wales Hospital. All patients were chemotherapy naïve. Twelve cirrhotic tissues from the nontumourous part of the resected specimens were also collected. The clinical information of HCC patients is listed in Table 3.1. There were 54 male and 13 female patients. The median age was 60 with a range of 30 to 97. Eighty-eight percent (59/67) of the patients were positive for hepatitis surface B antigen, which indicated a carrier status of HBV. Eighty-two percent (55/67) of the patients had underlying liver cirrhosis. Serum alpha fetal protein level (AFP) were raised above the diagnostic threshold of 500ng/ml in 28% (19/67) of patients.

The HCC were classified according to the tumour/node/metastasis (TNM) staging criteria (Beahrs *et al.*, 1993). Three cases (5%) were classified as stage I ($T_1N_0M_0$), 53 (79%) as stage II ($T_2N_0M_0$), and 11 (16%) as stage III ($T_3N_0M_0$). The maximal diameter and histological features of the tumours were recorded by

Table 3.1. The clinical background of 67 HCC patients

Sample No.	Age	Sex	TNM Staging	Size (cm)	Cirrhosis	HBsAg	AFP (ng/mL)
HCC 1	41	M	T2	2.2 x 2.8	+	+	< 10
HCC 2	60	M	T2	5 x 4.5	+	+	< 10
HCC 3	39	M	T2	5 x 3.5	+	+	< 10
HCC 4	71	M	T2	5 x 4.2	+	+	76
HCC 5	54	M	T2	11 x 7	-	+	< 10
HCC 6	58	M	T2	3 x 3	+	+	4788
HCC 7	40	F	T2	3 x 2.5	+	+	329
HCC 8	42	M	T2	1.2 x 2	+	+	115
HCC 9	46	F	T2	13 x 8	-	+	124
HCC 10	66	F	T3	15 x 12	+	+	14
HCC 11	66	M	T2	11 x 8	-	-	12
HCC 12	64	M	T2	4.5	+	+	35
HCC 13	70	F	T3	7 x 7.5	+	+	11
HCC 14	75	M	T2	6 x 2.5	-	-	11
HCC 15	67	M	T2	2.5	+	+	439
HCC 16	41	M	T2	5	-	+	40,000
HCC 17	49	M	T2	7.5 x 7	+	+	309
HCC 18	67	M	T2	6 x 4.5	+	+	38
HCC 19	51	M	T2	8.5	+	+	10
HCC 20	30	F	T2	8 x 7	+	+	3680
HCC 21	69	F	T2	8 x 7.5	+	+	3890
HCC 22	65	M	T2	6 x 5	+	+	3267
HCC 23	55	M	T3	5.8 x 5.3	+	+	307
HCC 24	55	M	T2	7 x 5.5	+	+	< 10
HCC 25	51	M	T2	3.5	+	N/A	N/A
HCC 26	61	F	T2	11 x 8	+	+	40
HCC 27	61	M	T2	2.5 x 2	+	-	233
HCC 28	32	M	T2	7.2 x 6.5	+	+	674
HCC 29	51	M	T2	5 x 3.5	+	+	27
HCC 30	53	M	T2	6.5 x 4.5	+	+	5462
HCC 31	67	M	T2	6 x 5	+	+	30
HCC 32	74	F	T2	3.2 x 2	+	-	< 10
HCC 33	71	M	T1	2	+	+	11
HCC 34	67	F	T2	3 x 1	+	+	44
HCC 35	74	F	T2	3.6 x 3	+	+	13
HCC 36	60	M	T2	11 x 7	-	+	1334
HCC 37	41	M	T2	3.5 x 3	-	+	616
HCC 38	39	M	T2	8.5 x 5.5	+	+	27170
HCC 39	68	M	T2	4.8 x 4.5	+	+	25
HCC 40	65	M	T1	1.4 x 1	+	+	2367
HCC 41	71	F	T2	6.5 x 5.4	+	+	10
HCC 42	33	M	T1	2 x 1.5	+	+	1503
HCC 43	97	M	T3	4 x 3	+	+	53
HCC 44	60	M	T2	2.6 x 1.8	+	+	308
HCC 45	32	M	T2	4 x 3.5	+	+	8760
HCC 46	65	M	T3	2.4 x 2	+	+	1601
HCC 47	62	M	T2	3 x 2	-	+	< 10
HCC 48	53	M	T2	4 x 3.6	+	+	26
HCC 49	66	M	T2	8 x 6.5	+	+	40
HCC 50	47	M	T3	7	+	+	189
HCC 51	46	M	T2	6	+	+	12
HCC 52	58	M	T2	12.8	+	+	2320
HCC 53	44	M	T2	3 x 2	+	+	146
HCC 54	68	M	T2	4.7	+	+	687
HCC 55	38	M	T2	3	+	+	878
HCC 56	62	M	T2	5.5 x 4	-	+	< 10
HCC 57	57	M	T3	2.8	+	+	< 10
HCC 58	34	M	T3	5.5 x 4	+	-	13500
HCC 59	63	M	T2	9.5 x 9	-	-	69
HCC 60	76	F	T2	2.8 x 2.8	-	-	661
HCC 61	68	M	T2	4.5	+	+	11
HCC 62	61	M	T3	1.8	+	+	21
HCC 63	57	M	T3	2.4	+	+	< 10
HCC 64	37	M	T3	3.8 x 4	+	+	325
HCC 65	60	M	T2	6.4 x 6.6	+	+	136
HCC 66	51	F	T2	13.5	-	+	231
HCC 67	34	M	T2	3 x 2.6	+	+	43

experienced pathologists at the Department of Anatomical and Cellular Pathology. Twenty specimens fell into the category of small tumours (<3 cm) and 47 into large tumours (>3 cm). Cirrhosis was defined as the presence of complete fibrous septa separating regenerating nodules. Within the non-tumourous liver parenchyma, an increase in fibrous tissue alone was not classified as cirrhosis. All tumour specimens received were first snap-frozen in embedding medium (Tissue-Tek, Elkhart, IN) and stored at -80°C until use. Tumour DNA was extracted as described in section 2.2.2.2.

3.2.2 Comparative Genomic Hybridization

CGH was performed according to procedure described in section 2.2.2. Briefly, biotinylated total tumour DNA and digoxigenin-labeled normal reference DNA was simultaneously hybridized to normal metaphase spreads in the presence of excess unlabeled human Cot-1 DNA. Fluorescent signals were captured with a cooled CCD camera and quantitatively analyzed by a digital image analysis software. The average ratio profiles were calculated based on the analysis of 8 to 10 selected metaphases.

3.2.3 Statistical Analysis

DNA gains or losses were compared between groups by the two-tailed unpaired Student's *t*-test. A difference was significant when the *P* value was less than 0.05. Individual chromosome copy number changes were compared by the nonparametric chi-square test and considered significant when the *P* value was less than 0.05.

3.3 Results

3.3.1 Overall Copy Number Aberrations in 67 HCC and Surrounding Cirrhotic Tissues

Complex pattern of genetic aberrations were identified in 63 HCC cases and no CGH abnormalities were found in the remaining 4 tumours (Fig. 3.1-3.3). The total number of genetic aberrations per sample was 8.5 ± 5.0. The total number of gains and losses per sample was 4.7 ± 2.5 and 3.8 ± 3.2 respectively. A remarkably high incidence of 1q copy number gain was found (72%, 48/67 cases). Other frequent gains included 8q (48%, 32/67 cases), 20q (37%, 25/67 cases), and 17q (28%, 19/67 cases). Copy number losses were commonly identified on 4q (43%, 29/67 cases), 13q (39%, 26/67 cases), 8p (37%, 25/67 cases) and 16q (28%, 19/67 cases). High-level gains involving the long arm of chromosome 1 were observed in 20/67 cases (30%). Of particular interest was a novel amplicon between chromosome 1q21-q25 was identified in 5 HCC cases.

No sequence gains or losses were detected in the twelve surrounding cirrhotic tissues studied.

3.3.2 TNM Staging

The total number of aberrations per tumour in stage T1, T2 and T3 was 9 ± 4.6, 8.5 ± 4.9 and 8.4 ± 6.4 respectively ($P > 0.86$). Average chromosomal gains and losses were compared between the two major stage groups T2 and T3. Mean copy number gains in stage T2 and T3 was 4.7 ± 2.5 and 3.8 ± 3.0 respectively ($P = 0.82$). Mean copy number losses in stage T2 and T3 was 4.9 ± 2.6 and 3.6 ± 4.5 ($P = 0.88$) respectively. There were no significant differences for individual chromosomal

Figure 3.1. Example of Chromosomal Aberrations Detected by CGH. The CGH image of hybridized chromosomes in case H20 is shown with the corresponding fluorescence ratio profile plotted alongside the chromosome ideogram. Green regions in the CGH image represent gains, while red represent losses. The mean ratio profile of 12 analyzed chromosomes or more (pink line) is depicted with the 95% confidence interval (gold lines). Red and green lines represent thresholds for chromosomal losses (0.75) and gains (1.25). A green-to-red fluorescent ratio over 1.5 is defined as high-level copy number gains or amplifications. The CGH profile of this specimen suggests high-level copy gains of 1q21-q22 and 8q, low-level copy gains of 1q, 9q32-qter, 10p, and 16pter-p11.2, and losses of 2q32-qter, 4q28-qter, 7q32-qer, 8p, 10q, 11q, 12p, 13q12-q31, 14q, and 16q. An amplicon on 1q21-q22 and high-level gain of 8q can be readily identified by the intense green signals.

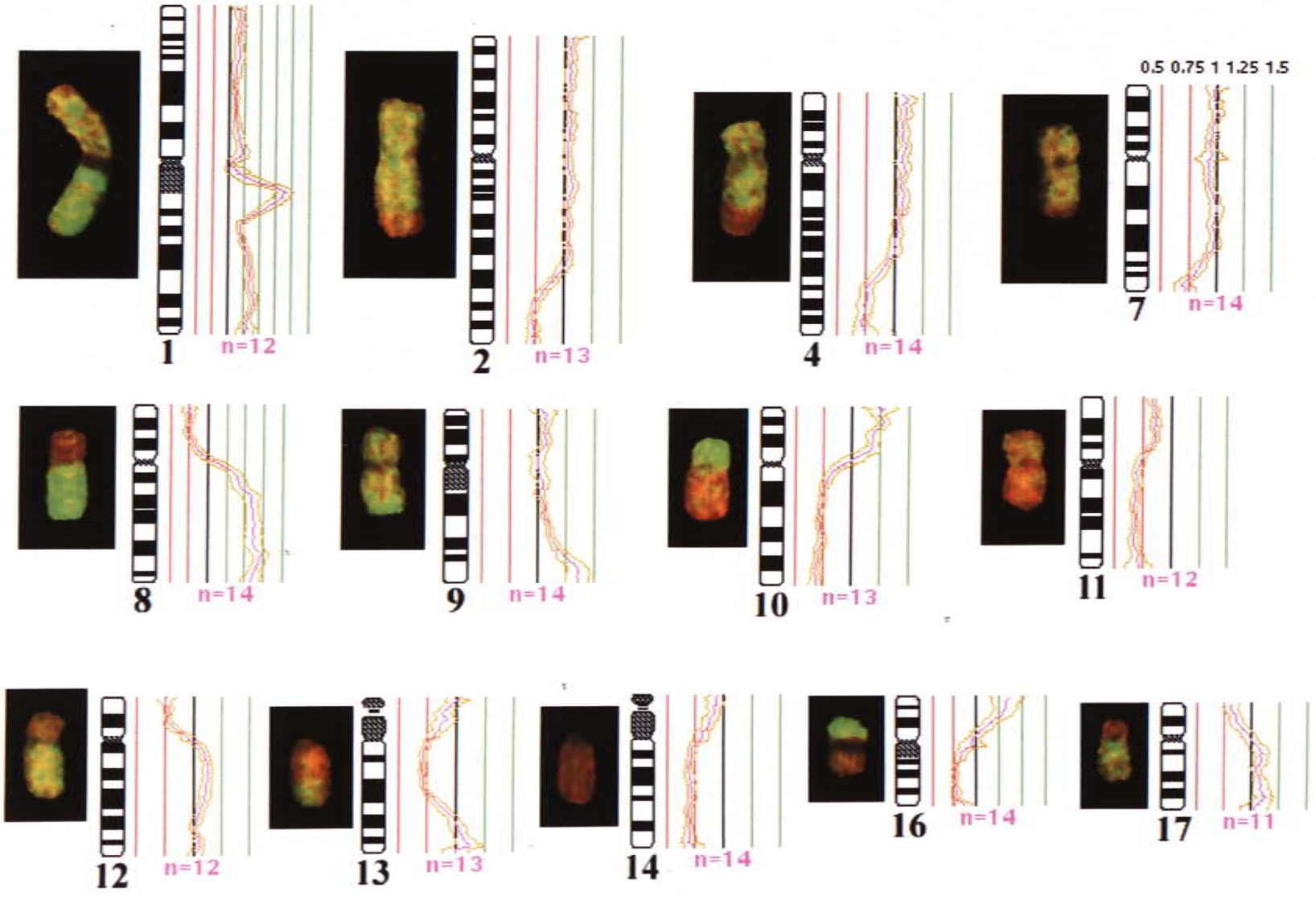
0.5 0.75 1 1.25 1.5
1
n=12
2
n=13
4
n=14
7
n=14
8
n=14
9
n=14
10
n=13
11
n=12
12
n=12
13
n=13
14
n=14
16
n=14
17
n=11

Figure 3.2. Examples of CGH Profiles.

A H37. Losses: 3q25-qter, 5, 9pter-p21, 13q, 15q
Gains: 4pter-q23, 7, 8p, 19q, 20, X, Y
Amplifications: 1q, 8q, 20q13, Xq22-ter

B H45. Losses: 1p, 2q33-qter, 4, 7q32, 8p, 9p, 13q, 16
Gains: 10, 20, Y
Amplifications: 1q, 8q

C H60. Losses: 4q28-qter, 8pter-p11.2, 10pter-q25
Gains: 8q21.3-qter, 20, X
Amplifications: 1q

D H66. Losses: 4, 8pter-p12, 10q22.3-qter, 13q14-qter, 14q
Gains: 7q11.2, 8p11.2-q13, 8q22-qter, 12q24.1-qter, 17q, 19p
Amplifications: 1q21-25, 19q, 20q13

A

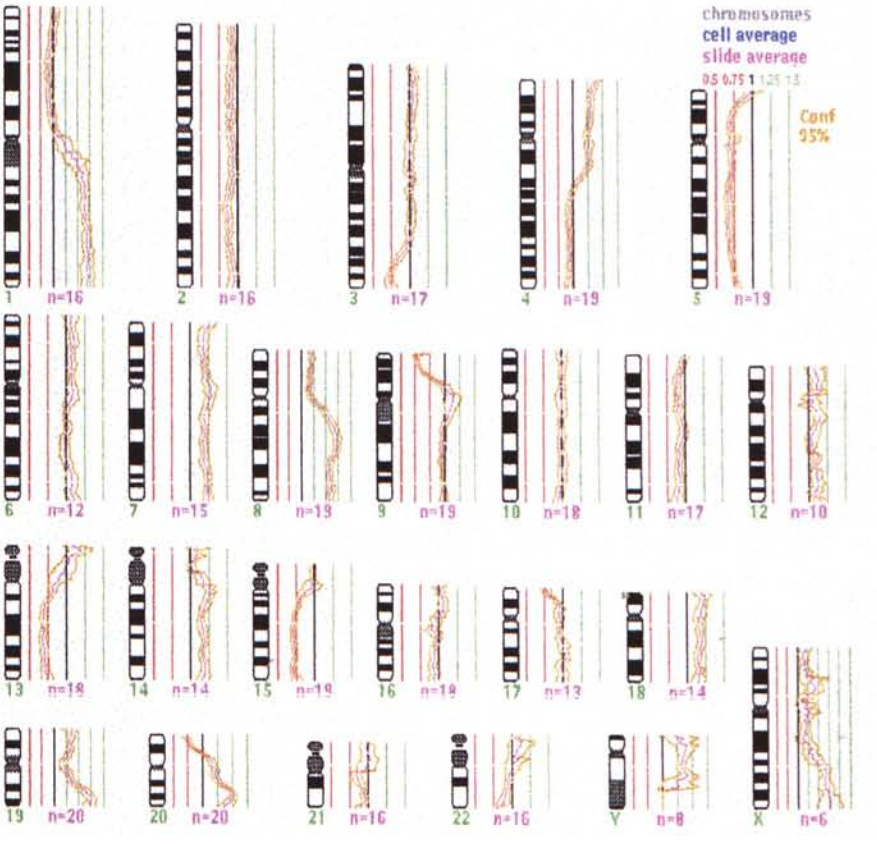
chromosomes
cell average
slide average
0.5 0.75 1 1.25 1.5
Conf 95%
1 n=16
2 n=16
3 n=17
4 n=19
5 n=19
6 n=12
7 n=15
8 n=19
9 n=19
10 n=18
11 n=17
12 n=10
13 n=18
14 n=14
15 n=19
16 n=18
17 n=13
18 n=14
19 n=20
20 n=20
21 n=16
22 n=16
Y n=8
X n=6

B

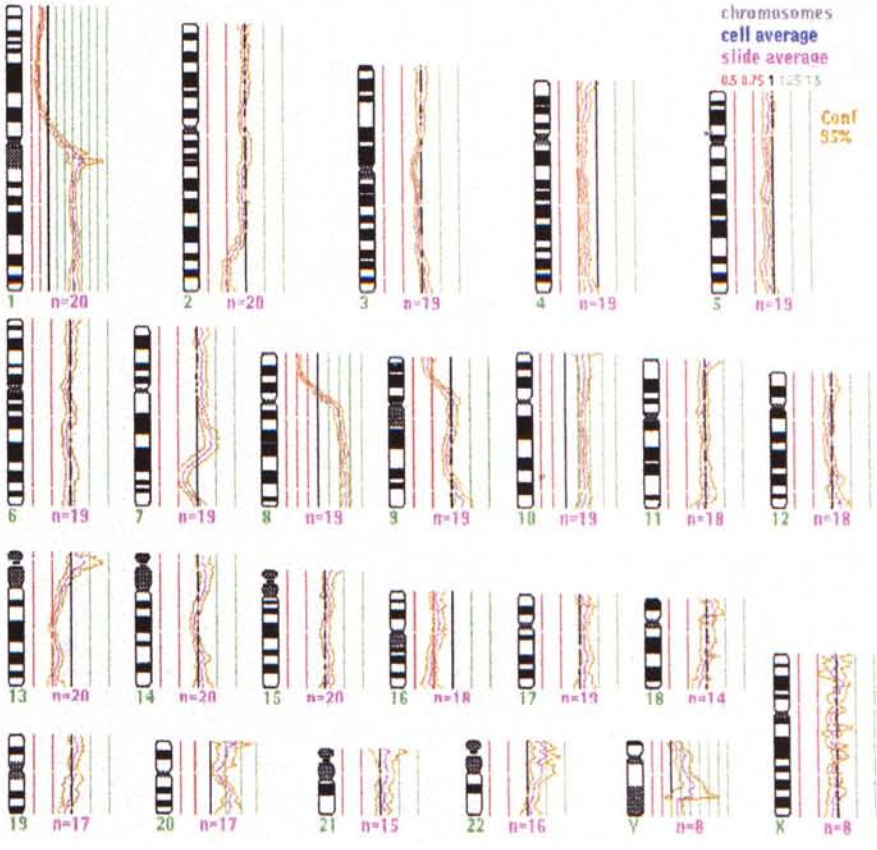
chromosomes
cell average
slide average
0.5 0.75 1 1.25 1.5
Conf 95%
1 n=20
2 n=20
3 n=19
4 n=19
5 n=19
6 n=19
7 n=19
8 n=19
9 n=19
10 n=19
11 n=18
12 n=18
13 n=20
14 n=20
15 n=20
16 n=18
17 n=19
18 n=14
19 n=17
20 n=17
21 n=15
22 n=16
Y n=8
X n=8

C

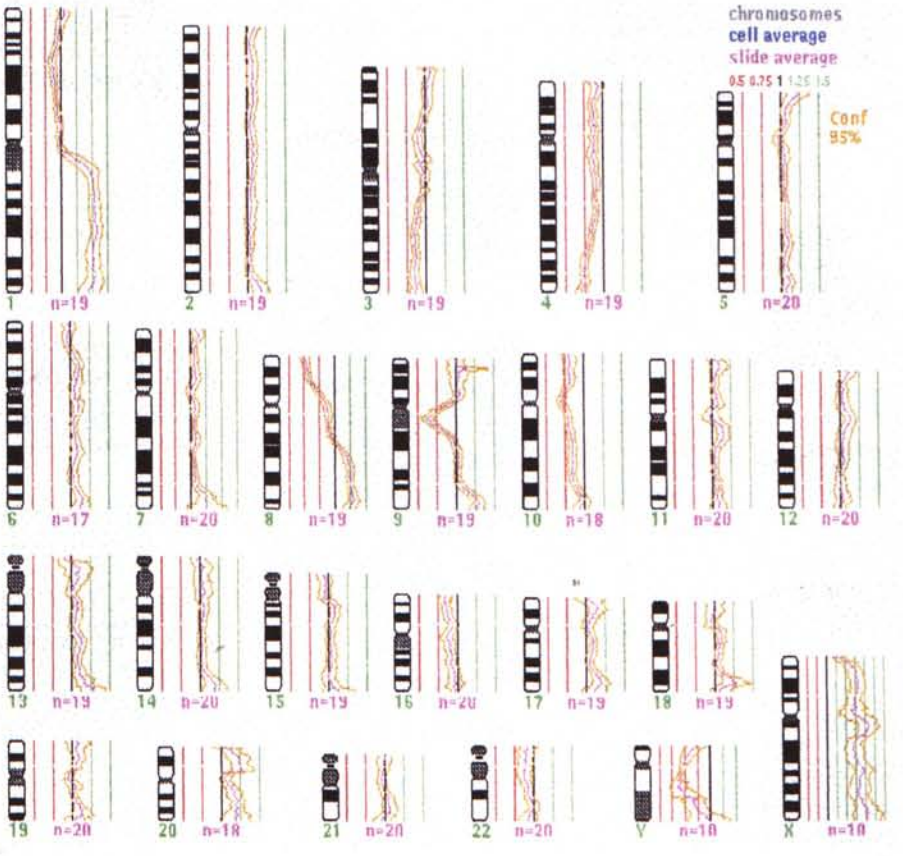
chromosomes
cell average
slide average
0.5 0.75 1 1.25 1.5
Conf 95%
1 n=19
2 n=19
3 n=19
4 n=19
5 n=20
6 n=17
7 n=20
8 n=19
9 n=19
10 n=18
11 n=20
12 n=20
13 n=19
14 n=20
15 n=19
16 n=20
17 n=19
18 n=19
19 n=20
20 n=18
21 n=20
22 n=20
Y n=10
X n=10

D

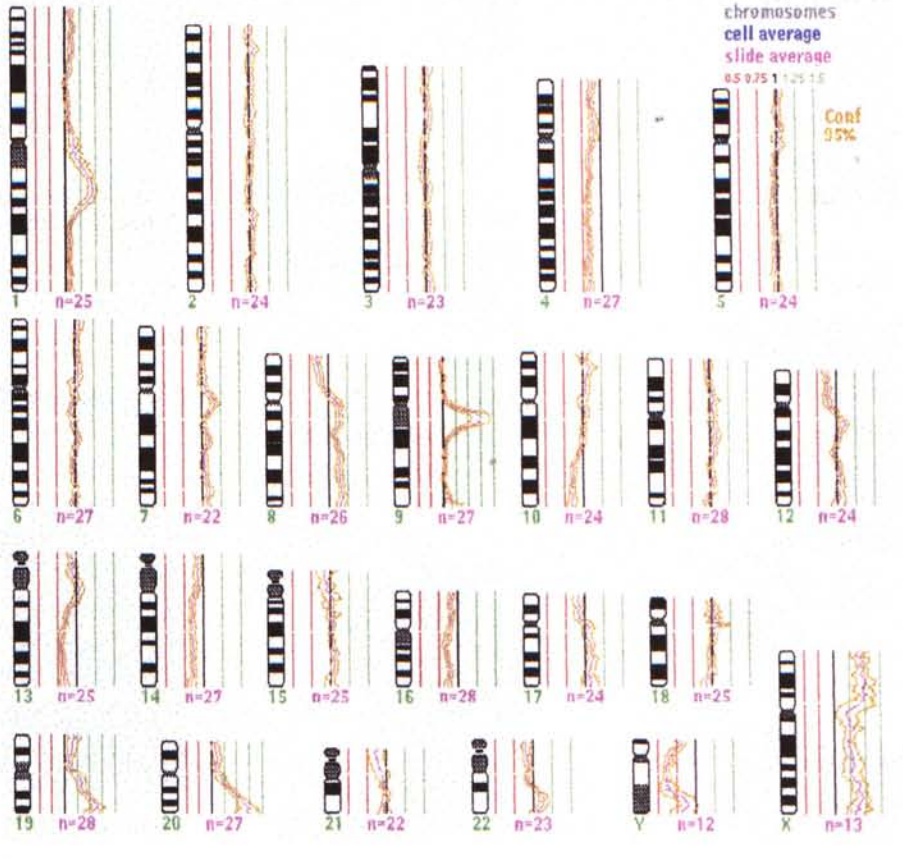
chromosomes
cell average
slide average
0.5 0.75 1 1.25 1.5
Conf 95%
1 n=25
2 n=24
3 n=23
4 n=27
5 n=24
6 n=27
7 n=22
8 n=26
9 n=27
10 n=24
11 n=28
12 n=24
13 n=25
14 n=27
15 n=25
16 n=28
17 n=24
18 n=25
19 n=28
20 n=27
21 n=22
22 n=23
Y n=12
X n=13

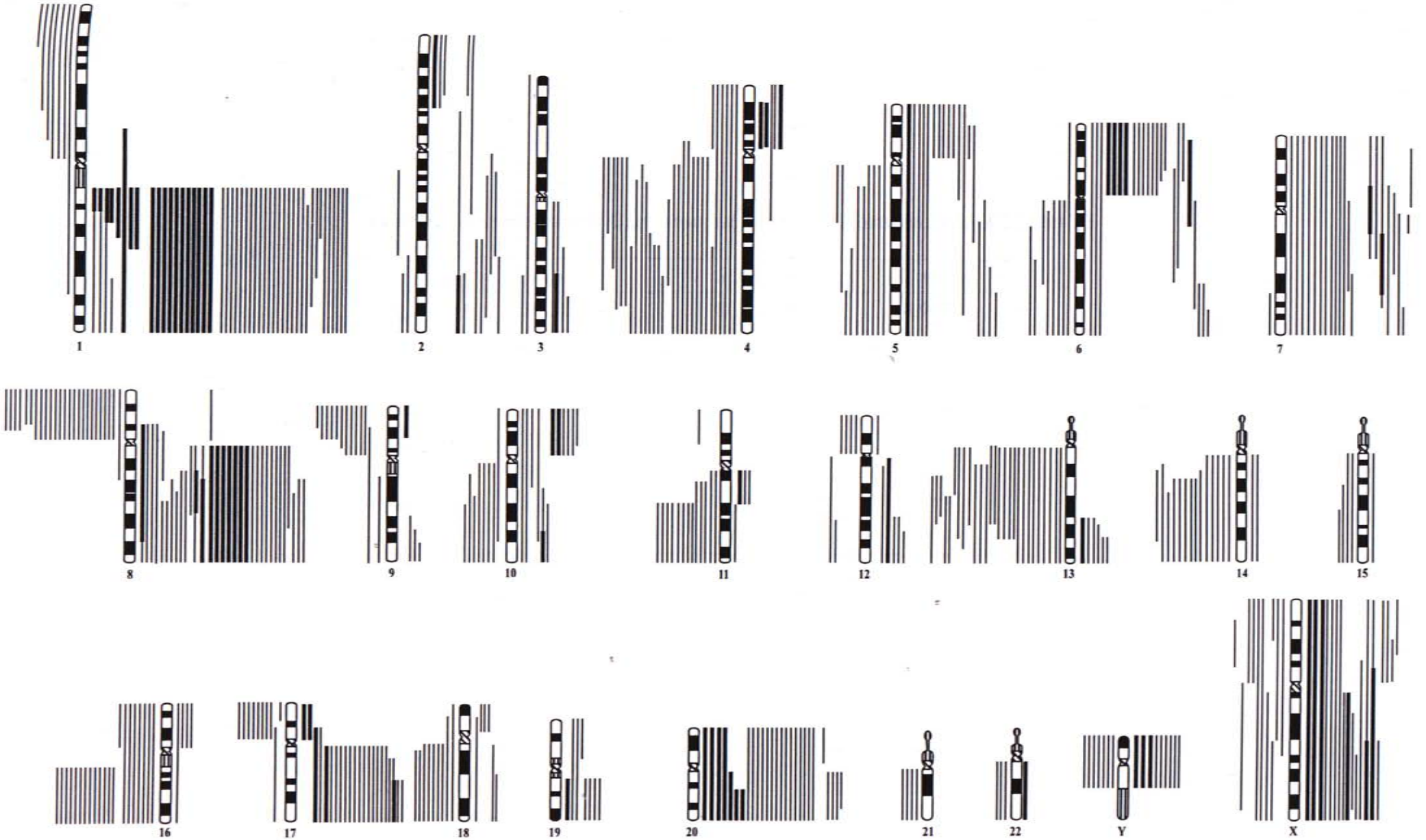

Figure 3.3. Summary of Gains and Losses of DNA Sequences Identified by CGH in 63 Cases. Gains are shown on the right side of the chromosome ideogram and losses on the left. High-level gains are shown as bold lines. Each vertical line represents the affected chromosomal region seen in a single tumour specimen.

Table 3.2. Comparison of Chromosomal Aberrations between Stages T2 and T3

	Stage T2	Stage T3	*P* value
+ 1q	39/53 (74%)	8/11 (73%)	0.953
+ 8q	29/53 (55%)	2/11 (18%)	0.027 *
+ 17q	17/53 (32%)	3/11 (27%)	0.755
+ 20q	19/53 (36%)	5/11 (46%)	0.549
- 4q	22/53 (42%)	5/11 (46%)	0.810
- 8p	20/53 (38%)	4/11 (36%)	0.932
- 13q	20/53 (38%)	4/11 (36%)	0.932
- 16q	17/53 (32%)	17/53 (32%)	0.359

Significant result was indicated with an arterisk*.

Table 3.3. Comparison of Chromosomal Aberrations between small (< 3cm) and large (> 3cm) tumours

	< 3cm	> 3cm	*P* value
+ 1q	12/60 (60%)	36/47 (77%)	0.168
+ 8q	9/20 (45%)	23/47 (49%)	0.768
+ 17q	6/20 (30%)	14/47 (21%)	0.986
+ 20q	5/20 (25%)	20/47 (43%)	0.174
- 4q	7/20 (35%)	22/47 (47%)	0.372
- 4q11-q23	3/20 (15%)	20/47 (43%)	0.009 *
- 8p	9/20 (45%)	16/47 (40%)	0.396
- 13q	6/20 (30%)	19/47 (40%)	0.419
- 16q	4/20 (20%)	16/47 (34%)	0.250

Significant result was indicated with an arterisk*.

Table 3.4. Correlation of genetic aberrations with elevation in alpha-fetal protein level above 10ng/ml was studied in 62 HCC in which the AFP levels were available.

	P value
+ 1q	0.942
+ 8q	1.000
+ 17q	0.637
+ 20q	0.583
- 4q	0.693
- 8p	0.278
- 13q	0.983
- 16q	0.715

Table 3.5. Comparison of Chromosomal Aberrations between HCC with and without Underlying Liver cirrhosis

	Cirrhotic HCC	Non-cirrhotic HCC	*P* value
+ 1q	38/55 (69%)	10/12 (83%)	0.321
+ 8q	20/55 (36%)	12/12 (100%)	0.0001 *
+ 17q	15/55 (27%)	5/12 (42%)	0.324
+ 20q	16/55 (29%)	9/12 (75%)	0.003 *
- 4q	20/55 (36%)	9/12 (75%)	0.014 *
- 8p	18/55 (33%)	7/12 (58%)	0.097
- 13q	18/55 (33%)	7/12 (58%)	0.097
- 16q	15/55 (27%)	5/12 (42%)	0.324

aberrations between stage T2 and T3, except for over-representation of 8q which was more commonly found in stage T2 ($P = 0.027$) (Table 3.2).

Tumour Size

Chromosomal aberrations were compared between the large (> 3cm) and small tumours (< 3cm). The total number of aberrations per tumour in large and small tumours was 9.3 $\pm$ 5.2 and 6.5 $\pm$ 4.0 respectively ($P = 0.036$). The mean copy number gains were 5.0 $\pm$ 2.6 in the large tumour group and 3.8 $\pm$ 1.9 in the small tumour group ($P = 0.072$). Mean copy number losses in the large and small tumour group were 4.3 $\pm$ 3.4 and 2.7 $\pm$ 2.6 respectively ($P = 0.066$). When individual aberrations were compared, loss on 4q11-q23 was more commonly found in larger HCC ($P = 0.009$) (Table 3.3).

3.3.3 Serum AFP Elevation

Individual chromosomal aberrations were tested for correlation with an elevation of serum AFP above 10ng/ml. No significant correlation was found (Table 3.4).

3.3.4 Chromosomal Aberrations in HCC arising from Cirrhotic and Non-cirrhotic Livers

The mean number ($\pm$SD) of DNA sequence copy changes per tumour in the cirrhotic and non-cirrhotic groups were 7.4 $\pm$ 5.3 and 12.8 $\pm$ 5.0 respectively ($P = 0.002$). On sub-division into gains and losses, the mean copy number gains were 4.1 $\pm$ 2.7 in the cirrhotic group and 7.5 $\pm$ 2.8 in the non-cirrhotic group ($P = 0.0002$). Copy number losses in the cirrhotic group were 3.3 $\pm$ 3.3 and 5.3 $\pm$ 2.9 in the non-

cirrhotic group (P = 0.046). When individual chromosomal aberrations was considered, gain of 8q (P = 0.001), 20q (P = 0.003) and loss on 4q (P = 0.014) were more commonly found in the non-cirrhotic group than the cirrhotics (Table 3.5).

3.4 Discussion

Using CGH, we were able to identify a number of consistent and nonrandom chromosomal aberrations in HCC. Whilst previous karyotypic studies on HCC has only reported a consistent deletion or rearrangement of chromosome 1p, our findings not only showed frequent 1q gains, but also common gains of 8q, 17q, 20q, and losses of 4q, 8p, 13q, 17p. Consistent with our findings (Wong *et al.*, 1999), Marchio *et al.* (1997) and Kusano *et al.* (1999) have also suggested the presence of these aberrations in HCC. Whilst amplicons at 11q12, 12p11, 14q12 and 19q31.1 reported by Marchio *et al.* (1997) were not detected, we have identified a novel amplicon on 1q21-q25. All recurrent gains and losses identified may signify chromosomal loci for growth control genes crucial to the initiation and /or progression of HCC.

3.4.1 Recurrent Gains

1q

In this study, gain of chromosome 1q was found in 72% (48/67 cases) of the tumours examined. High-level gain of regional or whole q-arm of chromosome 1 was also observed in 20 of 48 (42%) of HCC that showed 1q copy gain. Our finding of a novel amplicon at 1q21-q25 further implicates that proto-oncogenes important in the pathogenesis of HCC may reside on the long arm of chromosome 1. CGH studies on soft tissue sarcomas and osteosarcoma have also reported the presence of a

recurring 1q21-q22 amplicon (Forus *et al.*, 1995, Tirkkonen *et al.*, 1995). Characterisation of this amplicon showed that *FLG*, *SPRR2A*, *S100A6* and *S100A2* genes, located in 1q21, were amplified in human sarcomas (Forus *et al.*, 1998). Another gene in 1q21-q22, *MUC1*, coding for the epithelial tumour-associated antigen mucin 1, was also found to be amplified in some breast cancers (Bieche and Lidereau, 1997).

8q

Amplification of the long arm of chromosome 8 is common in a variety of solid tumours (Zitzelsberger *et al.*, 1997). In the present study, we detected 8q gain in 40% of HCC. The gain of 8q material may be related to an increased gene dosage of the *c-myc* proto-oncogene, which is located at 8q24. A previous study using a polymorphic marker for *c-myc* showed that the proto-oncogene was multiplied 2- to 6-fold in 44% of the informative HCC (Fujiwara *et al.*, 1993). As a gain of the whole chromosome 8q is often observed, one or more putative proto-oncogenes other than *c-myc* are likely.

20q

Chromosome 20q over-representation has not been described previously in HCC but is common in other solid tumours (Knuutila et al., 1998). Our results showed frequent low-level gain of 20q and high-level amplification of 20q13 in 37% of HCC cases. Studies on bladder cancer have shown that low-level 20q was associated with overcoming cellular senescence, which in turn enabled surviving cells to accumulate multiple genetic alterations (Schlegel *et al.*, 1995, Reznikoff *et al.*, 1996). In breast cancer, the amplified region in 20q is known to harbour specific

genes. *A1B1*, a steroid receptor co-activator, and *BTAK*, a serine/threonine kinase, have been shown to be amplified and over-expressed in breast cancer (Anzick *et al.*, 1997). Another candidate gene is *MYB12*, which is located at 20q13, encodes a transcription factor and plays an important role in cell cycle progression (Noben-Trauth *et al.*, 1996). The role of these genes in the liver carcinogenesis remains to be verified.

3.4.2 Recurrent Losses

4q

Under-representation of 4q is the most frequent loss (40%) in the 67 HCC studied and is more commonly found in the non-cirrhotic HCC. Loss of chromosome 4q is uncommon in other human cancers but frequent LOH has been reported in HCC (52% to 73%) (Nagai *et al.*, 1997; Piao *et al.*, 1998). Tumour suppressor(s) specifically associated with HCC development have hence been implicated in this chromosomal region. Several studies have defined the minimal deleted region on chromosome 4q to 4q11-12 (Buetow *et al.*, 1989), 4q12-q23 (Yeh *et al.*, 1996), 4q22-q24 and 4q35 (Nagai *et al.*, 1997). Since genes encoding growth factors or genes expressed predominantly in the liver such as albumin, alcohol dehydrogenase (ADH3), fibrinogen and UDP-glucuronyl-transferase are located at chromosome 4q, the deletion of this region might have profoundly alter cell growth conditions and hepatocyte functions (Nagai *et al.*, 1997).

8p

A frequent loss of chromosome 8p accompanied with a gain of 8q was detected (54%, 15 of 28 HCC cases with 8q gain). This may be suggestive of the

respective 8q iso-chromosome formation. Such chromosomal rearrangement has been observed in karyotypic analysis of an HCC (Lowichik *et al.*, 1996). Loss of heterozygosity on 8p is common in HCC and other human cancers like breast, colorectal, prostate and non-small cell lung cancers (Boige *et al.*, 1997; Emi *et al.*, 1992, Bova *et al.*, 1993, Macoska *et al.*, 1995). Further to the comprehensive allelotype study on HCC, Pineau *et al.* (1999) refine LOH on 8p to three minimal deleted areas: a 13cM region in the distal part of 8p21, a 9 cM area in the more proximal portion of 8p22 and a 5 cM area in 8p23. This in turn suggested that there were at least three novel tumour suppressor loci on 8p being involved in the HCC development.

13q

We detected loss of chromosome 13q in 39% of the 67 HCC. The retinoblastoma gene *Rb*, located at 13q14 may be a tumour suppressor gene involved. However, Zhang *et al.* (1994) detected somatic mutation of the *Rb* gene in only two of 13 HCC that displayed LOH of 13q or deficient Rb protein expression. Deletion mapping on 13q suggested *BRCA2* located on 13q12-13 to be another tumour suppressor involved in HCC (Kuroki *et al.*, 1995). Nevertheless, subsequent studies found mutations of *BRCA2* in only three of the 60 HCC examined (Katagiri *et al.*, 1996). Despite the low mutation rate, it is possible that these tumour suppressor genes are inactivated by epigenetic alteration such as hypermethylation, rather than somatic mutation.

3.4.3 Tumour Progression

Cirrhosis is considered as the final common response of liver to various insults, including chronic hepatitis B and C infection, and excessive alcoholic consumption. It is also regarded as the premalignant state that preceded HCC. The analysis of 12 surrounding cirrhotic livers by CGH suggested no gross gains or losses of DNA sequence copy number. Consistent with our findings, Kusano *et al.* (1999) has also found no chromosomal aberrations in surrounding cirrhotic tissues of HCC. Although no CGH alterations can be detected in the surrounding cirrhotic tissues, the presence of mutations and/or small regional alterations cannot be ruled out. Our study showed a significantly smaller total number of genetic aberrations in the cirrhosis-associated HCC compared with those without underlying cirrhosis. This may suggest that, although gross genotypic changes may not be present at the cirrhotic stage, the state of cirrhosis may increase the susceptibility of the normal hepatocytes to malignant transformation so that fewer genetic aberrations are required for tumour development. In addition, gains of 8q (100%) and 20q (75%) and loss of 4q (75%) were observed to be more frequent in noncirrhotic than cirrhotic HCC. This may be suggestive of these aberrations to be essential in the transformation of noncirrhotic liver to HCC, and providing the hepatocytes with proliferative stimulation and growth advantages.

Genetic alterations detected by CGH were correlated with clinical staging, tumour size and the presence of underlying cirrhosis. The pattern of genetic alterations between 53 cases of T2 and 11 cases of T3, showed no significant difference except a higher incidence of 8q gain in stage T2. This raised incidence could be explained by the fact that all noncirrhotic HCC cases studied fell within the T2 stage. However, we found that tumours greater than 3cm showed significantly

more aberrations than tumours smaller than 3cm. This supports that tumour size rather than TNM classification to be the better prognostic parameter for HCC. A higher incidence of 4q11-q23 loss in larger tumours found in this study suggested the presence of tumour suppressor gene(s) in this chromosomal locus, which might confer growth advantage in HCC progression.

3.5 Conclusion

CGH analysis on 67 HCC revealed a number of non-random chromosomal aberrations. These genetic aberrations are representative of HCC from Southern Chinese patients with prevalent HBV infection and underlying cirrhosis. A high frequency of 1q gain together with the identification of a novel amplicon at 1q21-q25 suggests a chromosomal region for further characterisation of gene(s) important in HCC development. The finding of loss of 4q11-q21 in large tumours (> 3 cm) suggested that this region may harbour a tumour suppressor that favours HCC progression. Besides, a consistent 8q gain in non-cirrhotic HCC in comparison to HCC arising from cirrhotic livers strongly suggested an essential role of genes residing on this chromosomal arm in the transformation of normal hepatocytes to malignant HCC. Although CGH did not reveal any aberrations in surrounding cirrhotic liver tissues, the smaller number of chromosomal aberrations in cirrhotic HCC than non-cirrhotic HCC suggests a role of underlying cirrhosis in enhancing HCC development.

Chapter 4.

Positional Mapping of a Novel Amplicon on Chromosome 1q21-q25 by Interphase Cytogenetics

4.1 Introduction

In Chapter 3, CGH study on HCC cases indicated the presence of an intense green signal hybridization (tumour DNA) below the heterochromatic region of chromosome 1 in 5 cases. The corresponding profile obtained suggested an approximate 2-fold gain (Fig. 4.1). This region of intense hybridization observed, 1q21-q25, was hence referred to as an 'amplicon' by criteria set forth in Materials & Methods, Chapter 2, Section 2.2.2.9. Since no putative oncogenes have been reported in this region, we have therefore undertaken a FISH study to further characterize this amplicon. Interphase FISH analysis on paraffin-embedded tissue sections was chosen over Southern blot or microsatellite analysis because of its higher sensitivity in detecting 1-2 fold copy number gain. Besides, FISH study on tissue sections has the advantage of histological correlation, thus allowing non-malignant stromal cells and inflammatory cells to be excluded from the analysis. The counting of FISH signals on a cell-by-cell basis can also allow intratumoural heterogeneity to be assessed at the same time.

Among the various sources of unique human DNA sequences, yeast artificial chromosomes are deemed most appropriate in this experiment. The large insert size of YAC can ensure maximum labeling so that intense FISH signals can be obtained. In this chapter, five YACs were chosen at approximately 10Mbp apart between 1q21-q25 to fine map this region on a locus-by-locus basis. These YACs were applied onto the corresponding paraffin-embedded formalin-fixed tissue sections of the five HCC patients that displayed regional 1q21-q25 gains by CGH.

Figure 4.1. Amplicons Found in the 5 HCC Cases. The corresponding fluorescent ratio profile indicates a DNA sequence copy number gain of around 2-fold.

4.2 Materials

HCC cases H20, H21, H50, H58 and H66 showed 1q21-25 gain by CGH analysis. The corresponding archival paraffin-embedded formalin-fixed tissue sections of these patients were kindly provided by Prof C.T. Liew, Department of Anatomical and Cellular Pathology of the Prince of Wales Hospital (Fig. 4.2).

CEPH mega-YAC clones (Albertsen *et al.*, 1990) were selected with reference to physical mapping data in the Whitehead institute/Massachusetts Institute of Technology Genome Centre database (http://www.genome.wi.mit.edu) and Centre d'Etudes du Polymorphisme humain (CEPH) infoclone program (http://www.cephb.fr/infoclone.html). The relative positions of the YACs were determined according to their sequence tagged site (STS) content and data in the contig WC1.16 (http://www-genome.wi.mit.edu). Potential YAC chimerisms were evaluated using data on STS content of YAC and hybridization of YAC *Alu*-PCR products against other members of the YAC libraries. Finally, five YAC clones (955_e_11, 910_c_8, 935_b_12, 757_a_7 and 964_h_4) spaced by approximately 10cM on chromosome 1q21-25 were obtained from Research Genetics (Huntsville AL, USA) and YAC Screening Centre in Italy (Fig. 4.3). The YAC clone 752_e_3, which is mapped to 1p31, is included as the reference probe to distinguish genuine local DNA amplification from overall ploidy state changes.

4.3 Methods

4.3.1 Preparation of Paraffin-embedded Tissue Sections

Paraffin-embedded tissue sections ranging from five to twenty microns were evaluated. Ten microns was found to be the optimum thickness for best nuclei

morphology with minimal overlapping. Consecutive 10μm sections mounted on 3-aminopropyltriethoxylsilane coated slides were therefore used in interphase study.

4.3.2 Verification of YAC Probes for Chimerism

The chromosomal location of YAC and the presence of chimerisms are verified by metaphase FISH before use (see section 2.3.3.3). Examples of the metaphase FISH images are depicted in Fig. 4.4.

4.3.3 Hybridization Efficiency of Test and Reference Probes

To minimize interference from yeast DNA sequences, human DNA contained in YAC were first enriched by inter-*Alu* PCR (see section 2.3.3.4). The inter-*Alu* PCR products were then labeled with biotin (test probes) and digoxigenin (reference probes) by nick translation to optimal fragment lengths of 200 to 500 base pairs. The labeled DNA was ethanol precipitated in excess human Cot-1 DNA and resuspended in Hybrisol VII. To ensure a similar hybridization efficiency of test and reference probes, differentially labeled test and reference probes were cohybridized onto normal lymphocytes. Digoxigenin-labeled DNA was detected with green-fluorescence (sheep anti-FITC) while biotin was visualised with red-fluorescence (avidin Texas Red). The number of nuclei that showed equal number of green and red signals was scored. Co-hybridization efficiency of test and reference probes employed was determined to be 80-90%.

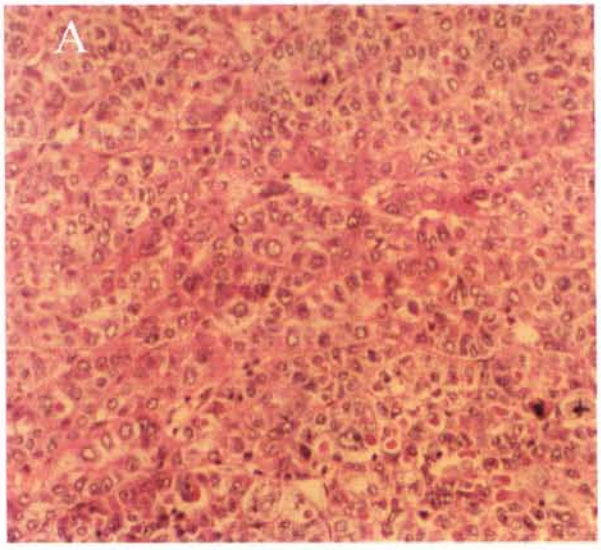

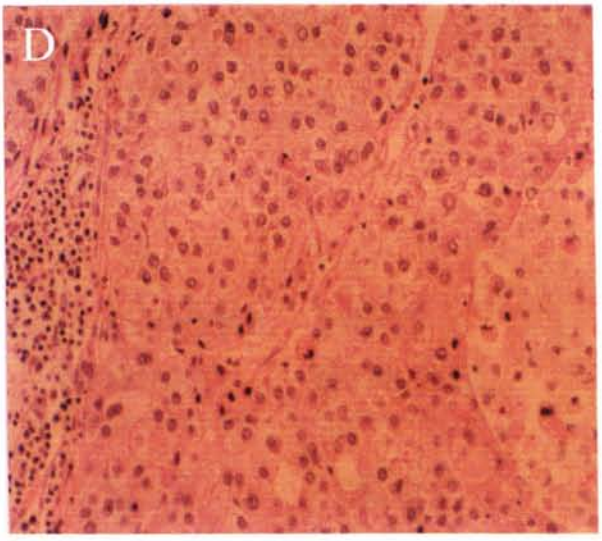

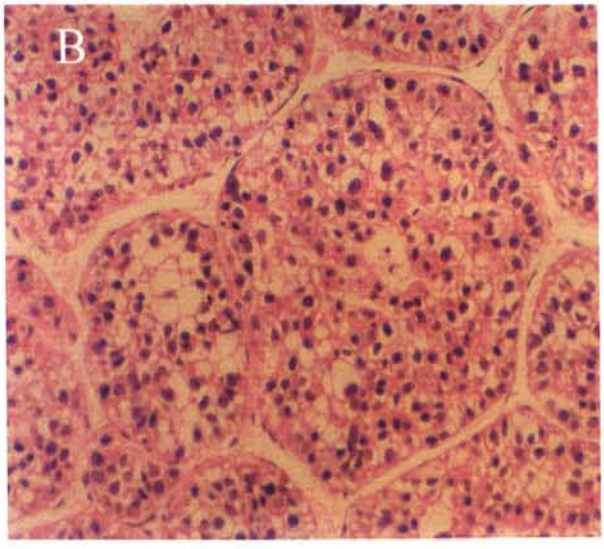

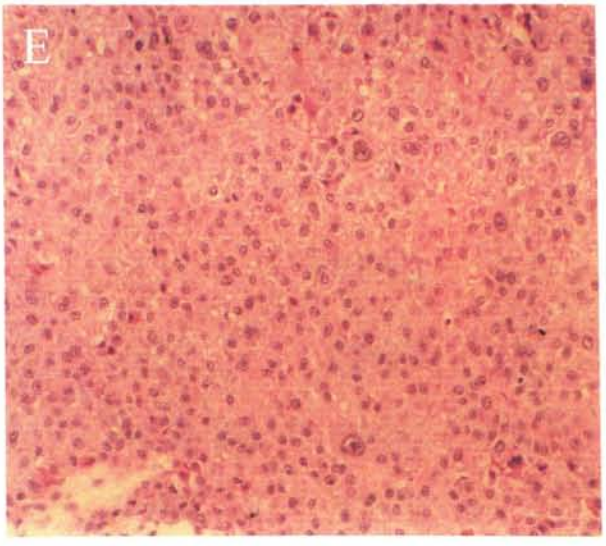

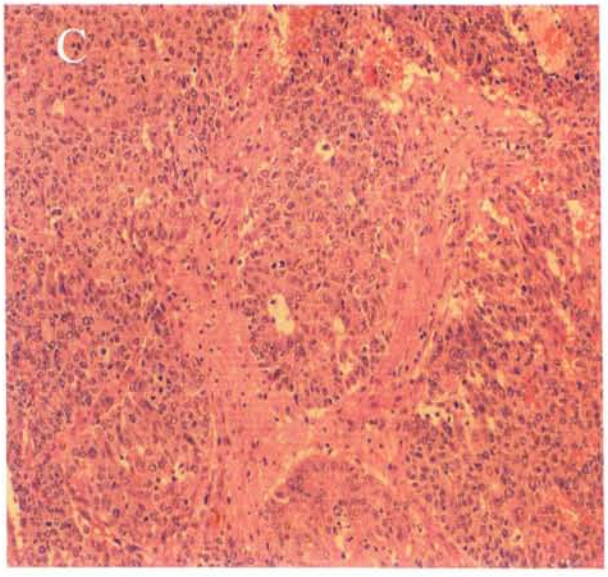

Figure 4.2. Haematoxylin and Eosin (H&E) Staining Showing the Morphology of the 5 HCC Cases Under Light Microscopy.

A. H20 (40x), well-differentiated HCC;

B. H21 (40x), moderately differentiated HCC;

C. H50 (10x), poorly differentiated HCC;

D. H58 (40x), well-differentiated HCC;

E. H66 (40x), well-differentiated HCC.

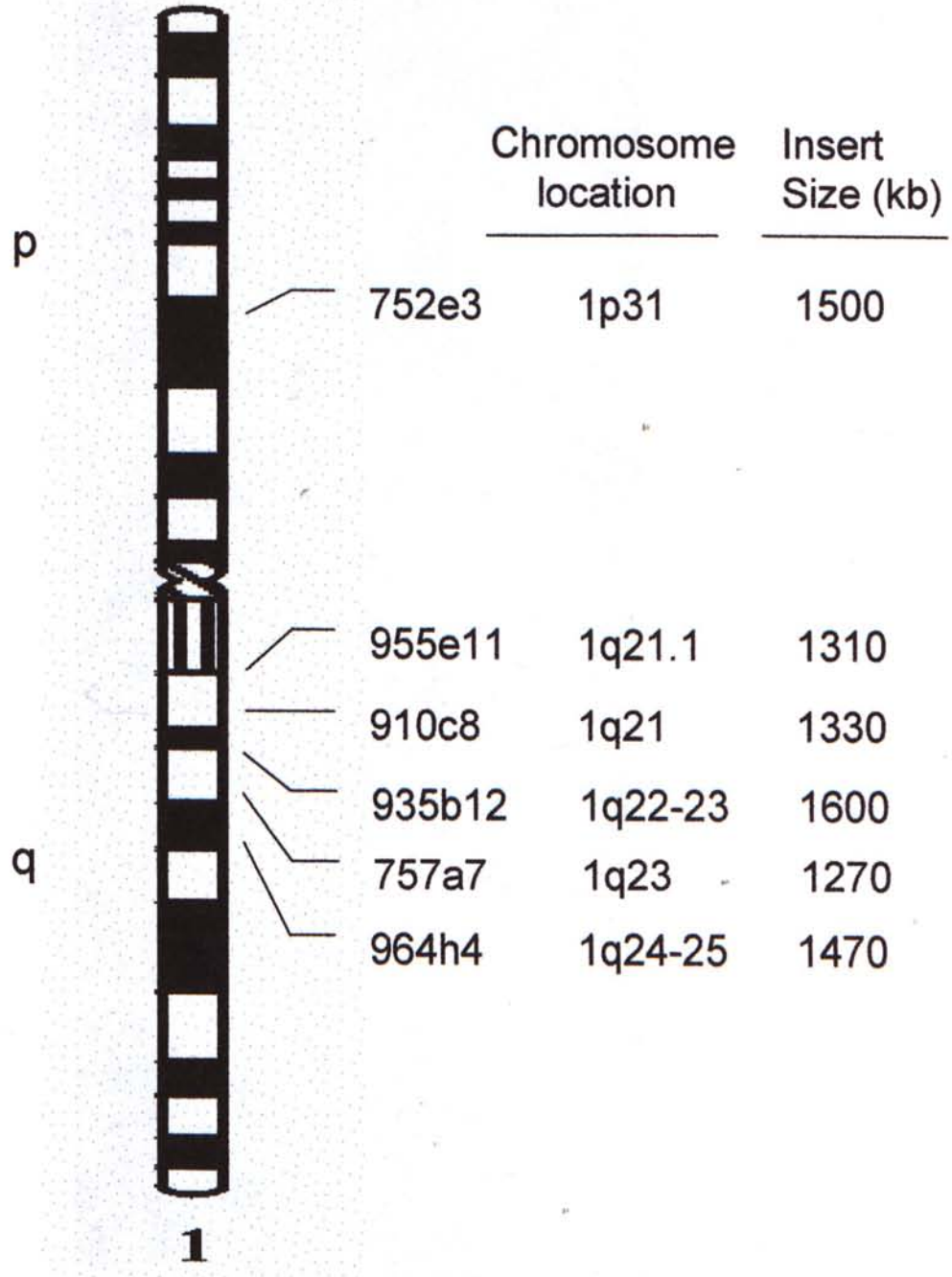

Figure 4.3. Map Locations for YAC Clones

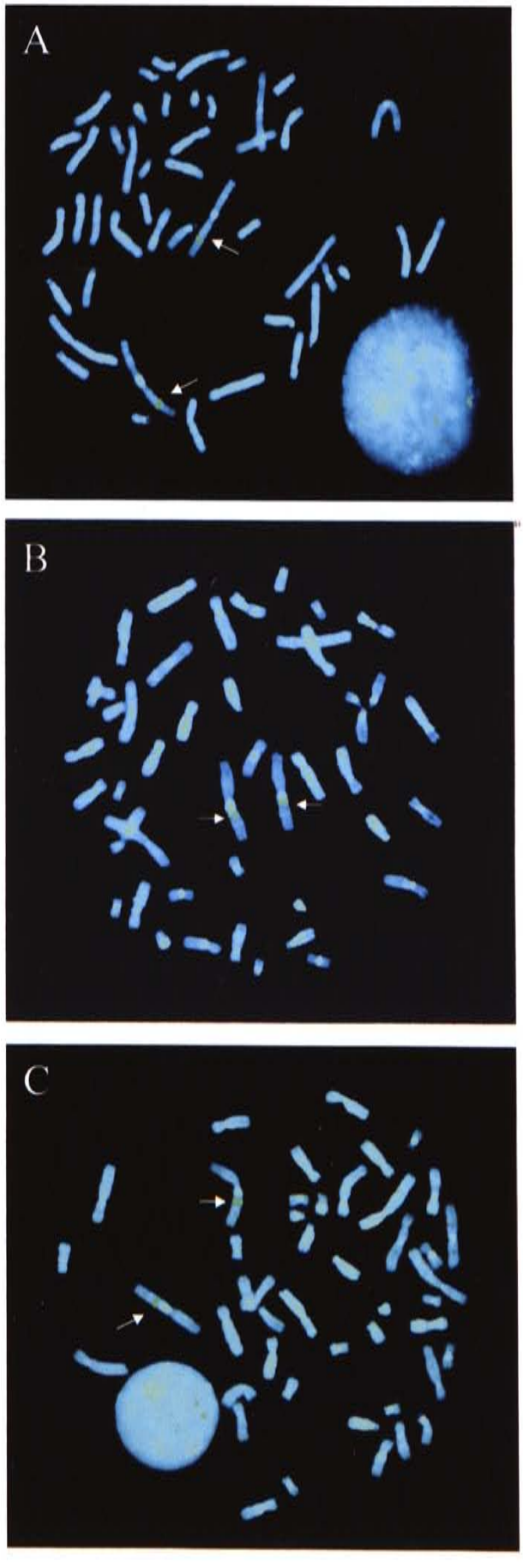
A
B
C

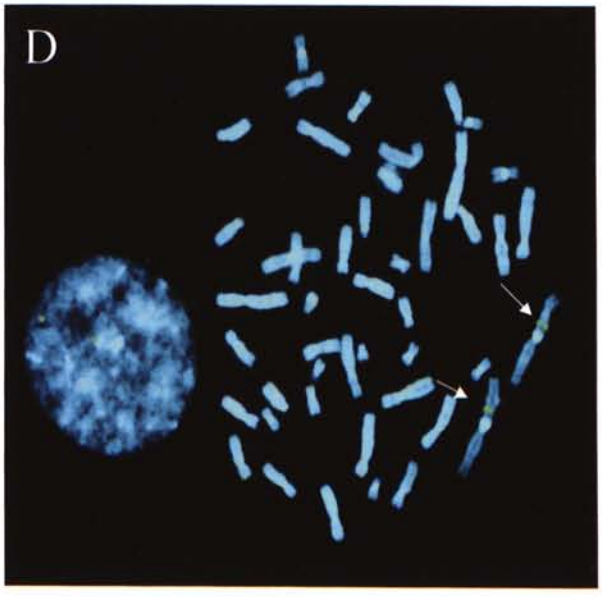

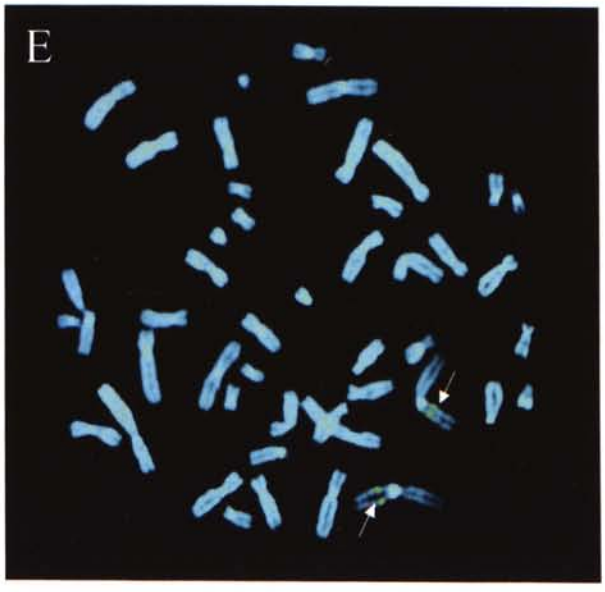

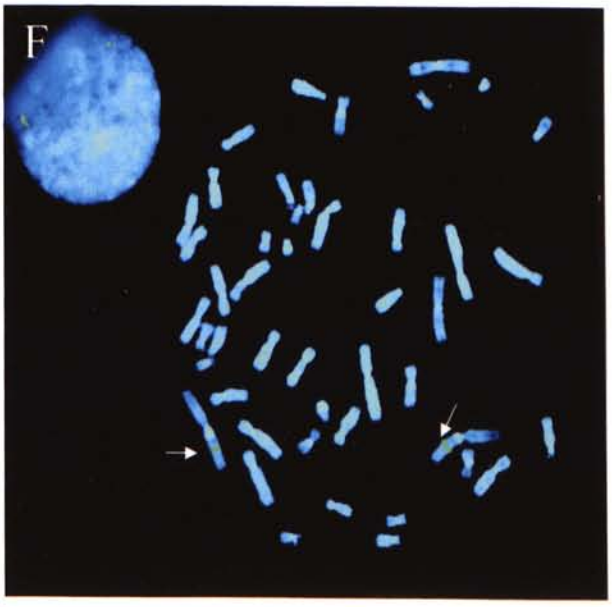

Figure 4.4. Metaphase FISH of 6 YACs. The total yeast DNA is extracted and labeled with digoxigenin. FISH signals are shown as green spots (indicated by arrows) on the corresponding chromosome locations or interphase nuclei. A. 752e3; B. 955e11; C. 910c8; D. 935b12; E. 757a7; F. 964h4.

4.3.4 Slide Pretreatment and FISH with YAC Probes

Tissue sections were dewaxed in three changes of xylene at 37°C for 1 hour each and dehydrated twice in methanol for 5 minutes. After treatment in 1M sodium thiocyanate at 80°C for 20 minutes, the tissue sections were digested with pepsin (1mg/ml to 2mg/ml in 0.2M HCl) for 20 to 30 minutes to remove cytoplasmic and nuclear proteins. This was followed by RNase treatment (200μg/ml in 2xSSC) at 37°C for 30 minute before heated in a microwave oven at low power (600 Watts) for 15 minutes. Nuclei DNA was denatured in 70% formamide/2xSSC at 72°C for 5 minutes and dehydrated in a cold ethanol series of 70%, 80% and 100%. After incubation at 37°C for 5 minutes, 300ng each of biotin-labeled test probe and digoxigenin-labeled reference probe were co-hybridized onto the pretreated tissue section. After an overnight incubation at 37°C, tissue section was washed in 40% formamide/1xSSC (pH 7.0) at 40°C for 5 minutes. Section was then blocked with 3% Marvel/4xSSC/0.1%Tween (pH 7.0). Fluorescent signals were developed by incubating the hybridized section in the following order of antibody layers, each for 30 minutes at 37°C (i) Avidin Texas Red and sheep anti-Dig FITC (ii) Goat biotinylated anti-avidin D (iii) Avidin Texas Red and anti-sheep IgG FITC. Nuclei were finally counterstained with 0.4μg/ml 4,6-diamino-2-phenylindole (DAPI) in an antifade solution.

4.3.5 Scoring of FISH Signals

Interphase FISH analysis was evaluated using Leitz DM RB (Leica, Wetzlar, Germany) fluorescence microscope. The whole tissue section was evaluated for areas of good hybridization. A total of 200 to 300 nuclei were scored by two independent observers and the following guidelines were employed:

1. To avoid misinterpretation due to inefficient hybridization, slides were analysed only when the hybridization efficiency was greater than 90%.
2. Only non-overlapping nuclei with well-defined nuclear outlines were scored. Damaged nuclei were disregarded.
3. The focal plane of the microscope was adjusted constantly so that signals hybridized at all planes of the nucleus were included.

Relative copy number changes for the q-arm probes were calculated by dividing the signal scored for the q-arm probes by that of the p-arm reference probe.

4.4 Results

4.4.1 Relative Copy Number Gain

There was an increased q-arm copy number relative to the p-arm probe in all HCC cases studied except for three loci in H66 (Fig. 4.5).

Case H20 the q/p-arm ratio was between 1.8 and 1.9 for YACs 910_c_8, 935_b_12, 757_a_7 and 964_h_4, and rose to 2.2 for 955_e_11 (Fig. 4.5A).

Case H21 the q/p-arm ratio ranged between 1.18 and 1.34 but gave a highest peak of 1.92 at 955_e_11 (Fig. 4.5B).

Case H50 similar to case H21, the q/p-arm ratio ranged between 1.47 and 1.79 and gave a peak of 2.14 at 955_e_11 (Fig. 4.5C).

Case H58 the q/p-arm ratio showed a steady increase from 1.75 at 964_h_4 to 1.91 at 955_e_11 (Fig. 4.5D).

Case H66 the q/p-arm ratio was 1.0 for YACs 935_b_12, 757_a_7 and 964_h_4 but increase sharply to 2.67 and 3.43 at 910_c_8 and 955_e_11 respectively (Fig. 4.5E).

In all five HCC cases studied, 955_e_11 was the chromosomal locus that consistently displayed the highest level of copy number gain.

4.4.2 Intratumour Heterogeneity

There was considerable heterogeneity among the nuclei examined. As indicated by the number of p-arm signals, the 5 HCC cases contained mainly disomies, trisomies and tetrasomies, but also pentasomies and octasomies. Heptasomies were only rarely detected. Disomic, trisomic and polysomic q-arm signals per nucleus were observed (Fig. 4.6 & 4.7). H66 showed a remarkable shift in signal distribution from a population with equal p- and q-arm signals for YACs 935_b_12, 757_a_7 and 964_h_4 to YAC 955_e_11 and 910_c_8 that displayed more than 2.5-fold increase (Fig. 4.7E). This clearly delineates the amplicon boundary in H66 to between 910_c_8 and 935_b_12. A similar shift in signal distribution, though less prominent, was also in cases H20 and H21 which presented the highest q/p ratio for YAC 955_e_11. In case H50, clustering of test signals in small subpopulation could be detected for 955_e_11, 910_c_8 and 935_b_12 (Fig. 4.6G-H).

4.5 Discussion

In this study, our CGH finding of the regional gain, 1q21-q25, below the heterochromatic region of chromosome 1 in 5 cases of HCC, H20, H21, H50, H58 and H66, was confirmed by FISH positional mapping. Our results also demonstrated the presence of intratumour heterogeneity in DNA ploidy in HCC. Hepatocytes of disomies, trisomies, up to heptasomies could be found in the 5 HCC cases studied. It is thought that genetic instability of tumour cells and the selection pressure of the

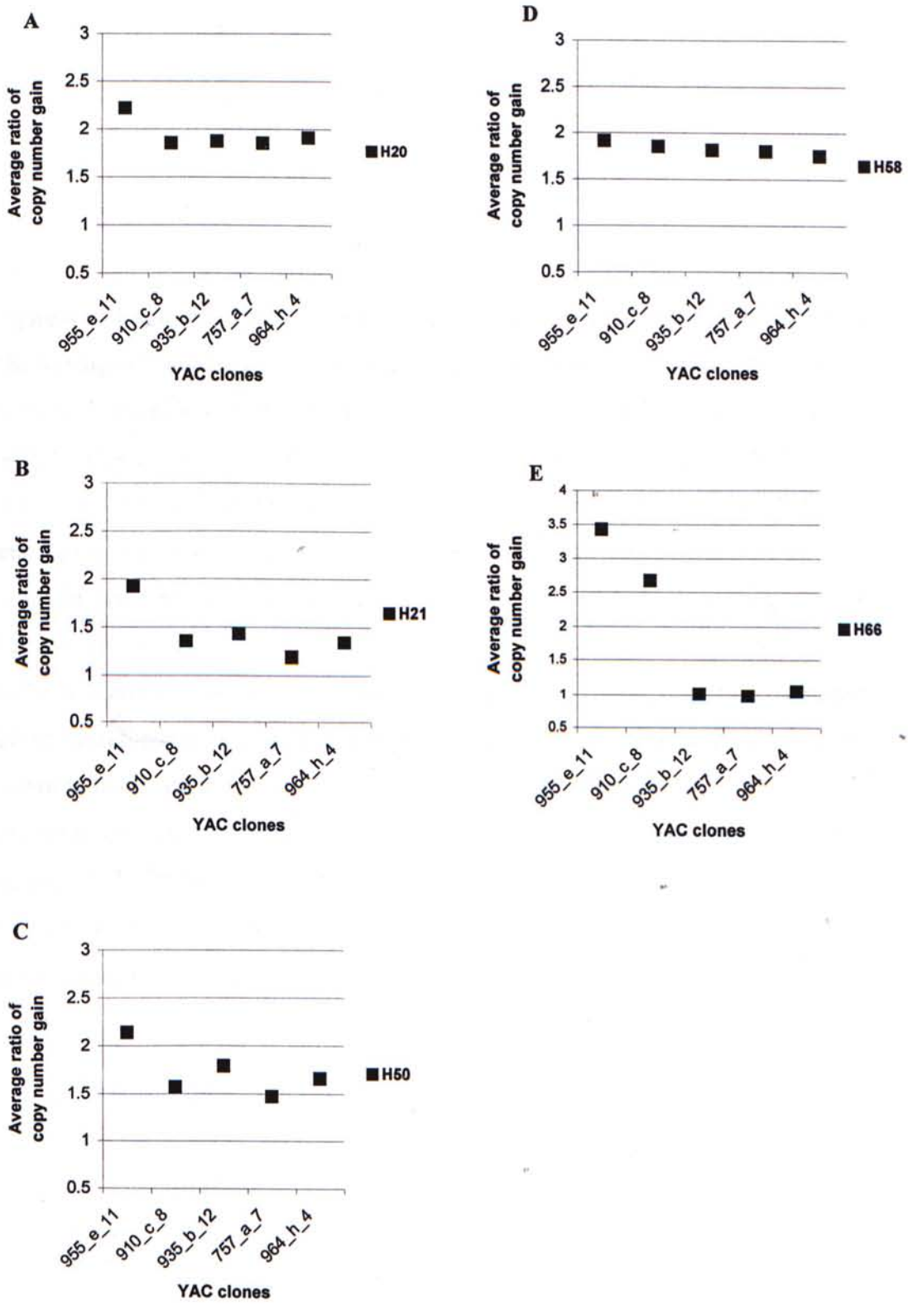

Figure 4.5. Relative copy number changes in five chromosomal loci on 1q21-q25 represented by the YAC clones. Most of the DNA copy number changes were below 2. 955e11 was the chromosomal locus that consistently displayed the highest copy number gains in the 5 HCC. A: H20; B: H21; C: H50; D: H58; E: H66.

Figure 4.6. Examples of Dual-colour FISH Results Obtained in the Five HCC Cases. The test signals and the reference signals are shown in red and green respectively. **A** 955e11, case H66; **B** 964h4, case H66; **C** 935b12, case H21; **D** 964h4, case H20; **E** 955e11, case H20; **F** 955e11, case H58; **G** 955e11, case H50; **H** 910c8, case H50; **I** 935b12, case H50. **A** 955e11 showed more than 3-fold increase in relative copy number in case H66. The signals were distributed across the nuclei. **B** 964h4 in case H66, however showed equal number of test and reference signals in the majority of nuclei scored. **C-E** Intratumour heterogeneity. Nuclei showing different number of test signals within the same tumour. In **D**, nuclei on the upper left showed three green and six red signals, while three green and red signals were shown in nuclei on the upper right. **F** Nuclei showed a 2-fold amplification of 955e11 in case 16556. Nuclei on the left showed three green signals and six red signals. **G-I** Clustering of test signals for 955e11, 910c8 and 964h4 in case H50. **G**: 955e11; **H**: 910c8; **I**: 964h4. The clustered arrangement of signals is suggested of intrachromosomal duplication of DNA sequences.

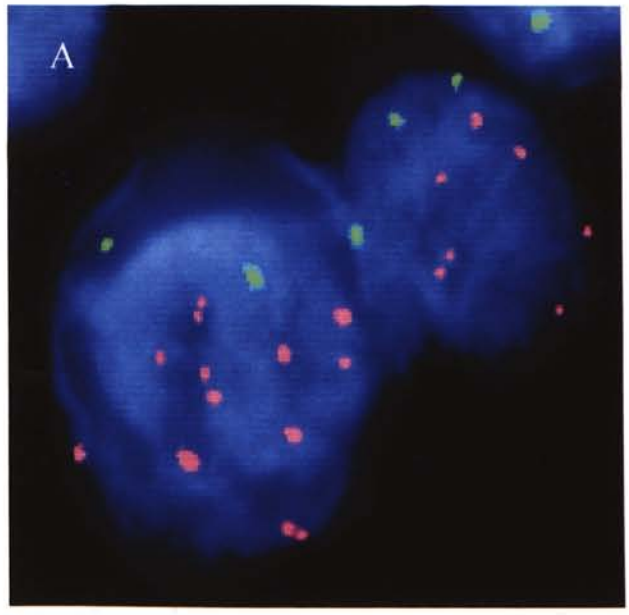
A

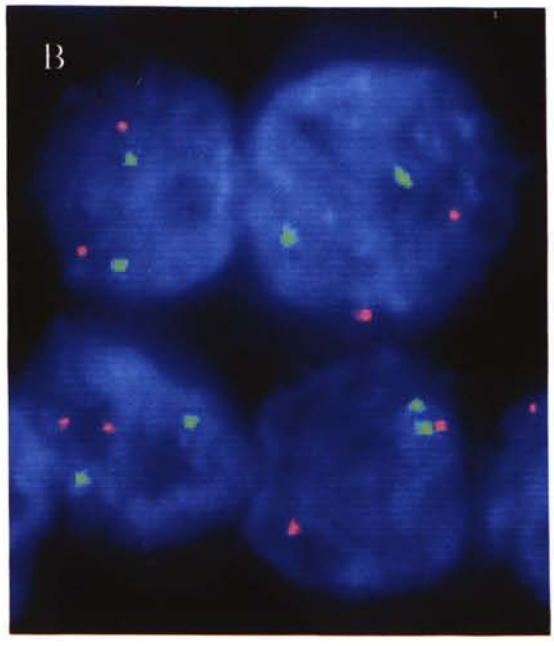
B

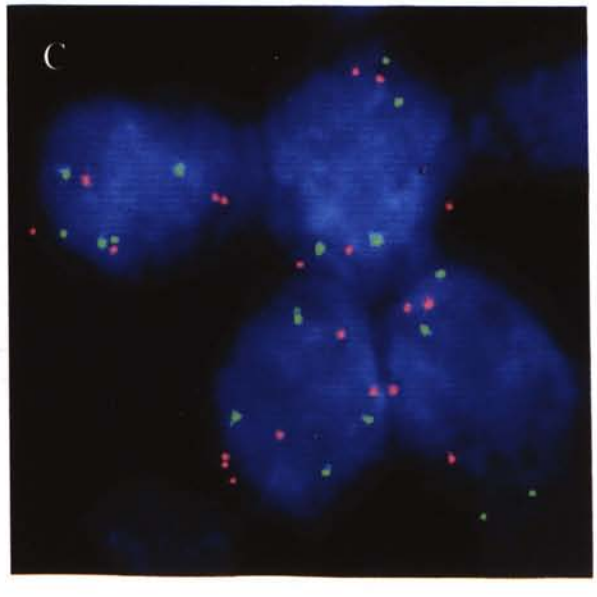
C

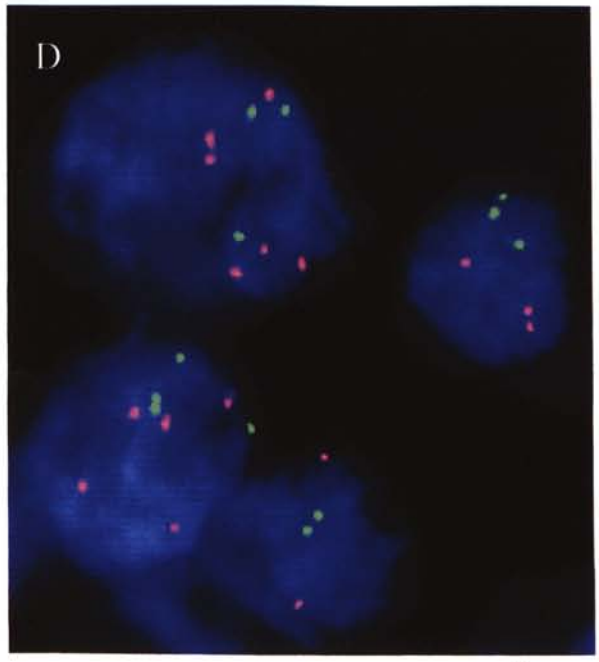
D

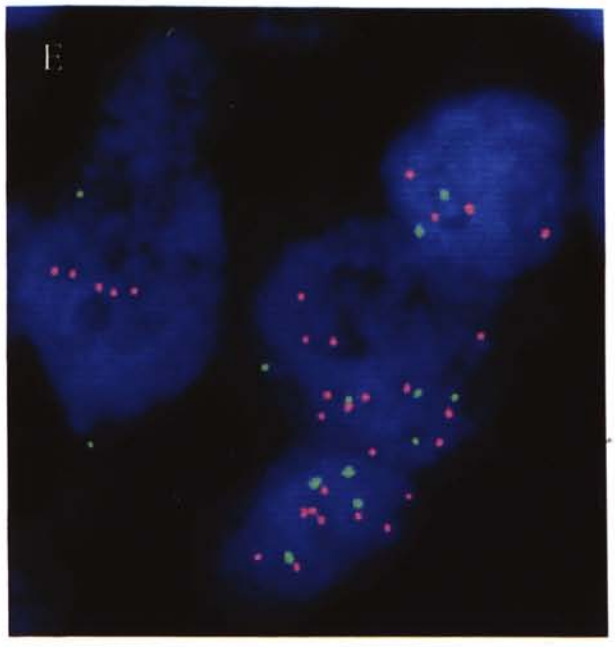
E

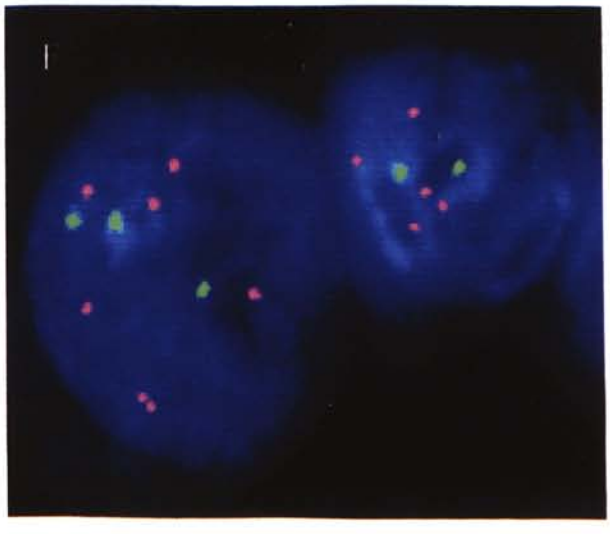
F

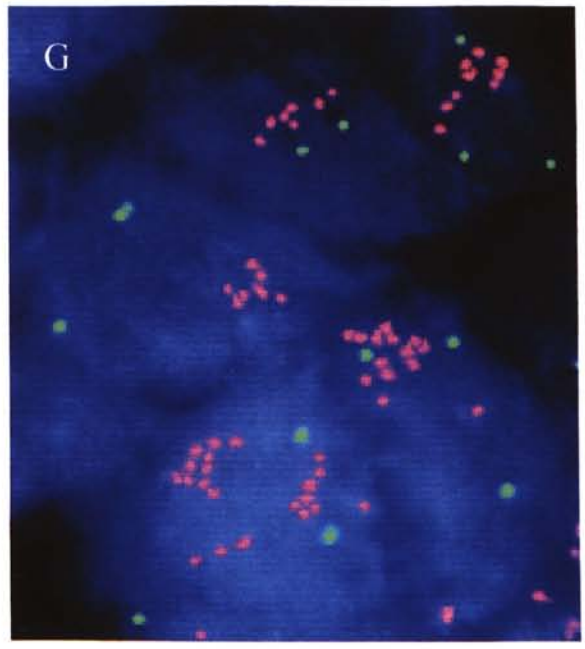
G

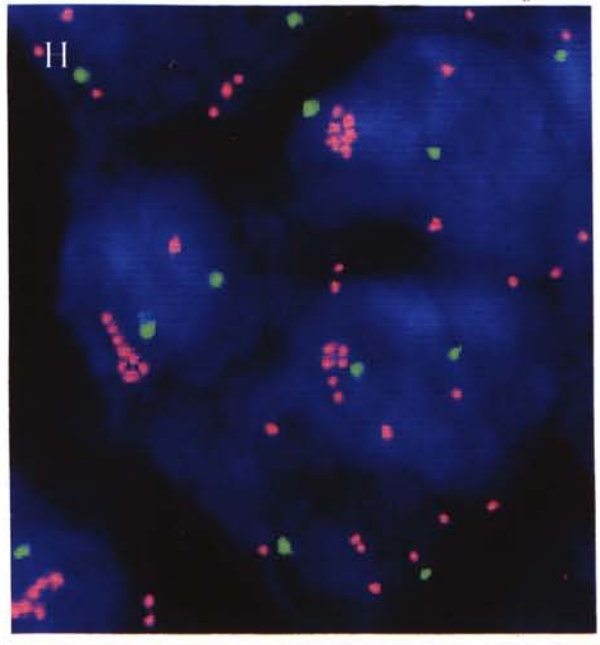
H

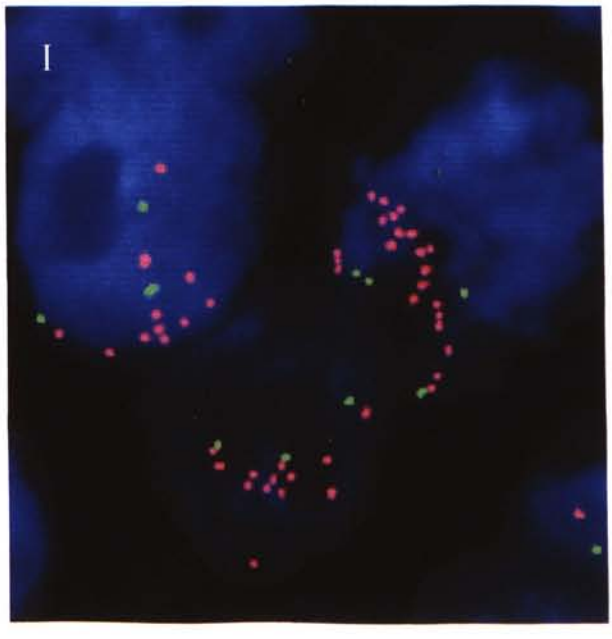
I

Figure 4.7. Frequency Histograms of Dual-colour FISH Results. A total of 200 to 300 nuclei were scored. The x-axis and y-axis represents the number of reference and test signals scored per nuclei respectively. The number of nuclei showing a combination of reference and test signals was then represented as a percentage of the total number of nuclei scored in the z-axis (shown as colour blocks). Intratumour heterogeneity can be recognized from the wide signal distribution in the histogram. **A**: H20, **B**: H21, **C**: H50, **D**: H58, **E**: H66.

H20-955_e_11

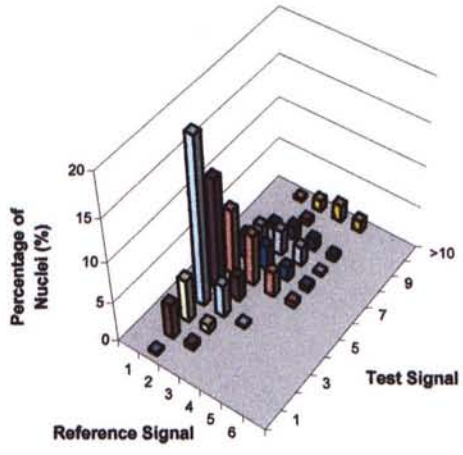

H20-757_a_7

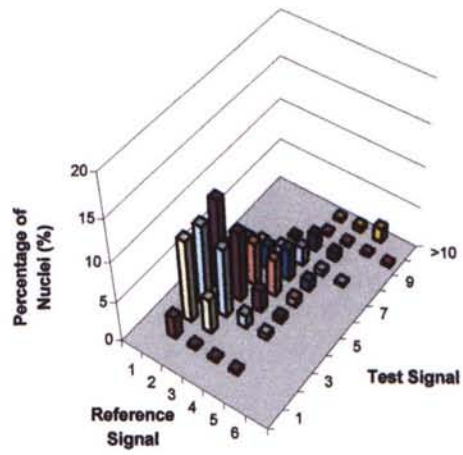

H20-910_c_8

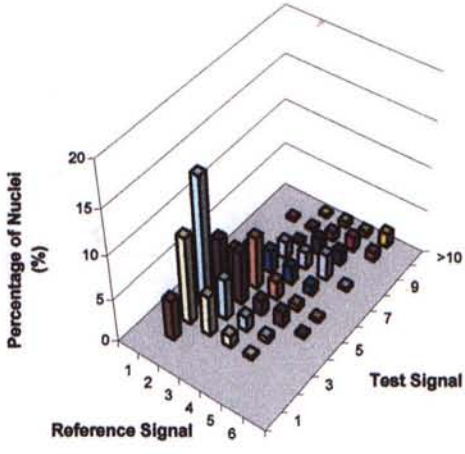

H20-964_h_4

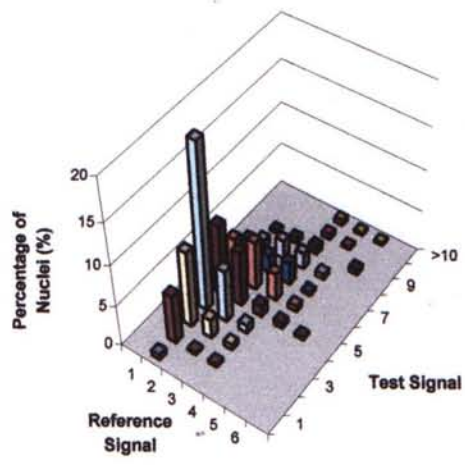

H20-935_b_12

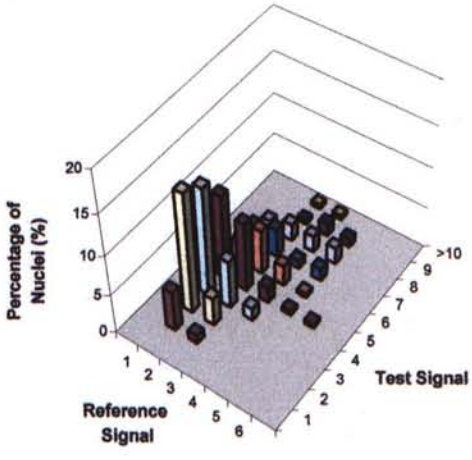

Figure 4.7A

H21-955_e_11

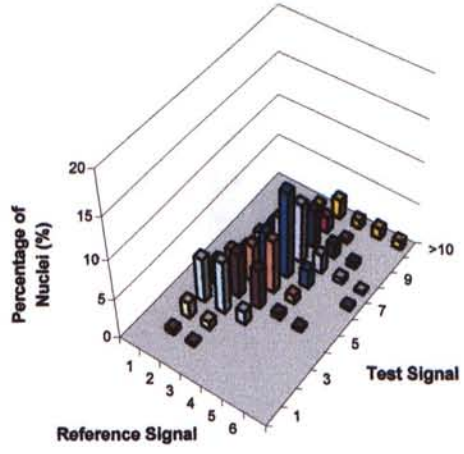

H21-757_a_7

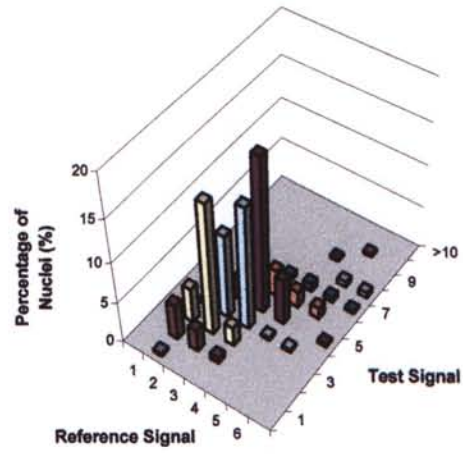

H21-910_c_8

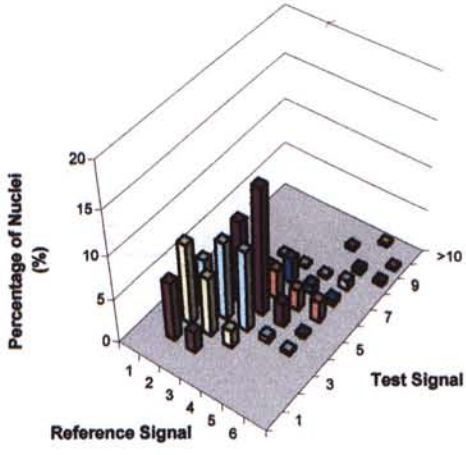

H21-964_h_4

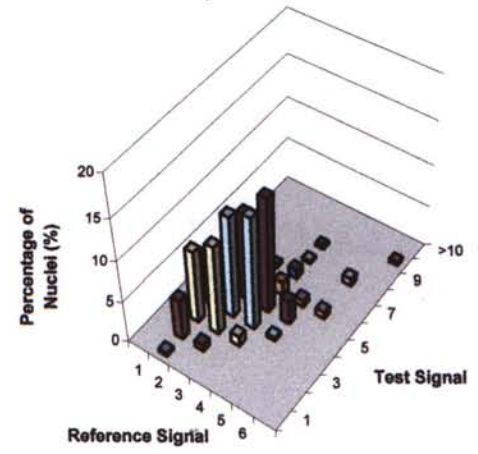

H21-935_b_12

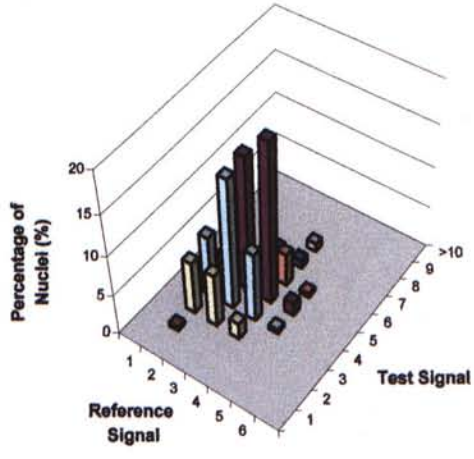

Figure 4.7B

H50-955_e_11

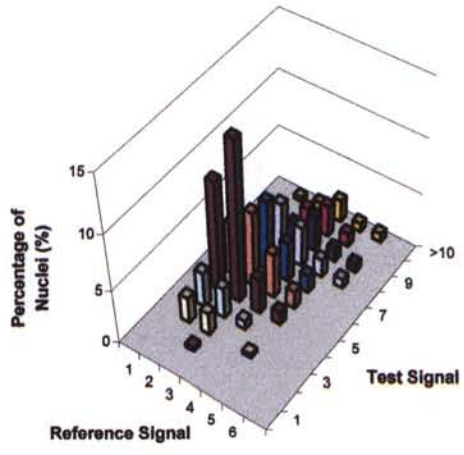

H50-757_a_7

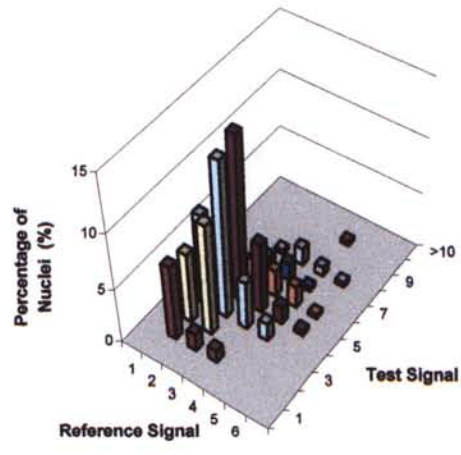

H50-910_c_8

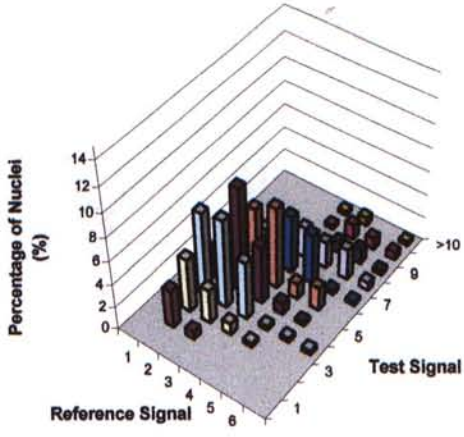

H50-964_h_4

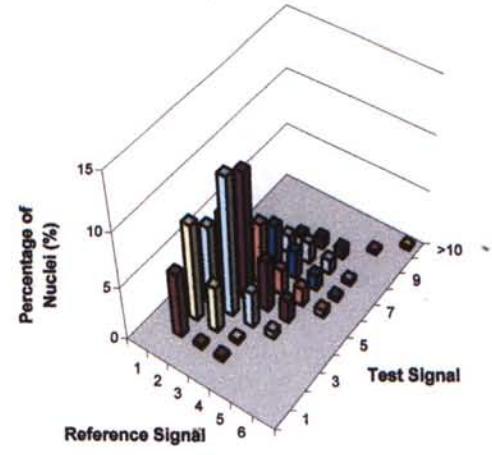

H50-935_b_12

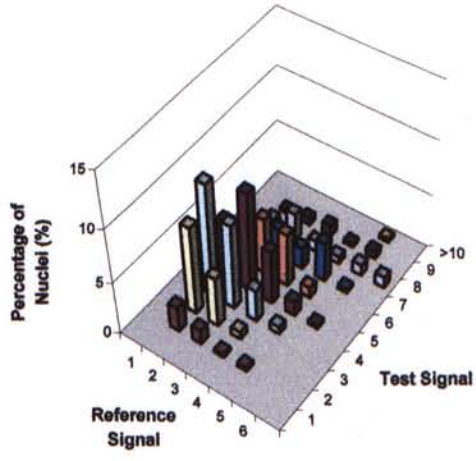

Figure 4.7C

H58-955_e_11

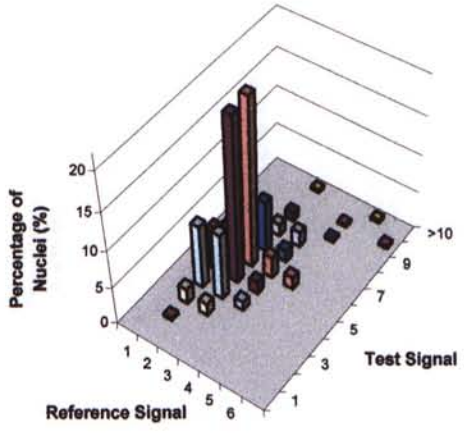

H58-757_a_7

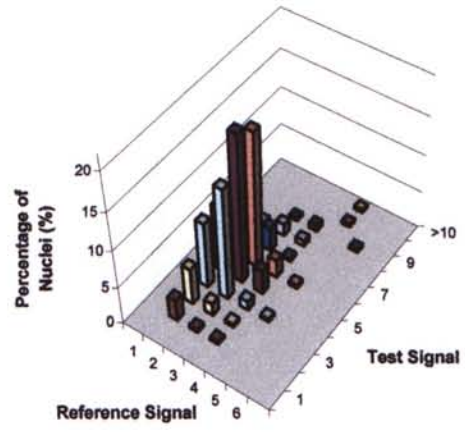

H58-910_c_8

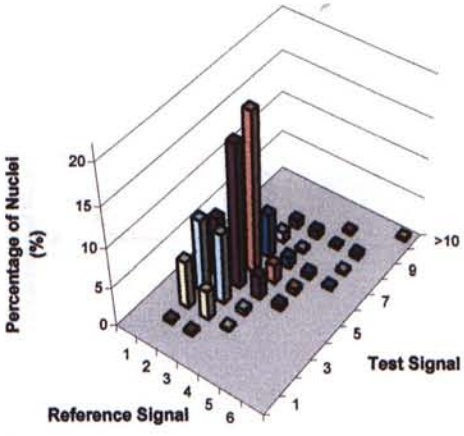

H58-964_h_4

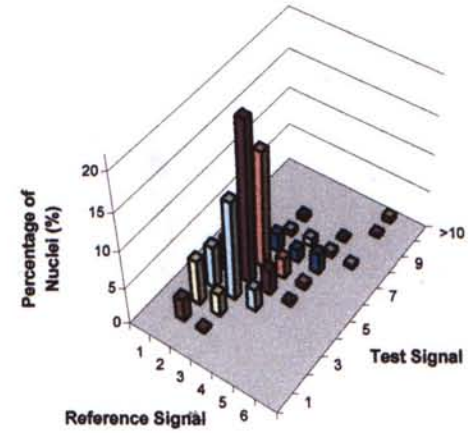

H58-935_b_12

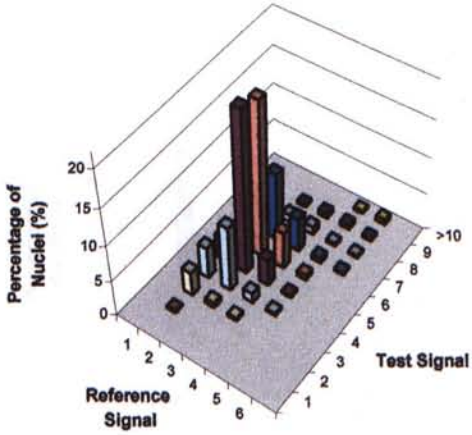

Figure 4.7D

H66-955_e_11

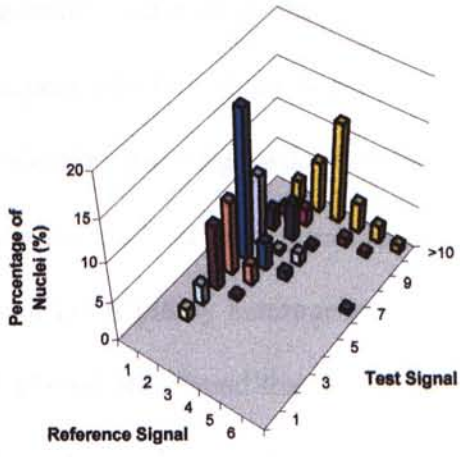

H66-757_a_7

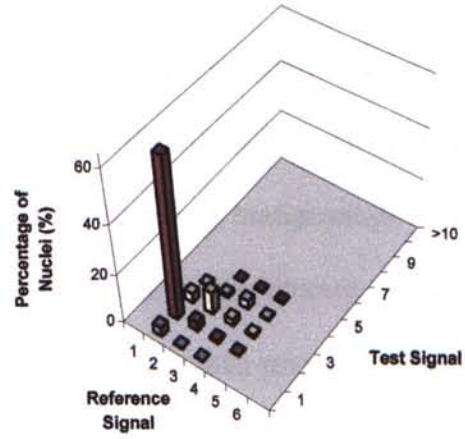

H66-910_c_8

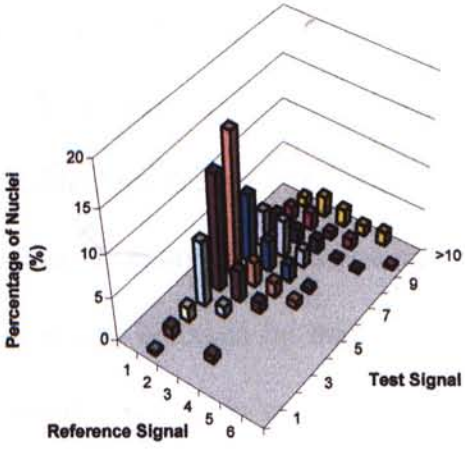

H66-964_h_4

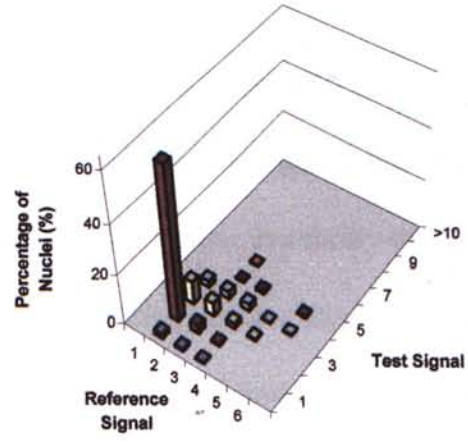

H66-935_b_12

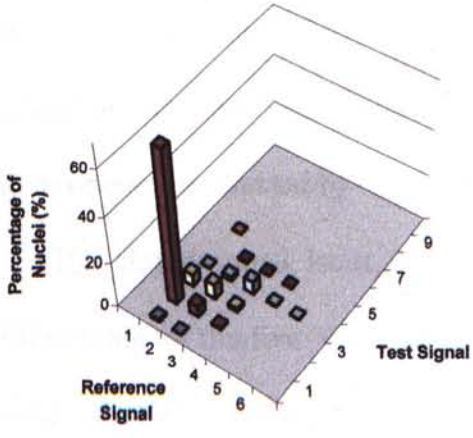

Figure 4.7E

growth environment (e.g., immune surveillance of the host, stromal or growth factor interactions, nutritional deficiencies, or hypoxia) favour the generation and subsequent selection of subclones of different ploidy state (Kuukasjarvi *et al.*, 1997). The selection and outgrowth of the more autonomous cells will then dominate in the population and lead to progression of the tumour to increasing malignancy. In the study of DNA ploidy heterogeneity in early and advanced gastric cancers, Fujimaki *et al.* (1996) also found that variation in DNA ploidy rather than presence of DNA aneuploidy correlated with progression of gastric cancer. If this observation applied to HCC, case H50 having a more diversified ploidy state, would be more likely to progress to an advanced stage.

Intratumoural signal heterogeneity was also observed in all 5 HCC studied. This implied the presence of clonal differences in the amplification status (Fig. 4.6). The clonal diversity observed was likely derived from the genetic instability of HCC cells that was enforced by the presence of host selection pressures from different microenvironments. In case H50, we were able to detect subpopulations of nuclei with highly amplified YAC 955e11, 910c8 and 935b12. The observation of clustered signals would be suggestive of intrachromosomal duplication of DNA sequences (homogeneously staining regions) rather than extrachromosomal amplification (double minutes). Such clonal diversity and clustering subpopulations would have been undetected by Southern blot and microsatellite analysis.

The chromosomal locus, 1q21.1, represented by 955_e_11 was the most amplified probe of the five YACs studied, and probably represented the core of the amplicon. A relative copy number gain of 1.9 to 3.4 copies of 955_e_11 was found. Whilst high-level amplification ($\geq$ 10-fold) of chromosomal material is thought to

contribute to oncogene over-expression, the role of a low-level copy gain in the liver tumourigenesis remained unclear.

A possible mechanism underlying the low-level chromosome gain in renal carcinogenesis was recently proposed by Zhuang *et al.* (1998). In hereditary papillary renal carcinomas (HPRC), trisomy 7 and germline mutation of the MET gene (7q31) are commonly found in tumours of these patients. The relationship between the two however is uncertain. By performing duplex PCR in 16 HPRC tumours that displayed both trisomy 7 and germline MET mutation, Zhang *et al.* detected the mutant MET gene in the duplicated chromosome 7 in all 16 tumours. It was therefore suggested that the tumourigenesis of HPRC might be initiated by a germline MET mutation, followed by a duplication of the mutated allele as a 'second activating hit'. Although no proto-oncogene has been implied on 1q21-q25 thus far, a similar mechanism of oncogene activation in the hepatocarcinogenesis cannot be ruled out since 1q copy number gain is frequent in HCC (Chapter 3).

Recent genetic mapping data showed that 955_e_11 lies in a large genomic region at 1q21 called the epidermal differentiation complex (EDC). EDC is one of the most gene-dense regions in the human genome. It contains three families of genes encoding proteins involved in the process of terminal differentiation of human epidermis, namely the cell envelope (CE) precursor proteins, the filament-associated proteins, and the S100A calcium-binding proteins (Marenholz *et al.,* 1996). It has been suggested that genes belonging to the same family evolved from a common ancestor by gene duplication mechanism (Lioumi *et al.*, 1998). Forus *et al.* (1998) have shown that the EDC genes including *SPRR3, SPRR2A, S100A6* and *S100A2* were highly amplified in human sarcomas. Although an increased expression of *S100A6* has been implicated in tumour progression and metastasis (Engelkamp *et al.*,

1993), the role of EDC genes in the development of HCC however remained to be verified.

A novel gene human *JTB* (*J*umping *T*ranslocation *B*reakpoint) was recently cloned (Hatakeyama *et al.*, 1999) and mapped within the EDC region in 955_e_11. H*JTB* however was not involved in epidermal differentiation when the expression pattern was considered. Interestingly, it was found that the region distal to the h*JTB* breakpoint was amplified to about 2.18-fold in tumour cells when compared to the normal cells. It is therefore possible that in HCC a breakpoint in the hJTB gene may have resulted in regional duplication of 1q21-q25 or a copy number gain in the whole long arm of chromosome 1.

In conclusion, by interphase FISH analysis, we have confirmed the presence of regional copy number gain on chromosome 1q21-q25. The amplicon core was also confined to 1q21.1. The YAC 955_e_11 defining the region of highest copy number increase should provide basis for further positional cloning of gene(s) that may be relevant to the development of HCC.

4.6 Further Studies

4.6.1 Fine Mapping of Chromosomal Region 1q21

Although the most amplified YAC identified in the amplicon 1q21-q25 was 955_e_11, it was not clear whether this YAC has the highest amplification, or that there were other amplified regions in the vicinity of 955_e_11. Therefore, further interphase FISH studies could be carried out to verify the amplification status of the region between the heterochromatic region (1q12) and 955_e_11, and region between 955_e_11 (1q21.1) and 910_c_8 (1q21).

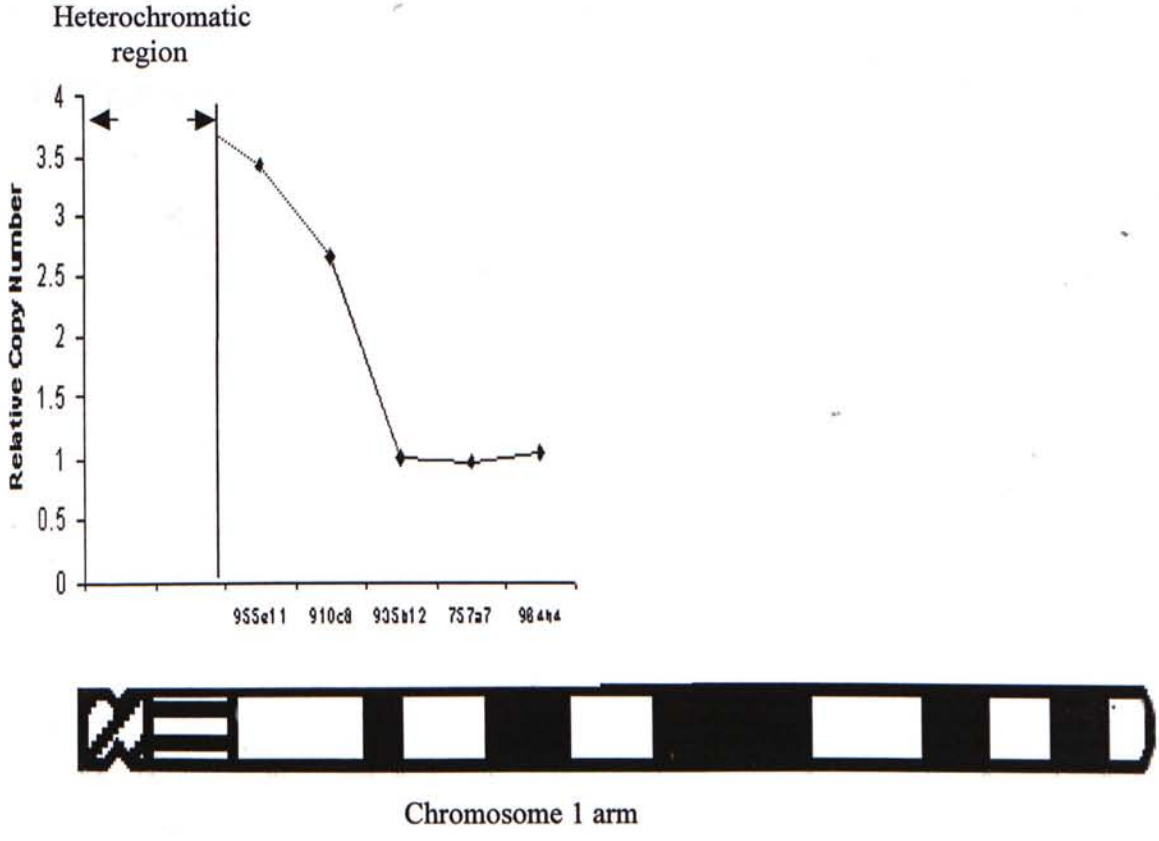

Figure 4.8. Further Interphase FISH studies to be done to verify the amplification status of the chromosome region between the heterochromatic region and 955e11, and region between 955e11 and 910c8.

4.6.2 Isolation of Novel Genes in the Amplicon

Once an amplified YAC is identified, it can be used to capture cDNAs by direct selection from a cDNA library constructed from the liver tumour that showed the highest corresponding level of YAC amplification (Elvin *et al.*, 1990). The differential expression of captured cDNA in normal and tumourous tissue will be first confirmed by Northern blotting. The overexpressed cDNA clones will then be sequenced and assessed for sequence homology with the database from the GenBank and EMBL using the online NCBI BLAST similarity program. It is probable that the cDNA identified may represent transcripts encoding proteins involved in apoptosis, cell cycle progression while functional studies on novel gene would verify its role in HCC pathogenesis.

References

Albertsen HM, Abderrahim H, Cann HM, Dausset J, Paslier DL, and Cohen D (1990). Construction and Characterization of a Yeast Artificial Chromosome Library Containing Seven Haploid Human Genome Equivalents. *Proc Natl Acad Sci USA* 87:4256-4260

Alitalo K and Schwab M (1986). Oncogene Amplification in Tumour Cells. *Adv Cancer Res* 47:235-281

Alter MJ (1995). Epidemiology of Hepatitis C in the West. *Semin Liver Dis* 15:5-14

Anzick SL, Kononen J, Walker RL, Azorsa DO, Tanner MM, Guan XY, Sauter G, Kallioniemi OP, Trent JM and Meltzer PS (1997). AIB1, a Steroid Receptor Coactivator Amplified in Breast and Ovarian Cancer. *Science* 277(5328):965-968

Beahrs OH, Henson DE, Hutter RVP, Kennedy BJ (1993). Handbook for Staging of Cancer. Philadelphia, JB Lippincott.

Beasley RP. (1988). Hepatitis B Virus. The Major Etiology of Hepatocellular Carcinoma. *Cancer* 61:1842-1856

Bentz M, Plesch A, Stilgenbauer S, Dohner H, Lichter P (1998). Minimal Size of Deletions Detected by Comparative Genomic Hybridization. *Gene Chromosom Cancer* 21(2):172-175

Bieche I and Lidereau R (1997). A Gene Dosage Effect is Responsible for High Overexpression of the *MUC1* Gene Observed in Human Breast Tumours. *Cancer Genet Cytogenet* 98:75-80

Boige V, Laurrent-Puig P, Fouchet P, Flejou JF, Monges G, Bedossa P, Bioulac-Sage P, Capron F, Schmitz A, Olschwang S, and Thomas G (1997). Concerted Nonsyntenic Allelic Losses in Hyperploid Hepatocellular Carcinoma as Determined by a High-Resolution Allelotype. *Cancer Res* 57:1986-1990

Boix L, Rosa JL, Ventura F, Castells A, Bruix J, Rodes J and Bartrons R (1994). C-*met* mRNA Overexpression in Human Hepatocellular Carcinoma. *Hepatology* 19:88-91

Bova GS, Carter BS, Bussemakers MJG, Emi M, Fujiwara Y, Kyprianou N, Jacobs SC, Robinson JC, Epstein JI, Walsh PC, and Issacs WB (1993). Homozygous Deletion and Frequent Allelic Loss of Chromosome 8p22 Loci in Human Prostate Cancer. *Cancer Res* 53:3869-3873

Brechot C, Pourcel C, Louis A, *et al.* (1980). Presence of Integrated Hepatitis B Virus DNA Sequences in Cellular DNA in Human Hepatocellular Carcinoma. *Nature* 286:533-535

Bressac B, Kew M, Wands J, Ozturk M (1991). Selective G to T Mutations of p53 Gene in Hepatocellular Carcinoma from Southern Africa. *Nature* 350:377-378

Bruix J, Barrera JM, Calvet X, et al. (1989). Prevalence of Antibodies to Hepatitis C Virus in Spanish Patients with Hepatocellular Carcinoma and Hepatic Cirrhosis. *Lancet* 2:1004-1006

Buetow KH, Murray JC, Israel JL, London WT, Smith M, Kew M, Blanquet V, Brechot C, Redeker A, and Govidnarajah S (1989). Loss of Heterozygosity Suggests Tumor Suppressor Gene Responsible for Primary Hepatocellular Carcinoma. *Proc Natl Acad Sci USA* 86:8852-8856

Burke DT, Carle GT, Olson MV (1987). Cloning of Large Segments of Exogenous DNA into Yeast by Means of Artificial Chromosome Vectors. *Science* 236:806-812

Chang MH, Chen CJ, Lai MS et al. (1997). Universal Hepatitis B Vaccination in Taiwan and the Incidence of Hepatocellular Carcinoma in Children. *N Engl J Med* 336:1855-1859

Chen DS, Hoyer BH, Nelson J *et al.* (1982). Detection and Properties of Hepatitis B Viral DNA in Liver Tissues From Patients with Hepatocellular Carcinoma. *Hepatology* 2:42s-46s

Chen SH, Hu CP, Chang C (1992). Hepatitis B Virus Replication in Well Differentiated Mouse Hepatocyte Cell Lines Transformed by Plasmid DNA. *Cancer Res* 52:1329-1335

Chu G, Vollrath D, Davis RW (1986). Separation of Large DNA Molecules by Contour-Clamped Homogeneous Electric Fields. *Science* 234:1582-1585

Cole CG, Goodfellow PN, Bobrow M, Bentley DR (1991). Generation of Novel Sequence Tagged Sites (STSs) from Discrete Chromosomal Regions Using *Alu*-PCR. *Genomics* 10:816-826

Cowan JM (1994). Fishing For Chromosomes. The Art and Its Applications. *Diagnostic Molecular Pathology* 3(4):224-226

De Souza AT, Hankins GR, Washington MK, Fine RL, Orton TC and Jirtle RL (1995). Frequent Loss of Heterozygosity on 6q at The Mannose 6-phosphate/insulin-like Growth Factor II Receptor Locus in Human Hepatocellular Tumours. *Oncogene* 10:1725-1729

De Souza AT, Hankins GR, Washington MK, Orton TC and Jirtle RL (1995). M6P/IGF2R Gene is Mutated in Human Hepatocellular Carcinomas with Loss of Heterozygosity. *Nat Genet* 11:447-449

Dejean A, Bougueleret L, Grzeschik KH, Tiollais P (1986). Hepatitis B Virus DNA Integration in a Sequence Homologous to *v-erb A* and Steroid Hormone Receptor in a Hepatocellular Carcinoma. *Nature* 322:70-72

Department of Health Annual Report 1997/1998. *Department of Health* 1999

Elvin P, Slynn G, Black D, Graham A, Butler R, Riley J, Anand R and Markham AF (1990). Isolation of cDNA Clones Using Yeast Artificial Chromosome Probes. *Nucleic Acids Res* 18:3913-3917

Emi M, Fujiwara Y, Nakajima T, Tsuchiya E, Tsuda H, Hirohashi S, Maeda Y, Tsuruta K, Miyaki M, and Nakamura Y (1992). Frequent Loss of Heterozygosity for Loci on Chromosome 8p in Hepatocellular Carcinoma, Colorectal Cancer, and Lung Cancer. *Cancer Res* 52:5368-5372

Engelkamp D, Schafer BW, Mattei MG, Erne P, Heizmann CW (1993). Six S100 Genes Are Clustered on Human Chromosome 1q21: Identification of Two Genes Coding for Previously Unreported Calcium-binding Proteins S100D and S100E. *Proc Natl Acad Sci USA* 90:6547-6551

Feitelson MA, Zhu M, Duan LX, London WT (1993). Hepatitis B X Antigen and p53 Associated *in vitro* and in Liver Tissues From Patients with Primary Hepatocellular Carcinoma. *Oncogene* 8:1109-1117

Fong TL, Di Bisceglie AM, Waggoner JG, *et al.* (1991). The Significance of Antibody to Hepatitis C Virus in Patients with Chronic Hepatitis B. *Hepatology* 14:64-67

Forus A, Weghuis DO, Smeets D, Fodstad O, Myklebost O, and van Kessel AG (1995). Comparative Genomic Hybridization Analysis of Human Sarcomas: I. Occurrence of Genomic Imbalances and Identification of a Novel major Amplicon at 1q21-22 in Soft Tissue Sarcomas. *Gene Chromosom Cancer* 14:8-14

Forus A, Berner J-M, Meza-Zepeda LA, Saeter G, Mischke D, Fodstad O and Myklebost O (1998). Molecular Characterization of a Novel Amplicon at 1q21-q22 Frequently Observed in Human Sarcomas. *Br J Cancer* 78(4):495-503

Fujiwara Y, Monden M, Mori T, Nakamura Y, and Emi M (1993). Frequent Multiplication of the Long Arm of Chromosome 8 in Hepatocellular Carcinoma. *Cancer Research* 53:857-860

Gall JG and Pardue ML (1969). Formation and Detection of RNA-DNA Hybrid Molecules in Cytological Preparations. *Proc Natl Acad Sci* USA 63:378-383

Hatakeyama S, Osawa M, Omine M and Ishikawa F (1999). *JTB*: A Novel Membrane Protein Gene at 1q21 Rearranged in a Jumping Translocation. *Oncogene* 18:2085-2090

Fujimaki E, Kohsuke S, Nakano O, et al (1996). DNA Ploidy Heterogeneity in Early and Advanced Gastric Cancers. *Cytometry* 26:131-136

Hohne M, Schaefer S, Seifer M *et al.* (1990). Malignant Transformation of Immortalized Transgenic Hepatocytes After Transfection with Hepatitis B Virus DNA. *EMBO J* 9:1137-1145

Hospital Authority Statistical Report 1997/1998. Hospital Authority 1999.

Hui AM, Sakamoto M, Kanai Y, et al. (1996). Inactivation of $p16^{INK4}$ in Hepatocellular Carcinoma. *Hepatology* 24:575-579

Ince N and Wands JR (1999). The Increasing Incidence of Hepatocellular Carcinoma. *N Engl J Med* 340:798-799

Johnson PJ, Williams R (1987). Cirrhosis and the Aetiology of Hepatocellular Carcinoma. *J Hepatol* 4:140-147

Kallioniemi A, Kallioniemi O-P, Sudar D, Rutovitz D, Gray JW, Waldman F, Pinkel D (1992). Comparative Genomic Hybridization for Molecular Cytogenetic Analysis of Solid Tumors. *Science* 258:818-821

Kallioniemi A, Kallioniemi O-P, Piper J, Tanner M, Stokke T, Chen L, Smith HS, Pinkel D, Gray JW, and Waldman FM (1994). Detection and Mapping of Amplified DNA Sequences in Breast Cancer by Comparative Genomic Hybridization. *Proc Natl Acad Sci USA* 91:2156-2160

Kariya Y, Kato K, Hayashizki Y, Himeno S, Tarui S and Matsubara K (1987). Revision of Consensus Sequence of Human *Alu* Repeats – A Review. *Gene* 53:1-10

Katagiri T, Nakamura Y, and Miki Y (1996). Mutations in the *BRCA2* Gene in Hepatocellular Carcinomas. *Cancer Res.* 56:4575-4577

Kimura H, Kagawa K, Deguchi T, *et al.* (1996). Cytogenetic Analyses of Hepatocellular Carcinoma by In Situ Hybridization with A Chromosome-specific DNA Probe. *Cancer* 77:271-277

Kita R, Nishida N, Fukuda Y et al. (1996). Infrequent Alterations of the $p16^{INK4A}$ Gene in Liver Cancer. *Int J Cancer* 67:176-180

Kiyosawa K, Furuta S (1991). Review of Hepatitis C in Japan. *J Gastroenterol Hepatol* 6:383-391

Knuutila S, Bjorkqvist A-M, Autio K, Tarkkanen M, Wolf M, Monni O, Szymanska J, Larramendy ML, Tapper J, Pere H, El-Rifai W, Hemmer S, Wasenius V-M, Vidgren V, Zhu Y (1998). DNA Copy Amplifications in Human Neoplasms. Review of Comparative Genomic Hybridization Studies. *Am J Pathol* 152:1107-1123

Kuukasjarvi T, Karhu R, Tanner M et al (1997). Genetic Heterogeneity and Clonal Evolution Underlying Development of Asynchronous Metastasis in Human Breast Cancer. *Cancer Res* 57:1597-1604

Kouprina N, Eldarov M, Moyzis R, Resnick M, Larionov V (1994). A Model System to Assess the Integrity of Mammalian YACs During Transformation and Propagation in Yeast. *Genomics* 21(1):7-17

Kress S, Jahn UR, Buchmann A, Bannasch P, Schwarz M (1992). P53 Mutations in Human Hepatocellular Carcinomas From Germany. *Cancer Res* 52:3220-3223

Kuroki T, Fujiwara Y, Nakamori S, Imaoka S, Kanematsu T and Nakamura Y (1995). Evidence for the Presence of Two Tumour-suppressor Genes for Hepatocellular Carcinoma on Chromosome 13q. *Br J Cancer* 72:383-385

Kuroki T, Fujiwara Y, Tsuchiya E, Nakamori S, Imaoka S, Kanematsu T, and Nakamura Y (1995). Accumulation of Genetic Changes During Development and Progression of Hepatocellular Carcinoma: Loss of Heterozygosity on Chromosome Arm 1p Occurs at an Early Stage of Hepatocarcinogenesis. *Gene Chromosom Cancer* 13:163-167

Kusano N, Shiraishi K, Kubo K, Oga A, Okita, and Sasaki K (1999). Genetic Aberrations Detected by Comparative Genomic Hybridization in Hepatocellular Carcinomas: Their Relationship to Clinicopathological Features. *Hepatology* 29:1858-1862

Larionov V, Kouprina N, Nikolaishvili N and Resnick MA (1994). Recombination During Transformation as a Source of Chimeric Mammalian Artificial Chromosomes in Yeast (YACs). *Nucleic Acid Res* 22:4154-4162

Leversha MA. "Fluorescence *in situ* Hybridization" in *Genome Mapping A Practical Approach* edited by Dear PH, IRL Press, 1997)

Levrero M, Tagger A, Balsano C *et al.* (1991). Antibodies to Hepatitis C Virus in Patients With Hepatocellular Carcinoma. *J Hepatol* 12:60-63

Liew CT, Li HM, Lo KW, Leow CK, Chan JY, Hin LY, Lau WY, Lai PB, Lim BK, Huang J, Leung WT, Wu S, Lee JC (1999). High Frequency of $p16^{INK4A}$ Gene Alterations in Hepatocellular Carcinoma. *Oncogene* 18:789-795

Lioumi M, Olavesen MG, Nizetic D, and Ragoussis J (1998). High-resolution YAC Fragmentation Map of q21. *Genomics* 49:200-208

Lowichik A, Schneider NR, Ansari MQ, and Timmons CF (1996). Report of a Complex Karyotype in Recurrent Metastatic Fibrolamellar Hepatocellular Carcinoma and a Review of Hepatocellular Carcinoma Cytogenetics. *Cancer Genet Cytogenet* 88:170-174

Luke S, Varkey JA, Belogolovkin V and Ladoulis CT (1997). Current State of Fluorescence *in situ* Hybridization (FISH) in Diagnostic Pathology. *Cell Vision* 4:16-31

Macoska JA, Trybus TM, Benson PD, Sakr WA, Grignon DJ, Wojno KD, Pietruk T, and Powell IJ (1995). Evidence for Three Tumour Suppressor Gene Loci on Chromosome 8p in Human Prostate Cancer. *Cancer Res* 55:5390-5395

Maniatas T, Fritsch EF, Sambrook J. *Molecular Cloning: A Laboratory Manual* (Cold Spring Harbour Laboratory, Cold Spring Harbour, NY, 1989).

Mansell CJ, Locarnini SA (1995). Epidemiology of Hepatitis C in the East. *Semin Liver Dis* 15:15-32

Marchio A, Meddeb M, Pineau P, Danglot G, Tiollais P, Bernheim A, and Dejean A (1997). Recurrent Chromosomal Abnormalities in Hepatocellular Carcinoma Detected by Comparative Genomic Hybridization. *Genes Chromosom Cancer* 18:59-65

Marenholz I, Volz A, Ziegler A, Davies A, Ragoussis I, Korge BP, and Mischke D (1996). Genetic Analysis of the Epidermal Differentiation Complex (EDC) on Human Chromosome 1q21: Chromosomal Orientation, New Marker, and a 6-Mb YAC Contig. *Genomics* 37:295-302

Nagai H, Pineau P, Tiollais P, Buendia MA and Dejean A (1997). Comprehensive Allelotyping of Human Hepatocellular Carcinoma. *Oncogene* 14:2927-2933

Nalpas B, Driss F, Pol S *et al.* (1991). Association Between HCV And HBV Infection in Hepatocellular Carcinoma And Alcoholic Liver Disease. *J Hepatol* 12:70-74

Nasarek A, Werner M, Nolte M, Klempnauer J, Georgii A (1995). Trisomy 1 and 8 Occur Frequently in Hepatocellular Carcinoma But Not in Liver Cell Adenoma And Focal Nodular Hyperplasia. A Fluorescence *In Situ* Hybridization Study. *Virchows Arch* 47:373-378

Nelson DL, Ledbetter SA, Corbo L, Victoria MF, Ramirez-Solis R, Webster TD, Ledbetter DH, and Caskey CT (1989). Alu Polymerase Chain Reaction: A Method for Rapid Isolation of Human-specific Sequences From Complex DNA Sources. *Proc Natl Acad Sci USA* 86:6686-6690

Ng IO, Srivastava G, Chung LP, Tsang SW, Ng MM (1994). Over-expression and Point Mutations of p53 Tumor Suppressor Gene in Hepatocellular Carcinomas in Hong Kong Chinese People. *Cancer* 74(1):30-7

Nishida N, Fukuda Y, Kokuryu H, et al. (1992). Accumulation of Allelic Loss on Arms of Chromosomes 13q, 16q and 17p In the Advanced Stages of Human Hepatocellular Carcinoma. *Int J Cancer* 51:862-868

Noben-Trauth K, Copeland NG, Gilbert DJ, Jenkins NA, Sonoda G, Testa JR, Klempnauer KH (1996): *Myb12* (*Bmyb*) Maps to Mouse Chromosome 2 and Human Chromosome 20q13.1. *Genomics* 35:610-612

Nose H, Imazeki F, Ohto M, Omata M (1993). p53 Gene Mutation And 17p Allelic Deletions in Hepatocellular Carcinoma from Japan. *Cancer* 72:355-360

Nousbaum JB, Pol S, Nalpas B, Landais P, Berthelot P, Brechot C (1995). Hepatitis C Virus Type 1b(II) Infection in France and Italy. *Annal Int Med* 122(3):161-168

Ohsawa N, Sakamoto M, Saito T, Kobayashi M, Hirohashi S (1996). Numerical Chromosome Aberrations in Hepatocellular Carcinoma Detected by Fluorescence *in situ* Hybridization. *J Hepatology* 25(5):655-662

Ohkoshi S, Kojima H, Tawaraya H *et al.*(1990). Prevalence of Antibody Against Non-A, Non-B hepatitis Virus in Japanese Patients With Hepatocellular Carcinoma. *Jpn J Cancer Res* 81:550-553

Okuda K. "Hepatitis C Virus And Hepatocellular Carcinoma." in *Liver Cancer* (edited by Okuda K and Tabor E., Churchill Livingstone, 1997)

Ozturk M, Bressac B, Puisieux A, *et al.* (1991). P53 Mutation in Hepatocellular Carcinoma After Aflatoxin Exposure. *Lancet* 338:1356-1359

Parkin DM, Pisani P and Ferlay J (1999). Estimates of the Worldwide Incidence of 25 Major Cancers in 1990. *Int J Cancer* 80:827-841

Piao Z, Park C, Park JH, and Kim H (1998). Allelotype Analysis of Hepatocellular Carcinoma. *Int J Cancer* 75:29-33

Pineau P, Nagai H, Prigent S, Wei Y, Gyapay G, Weissenbach J, Tiollais P, Buendia MA and Dejean A (1999). Identification of Three Distinct Regions of Allelic Deletions on the Short Arm of Chromosome 8 in Hepatocellular Carcinoma. *Oncogene* 18:3127-3134

Pinkel D, Straume T, and Gray JW (1986). Cytogenetic Analysis Using Quantitative High-sensitivity Fluorescence Hybridization. *Proc Natl Acad Sci USA* 83:2934-2938

Piper J, Rutovitz D, Sudar D, Kallioniemi A, Kallioniemi Olli-P, Waldman FM, Gray JW, and Pinkel D (1995). Computer Image Analysis of Comparative Genomic Hybridization. *Cytometry* 19:10-26

Reznikoff CA, Belair CD, Yeager TR, Savelieva E, Blelloch RH, Puthenveettil JA, Cuthill S (1996). A Molecular Genetic Model of Human Bladder Cancer Pathogenesis. *Semin Oncol* 23:571-584

Schlegel J, Stumm G, Scherthan H, Bocker T, Zirngibl H, Ruschoff J, Hofstadter F (1995). Comparative Genomic in situ Hybridization of Colon Carcinomas with Replication Error. *Cancer Res* 55:6002-6005

Schmid CW and Jelinek WR (1982). The *Alu* Family of Dispersed Repetitive Sequences. *Science* 216:1065-1070

Sheu JC, Huang GT, Lee PH, Chung JC, Chou HC, Lai MY, Wang JT, Lee HS, Shih Ln, Yang PM (1992). Mutation of p53 Gene in Hepatocellular Carcinoma in Taiwan. *Cancer Res* 52:6098-6100

Simmonds P, Alberti A, Alter HJ *et al.* (1994). A Proposed System for the Nomenclature of Hepatitis C Viral Genotypes. *Hepatology* 19:1321-1324

Simon D, Aden DP and Knowles BB (1982). Chromosomes of Human Hepatoma Cell Lines. *Int. J. Cancer* 30:27-33

Simonetti R, Cottonoe M, Craxi A, *et al.* (1989). Prevalence of Antibodies to Hepatitis C Virus in Hepatocellular Carcinoma. *Lancet* ii:1338

Singer MF (1982). SINEs and LINEs: Highly Repeated Short and Long Interspersed Sequences in Mammalian Genomes. *Cell* 28:433-434

Tada M, Omata M, and Ohto M (1990). Analysis of *ras* Gene Mutations in Human Hepatic Malignant Tumours By Polymerase Chain Reaction And Direct Sequencing. *Cancer Res* 50:1121-1124

Tirkkonen M, Karhu R, Kallioniemi A, Elomaa I, Kivioja AH, Nevalainen B, Karaharju E, Hyytinen E, Knuutila S, Kallioniemi OP (1995). Gains and Losses of DNA Sequences in Osteosarcomas by Comparative Genomic Hybridization. *Cancer Res* 55:1334-1338

Truant R, Antunovic J, Greenblatt J *et al.* (1995). Direct Interaction of the Hepatitis B Virus HBx Protein with p53 Leads to Inhibition by HBx of p53 Response Element-directed Transactivation. *J Virol* 69:1851-1859

Tsuda H, Hirohashi S, Shimosato Y, Ino Y, Yoshida T, and Terada M (1989). Low Incidence of Point Mutation of c-Ki-*ras* and N-*ras* Oncogenes in Human Hepatocellular Carcinoma. *Jpn J Cancer Res* 80:196-199

Tsuda H, Zhang W, Shimosato Y *et al.* (1990). Allele Loss On Chromosome 16 Associated With Progression of Human Hepatocellular Carcinoma. *Proc Natl Acad Sci USA* 87:6791-6794

Tulpule PG (1981). Aflatoxins - Experimental Studies. *J Cancer Res & Clin Oncol* 99(1-2):137-142

Wang J, Chenivesse X, Heigliein B, Brechot C (1990). Hepatitis B Virus Integration in a Cyclin A gene in a Hepatocellular Carcinoma. *Nature* 343:555-557

Wang XW, Forester K, Yeh H *et al.* (1994). Hepatitis B Virus X Protein Inhibits p53 Sequence-specific DNA Binding, Transcriptional Activity And Association with Transcriptional Factor ERCC3. *Proc Natl Acad Sci USA* 91:2230-2234

Wang Z, Xiang Q, Li D and Li S (1991). Correlation Between Gene Expression And Chromatin Conformation of *c-fos* and *N-ras* in Human Liver And Hepatoma. *Chin Med Sci J* 6:6-8

Wong N, Lai P, Lee SW, Fan S, Pang E, Liew CT, Zhong S, Lau JWY, and Johnson PJ (1999). Assessment of Genetic Changes in Hepatocellular Carcinoma by Comparative Genomic Hybridization Analysis. Relationship to Disease Stage, Tumour Size, and Cirrhosis. *Am J Pathol* 154:37-43

World Health Report 1996. World Health Organization.

Yeh SH, Chen PJ, Chen HL, Lai MY, Wang CC, and Chen DS (1994). Frequent Genetic Alterations at the Distal Region of Chromosome 1p in Human Hepatocellular Carcinomas. *Cancer Res.* 54:4188-4192

Yeh SH, Chen PJ, Lai MY, and Chen DS (1996). Allelic Loss on Chromosomes 4q and 16q in Hepatocellular Carcinoma: Association with Elevated α-Fetoprotein Production. *Gastroenterology* 110:184-192

Zhang YJ, Jiang W, Chen CJ, Lee CS, Kahn SM, Saetella RM and Weinstein IB (1993). Amplification and Overexpression of Cyclin D1 in Human Hepatocellular Carcinoma. *Biochem Biophys Res Commun* 196:1010-1016

Zhang X, Xu HJ, Murakami Y, Sachse R, Yashima K, Hirohashi S, Hu SX, Benedict WF, and Sekiya T (1994). Deletions of Chromosome 13q, Mutations in *Retinoblastoma 1*, and Retinoblastoma Protein State in Human Hepatocellular Carcinoma. *Cancer Res* 54:4177-4182

Zhao M, Zhang NX, Economou M, Blaha I, Laissue JA and Zimmermann A (1994). Immunohistochemical Detection of *bcl*-2 Protein in Liver Lesions: *bcl*-2 Protein is Expressed in Hepatocellular Carcinomas but Not in Liver Cell Dysplasia. *Histopathology* 25:237-245

Zhuang ZP, Park WS, Pack S, Schmidt L, Vortmeyer AO, Pak E, Pham T, Weil RJ, Candidus S, Lubensky IA, Linehan WM, Zbar B and Weirich G (1998). Trisomy 7-harbouring Non-random Duplication of the Mutant *MET* Allele in Hereditary Papillary Renal Carcinomas. *Nat Genet* 20:66-69

Zimmermann U, Feneux D, Mathey G *et al.* (1997). Chromosomal Aberrations in Hepatocellular Carcinomas: Relationship with Pathological Features. *Hepatology* 26:1492-1498

Zitzelsberger H, Lehmann L, Werner M, Bauchinger M (1997). Comparative Genomic Hybridisation for the Analysis of Chromosomal Imbalances in Solid Tumours and Haematological Malignancies. *Histochem Cell Biol* 108:403-417